

Assessment of Channel Routing for WRIMS CalLite Application:
North of the Sacramento Delta

By

Kevin Fung
B.S. (University of California, Davis) 2009

THESIS

Submitted in partial fulfillment of the requirements for the degree of

MASTER OF SCIENCE

In

Civil and Environmental Engineering

in the

OFFICE OF GRADUATE STUDIES

of the

UNIVERSITY OF CALIFORNIA

DAVIS

Approved by: _____
Jay R. Lund, Ph.D.

Fabián A. Bombardelli, Ph.D.

Z.Q. Richard Chen, Ph.D.

2011

Abstract

This thesis explores the use of hydrologic channel routing methods in a linear programming setting. The focus is on trying to implement channel routing in a large scale planning model similar to CalLite or CalSim. Three methods are compared in this study: 1) Muskingum 2) Lag and 3) Storage routing all of which are coefficient based. The models are calibrated using the Sacramento Basin WARMF model. WARMF and HEC-RAS are used for input hydrology and comparison. Downstream and minimum inflow requirements constrain the routing and optimization. Forecasts are run for each day to predict downstream conditions 2-3 days into the future, which are used to make present day allocations subject to routing constraints. The results show that all methods are applicable, with lag and storage being simpler to run and less susceptible to large fluctuations. The Muskingum method has more potential for greater accuracy than the other methods, but requires more hydrological data and calibration.

Acknowledgements

Special thanks to everyone at the Department of Water Resources (DWR) Bay-Delta Office, Modeling Branch, Central Valley Section for all their help, funding and support. Thanks to my supervisors Nazrul Islam and Sanjaya Seneviratne for hiring me, putting me up to this task, and believing in me.

Many people have assisted along the way, special thanks to other members at DWR including: Hao Xie, Eric Reyes, Francis Chung, Dustin Jones and Richard Chen, who is also part of my committee. Also, thanks go out to David Ford (David Ford Consulting), Jason Needham (HEC), and especially Beth Faber (HEC) for providing code and documentation for the FCLP program. Thank you Patrick Ji for helping me learn HEC-RAS on your own time outside of Davis.

I appreciate everyone willing to dedicate some time to helping me with various parts of this research. I can not believe how fortunate I am to be surrounded by such brilliant people on a daily basis. This includes the members of my committee Dr. Jay Lund (Chair), Dr. Bombardelli, and Dr. Chen for providing insight and constructive reviews.

Finally, thank you to all my family and friends who have been supporting my endeavors and Shirley Chan who has been a steady rock in my life. I wish you all the best and thank you a hundred times over.

TABLE OF CONTENTS

CHAPTER 1 INTRODUCTION	1
1.1 PURPOSE	1
1.2 STATE WATER AND CENTRAL VALLEY PROJECTS	1
1.3 CALSIM AND CALLITE	2
1.3.1 CalSim II	2
1.3.2 CalLite	2
1.4 OBJECTIVE	2
1.5 REPORT ORGANIZATION	3
Chapter 2 WRIMS, LIMITATIONS, AND OTHER LP MODELS	4
2.1 WRIMS OVERVIEW	4
2.2 WRESL	4
2.2.1 Objective	4
2.2.2 Soft Constraints	5
2.2.3 Coding	5
2.3 EXISTING LINEAR PROGRAMMING MODELS WITH ROUTING	5
2.3.1 ModSim	5
2.3.2 HEC-FCLP	6
2.3.3 HFAM-II	6
2.3.4 Aquatool	7
2.3.5 OASIS	7
2.4 LIMITATIONS OF WRESL	7
Chapter 3 REVIEW OF ROUTING METHODS	9
3.1 HYDROLOGIC VERSUS HYDRAULIC ROUTING	9
3.1.1 Hydraulic Routing Methods	9
3.1.2 Hydrologic Routing Methods	10
3.2 COEFFICIENT AND MUSKINGUM ROUTING	11
3.2.1 Storage and Routing Equations	11
3.2.2 General Muskingum Method	11
3.2.3 Coefficient Muskingum Method	12
3.2.4 Other Coefficient-Based Methods	14
3.3 STORAGE ROUTING	14
3.4 LAG ROUTING	15
3.5 ROUTING APPLIED TO WRIMS	15
3.6 ROUTING METHODS SUMMARY	16
Chapter 4 MODEL APPLICATION AND NETWORK SYSTEM	19
4.1 GENERAL APPROACH	19
4.2 DATA COLLECTION & WARMF MODEL	21
4.2.1 WARMF Background and Routing Procedures	22
4.2.2 Data Collection from WARMF Model	22
4.2.3 Data Compilation from WARMF Model	22

4.3 MODELLING APPROACH	23
4.3.1 Scenarios and Hydrology	24
4.4 MODEL CALIBRATION	24
4.4.1 Muskingum Coefficient Routing Application and Sensitivity	24
4.4.2 Storage Routing Application and Sensitivity	28
4.4.3 Lag Routing Application	32
4.4.4 Forecasting	32
Chapter 5 RESULTS AND DISCUSSION	34
5.1 OVERVIEW	34
5.2 FLOOD ROUTING TESTING	34
5.3 OUTFLOWS TO DELTA OPTIMIZATION	39
5.4 MULTIPLE MINIMUM INFLOWS TEST	44
5.5 COMPARISON OF ROUTING METHODS AND LIMITATIONS	49
5.5.1 Comparison of Routing Methods	49
5.5.2 Model Limitations	50
5.5.3 Run Time	50
Chapter 6 CONCLUSION	51
REFERENCES	53
APPENDIX	56
APPENDIX A: WARMF STREAM PROPERTIES	57
APPENDIX B: WATER TRAVEL TIMES	58
APPENDIX C: ESTIMATING THE NUMBER OF FORECASTING DAYS	59
APPENDIX D: ALL ROUTING FIGURES	61

LIST OF FIGURES

Figure 1. Geographical Coverage of CalSim II	3
Figure 2. Feasible region for Muskingum model parameters	13
Figure 3. Study area of Sacramento River on CalLite. Schematic circled in red	19
Figure 4. Study area of Sacramento River on Northern California Map from Google Maps	20
Figure 5. WARMF Interface	21
Figure 6. Plot of Muskingum sensitivity by varying K	26
Figure 7. Plot of Muskingum sensitivity by varying Δt .	27
Figure 8. Plot of Muskingum sensitivity by varying X	28
Figure 9. Muskingum variable error for X, t, and K	28
Figure 10. Plot of storage routing sensitivity by varying K	30
Figure 11. Plot of storage routing sensitivity by varying Δt .	31
Figure 12. Storage variable error for t and K	31
Figure 13. Example parallel system of releases	33
Figure 14. Example aggregation and averaged daily flow for a single channel	33
Figure 15. Outflow at Shasta for a 5 day release from Shasta Reservoir using WARMF calibrated coefficients	35
Figure 16. Outflow at Shasta for a 5 day release from Shasta Reservoir using HEC-RAS calibrated coefficients	36
Figure 17. Outflow at Shasta for a 5 day release from Shasta Reservoir using HEC Hydraulics Manual calibrated coefficients	36
Figure 18. Outflow at Hood for a 5 day release from Sacramento R.iver at American Confluence Channel using WARMF calibrated coefficients	37
Figure 19. Outflow at Hood for a 5 day release from Sacramento R.iver at American Confluence Channel using HEC-RAS calibrated coefficients	38
Figure 20. Outflow at Hood for a 5 day release from Sacramento R.iver at American Confluence Channel using HEC Hydraulics Manual calibrated coefficients	38
Figure 21. Outflow at Shasta channel for time series demand at the Hood using WARMF calibrated coefficients	40
Figure 22. Outflow at Shasta channel for time series demand at the Hood using HEC Hydraulics Manual calibrated coefficients	41
Figure 23. Outflow at Hood for a time series demand using WARMF calibrated coefficients	42
Figure 24. Outflow at Hood for a time series demand using HEC Hydraulics Manual calibrated coefficients	43
Figure 25. Outflow at Shasta channel for time series demands at Hood and Keswick using WARMF calibrated coefficients	45
Figure 26. Outflow at Shasta channel for time series demands at Hood and Keswick using HEC hydraulics manual calibrated coefficients	46
Figure 27. Outflow at Hood for time series demands at Hood and Keswick using WARMF calibrated coefficients	47
Figure 28. Outflow at Hood for time series demands at Hood and Keswick using HEC Hydraulics Manual calibrated coefficients	48
Figure 29. Water travel times during flood seasons	58
Figure 30. Outflow from C_Shsta at Keswick with WARMF calibrated coefficients	61
Figure 31. Outflow from C_Shsta at Keswick with HEC-RAS calibrated coefficients	61
Figure 32. Outflow from C_Shsta at Keswick with theoretically calibrated coefficients	62
Figure 33. Outflow from C_Kswck at Red Bluff with WARMF calibrated coefficients	62
Figure 34. Outflow from C_Kswck at Red Bluff with HEC-RAS calibrated coefficients	63
Figure 35. Outflow from C_Kswck at Red Bluff with theoretically calibrated coefficients	63
Figure 36. Outflow from C_RedBlf at Wilkins Slough with WARMF calibrated coefficients	64
Figure 37. Outflow from C_RedBlf at Wilkins Slough with HEC-RAS calibrated coefficients and Feather R. confluence with WARMF calibrated coefficients	64
Figure 38. Outflow from C_RedBlf at Wilkins Slough with theoretically calibrated coefficients and Feather R. confluence with HEC-RAS calibrated coefficients	65

Figure 39. Outflow from C_Wilkns at Sacramento R. and Feather R. confluence with theoretically calibrated coefficients	65
Figure 40. Outflow from C_Wilkns at Sacramento R. and American R. confluence with WARMF calibrated coefficients	66
Figure 41. Outflow from C_Wilkns at Sacramento R. and American R. confluence with HEC-RAS calibrated coefficients	66
Figure 42. Outflow from C_SacFea at Sacramento R. and American R. confluence with theoretically calibrated coefficients	67
Figure 43. Outflow from C_SacFea at Sacramento R.	67
Figure 44. Outflow from C_SacFea at Sacramento R.	68
Figure 45. Outflow from C_SacAme at Hood with WARMF calibrated coefficients	68
Figure 46. Outflow from C_SacAme at Hood with HEC-RAS calibrated coefficients	69
Figure 47. Outflow from C_SacAme at Hood with theoretically calibrated coefficients	69
Figure 48. Outflow from C_Shsta at Keswick with Delta flow requirement using WARMF calibrated coefficients	70
Figure 49. Outflow from C_Shsta at Keswick with Delta flow requirement using theoretically calibrated coefficients	70
Figure 50. Outflow from C_Kswck at Red Bluff with Delta flow requirement using WARMF calibrated coefficients	71
Figure 51. Outflow from C_Kswck at Red Bluff with Delta flow requirement using theoretically calibrated coefficients	71
Figure 52. Outflow from C_RedBlf at Wilkins Slough with Delta flow requirement using WARMF calibrated coefficients and Feather R. confluence with Delta flow requirement using WARMF calibrated coefficients	72
Figure 53. Outflow from C_RedBlf at Wilkins Slough with Delta flow requirement using WARMF calibrated coefficients and Feather R. confluence with Delta flow requirement using theoretically calibrated coefficients	72
Figure 54. Outflow from C_Wilkins at Sacramento R. and American R. confluence with Delta flow requirement using WARMF calibrated coefficients	73
Figure 55. Outflow from C_Wilkins at Sacramento R. and American R. confluence with Delta flow requirement using theoretically calibrated coefficients	73
Figure 56. Outflow from C_SacFea at Sacramento R.	74
Figure 57. Outflow from C_SacFea at Sacramento R.	74
Figure 58. Outflow from C_SacAme at Hood with Delta flow requirement using WARMF calibrated coefficients	75
Figure 59. Outflow from C_SacAme at Hood with Delta flow requirement using theoretically calibrated coefficients	75
Figure 60. Outflow from C_Shsta at Keswick with Delta and upstream flow requirements using WARMF calibrated coefficients	76
Figure 61. Outflow from C_Shsta at Keswick with Delta and upstream flow requirements using theoretically calibrated coefficients	76
Figure 62. Outflow from C_Kswck at Red Bluff with Delta and upstream flow requirements using WARMF calibrated coefficients	77
Figure 63. Outflow from C_Kswck at Red Bluff with Delta and upstream flow requirements using theoretically calibrated coefficients	77
Figure 64. Outflow from C_RedBlf at Wilkins Slough with Delta and upstream flow requirements using WARMF calibrated coefficients and Feather R. confluence with Delta and upstream flow requirements using WARMF calibrated coefficients	78
Figure 65. Outflow from C_RedBlf at Wilkins Slough with Delta and upstream flow requirements using theoretically calibrated coefficients and Feather R. confluence with Delta and upstream flow requirements using WARMF calibrated coefficients	78
Figure 66. Outflow from C_Wilkins at Sacramento R. and American R. confluence with Delta and upstream flow requirements using WARMF calibrated coefficients	79
Figure 67. Outflow from C_Wilkins at Sacramento R. and American R. confluence with Delta and upstream flow requirements using theoretically calibrated coefficients	79
Figure 68. Outflow from C_SacFea at Sacramento R.	80

Figure 69. Outflow from C_SacFea at Sacramento R.	80
Figure 70. Outflow from C_SacAme at Hood with Delta and upstream flow requirements using WARMF calibrated coefficients	81
Figure 71. Outflow from C_SacAme at Hood with Delta and upstream flow requirements using theoretically calibrated coefficients	81

LIST OF TABLES

Table 1. Channel Routing Methods Summary Table Compilation _____	17
Table 2. Channel characteristics _____	23
Table 3. K, X, ,and Δt coefficients from HEC Manual based Formulas	25
Table 4. K, X, ,and Δt coefficients from WARMF calibration _____	25
Table 5. K, X, ,and Δt coefficients from HEC-RAS calibration _____	25
Table 6. Muskingum Sensitivity by varying K _____	26
Table 7. Muskingum Sensitivity by varying X _____	27
Table 8. Muskingum Sensitivity by varying Δt _____	27
Table 9. K, Δt , and C coefficients from HEC Manual based Formulas _____	29
Table 10. K, Δt , and C coefficients from WARMF calibration _____	29
Table 11. K, Δt , and C coefficients from HEC-RAS calibration _____	29
Table 12. Storage Routing Sensitivity by varying K _____	30
Table 13. Muskingum Sensitivity by varying Δt _____	30
Table 14. Lag Reach parameters _____	32
Table 15. Flood routing test for Shasta channel summary table _____	35
Table 16. Flood routing test for SacAme channel summary table _____	37
Table 17. WARMF calibrated Delta outflow routing test for SacAme channel _____	40
Table 18. HEC hydraulics manual calibrated Delta outflow routing test for SacAme channel _____	41
Table 19. WARMF calibrated Delta outflow routing test for Shasta channel _____	42
Table 20. HEC hydraulics manual calibrated Delta outflow routing test for Shasta channel _____	43
Table 21. WARMF calibrated minimum in-stream flows routing test for Shasta channel _____	45
Table 22. HEC hydraulics manual calibrated minimum in-stream flows routing test for Shasta channel _____	46
Table 23. WARMF calibrated minimum in-stream flows routing test for SacAme channel _____	47
Table 24. HEC hydraulics manual calibrated minimum in-stream flows routing test for SacAme channel _____	48
Table 25. Comparison of routing methods tested _____	50
Table 26. Channel Properties from WARMF model _____	57
Table 27. Muskingum routing with WARMF based coefficients number of days Summary _____	59
Table 28. Muskingum routing with theoretical based coefficients number of days Summary _____	59
Table 29. Storage routing with WARMF based coefficients number of days Summary _____	59
Table 30. Storage routing with theoretical based coefficients number of days Summary _____	59
Table 31. Lag routing with theoretical based coefficients number of days Summary _____	60

Chapter 1
INTRODUCTION

1.1 PURPOSE

This document describes an optimization-based simulation model with channel routing for flood, delta salinity, and minimum in stream flows for the Sacramento River Basin. The purpose of this analysis is to assess the feasibility and extent of integrating channel routing to a daily linear programming-based simulation model in Water Resources Simulation Language (WRESL) for the applications of flood routing, delta salinity flows and minimum in-stream flow requirements. By applying generic tests to simple cases, it may be possible to infer improved release schedules from reservoirs to meet all demands efficiently. The modeled releases and outflows can be plotted against those of other simulation models and gage station data for comparison.

1.2 STATE WATER AND CENTRAL VALLEY PROJECTS

The State Water Project (SWP) is the largest man-made water conveyance project in the United States and is run by the California Department of Water Resources (DWR). The project begins in Oroville and runs down the Sacramento River to the Sacramento-San Joaquin Delta where water is pumped into the California Aqueduct. There are 34 storage facilities, 5 hydroelectric power plants and delivers an annual average of 2.4 million acre-feet and a total storage capacity of 5.8 million acre-feet (DWR, 2003). The project began in the Pat Brown administration and has since added various local interties since its completion in 1973. A major objective is to bring water to southern California, where rainfall and runoff is sparse. Today, the SWP serves over 25 million Californians and supplies water for over 750,000 acres of farmland (DWR, 2003).

The Central Valley Project (CVP) is run by the United State Bureau of Reclamation (USBR). It begins with Shasta and Trinity Reservoirs in the north, which leads to the Sacramento River and out into the Delta. The CVP extends to the Delta Mendota canal where it is conveyed to San Luis Reservoir. Work on the CVP began in 1933, during the great depression, funded by the federal government. Construction went on through the 70s. The network has 22 reservoirs have a total capacity of 11 million acre-feet and an average annual delivery of 7 million acre-feet. The CVP irrigates over 3 million acres of farmland and provides drinking water to more than 2 million consumers. The CVP has long-term contracts with more than 250 direct or indirect contractors in 29 out of 58 counties; while 29 agencies have contracts with the SWP. When the SWP is combined with the CVP, the projects extend north from Shasta Lake south to the Los Angeles Area, consisting of 701 miles of pipes, canals and aqueducts (DWR, 2010).

1.3 CALSIM AND CALLITE

The California Department of Water Resources maintains two planning system models for the combined CVP and SWP system, CalSim and CalLite. They are monthly comparative models that use optimization as the basis for simulation. The motivation behind this study is to add the daily time step capability to CalLite or CalSim.

1.3.1 *CalSim II*

CalSim II is a water network optimization driven simulation model created by the DWR and USBR. CalSim was preceded by two separate project models for the CVP (PROSIM) and SWP (DWRSIM). These two models replaced by a merged model with the addition of user specified constraints and objectives, called CalSim. This presented a major shift from a procedural model to a priority-preserving optimization-based simulation approach (DWR, 2000). Currently there are two versions of CalSim, with a third is to be released, which will feature more hydrologic detail. CalSim is a monthly comparative planning model that simulates release rules and environmental and water quality regulations such as D1641, COA and the biological opinions (DWR, 2002). Both the Bureau and DWR use CalSim studies in their OCAP and reoperations reports. Some local agencies use CalSim output for water allocation planning (DWR, 2003). A map of the system is shown in Figure 1.

1.3.2 *CalLite*

In 2007, a screening model was developed to bridge the gap between detailed CalSim modeling and policy and stakeholder demand for easier policy evaluations. This tool became known as CalLite and is available in a GoldSim software package online. CalLite can be used to run future development conditions and show impacts of climate change on the system. The goal of CalLite is to simulate Central Valley operations for 82 years in under 5 minutes of runtime. CalSim runs can take hours if not days to complete. To accomplish this, CalLite uses a simplified version of the CalSim system (DWR, 2009).

1.4 OBJECTIVE

CalLite currently is being shifted from the proprietary GoldSim environment to the Water Resources Integrated Modeling System (WRIMS) environment, which is the same as CalSim, for better transparency. The new version will retain the features of the GoldSim model, with a few tweaks. However, there is a demand for CalSim and CalLite to be used for more predictive policy applications. A daily model is being proposed for CalLite. Due to the complexity of such a change, the simpler CalLite would be easier to implement. This may increase run time, but a daily time step allows more flexibility for daily or weekly regulations. Since both CalSim and CalLite are monthly time step models, like many large scale planning models, changing to a finer daily time step involves many changes, some of which include reworking of the hydrology, regulations, and allocation logic. Also there is now a need for channel routing to simulate flows of water from upstream to downstream that require more than a single time step.

This study tests the feasibility of channel routing methods to a linear programming (LP) WRIMS model, with some form of regulation driving operations. Channel routing in LP models have been done, but for smaller systems and none use the WRIMS environment. Successful implementation will have benefits for reoperation, environmental, and other uses (DWR, 2000). The objectives for selecting a routing method include ease of implementation, quick run-time, and accuracy.

1.5 REPORT ORGANIZATION

Chapter 2 of this report provides an overview of WRIMS and WRESL code. A comparison of other similar types of models currently available is also presented. Chapter 3 discusses the channel routing approaches and a synopsis of findings. Chapter 4 covers the model application, including the incorporation of proprietary software (WARMF) in this research and assumptions made. The results are discussed in Chapters 5. Conclusions are drawn in Chapter 6.



Figure 1. Geographical Coverage of CalSim II

Chapter 2
WRIMS, LIMITATIONS, AND OTHER LP MODELS

2.1 WRIMS OVERVIEW

CalSim II and the next CalLite are written in a Water Resources Simulation (WRESL) script also developed by DWR and the Bureau. This script is used for all relationships and equations in the system and is used as a way to interface with the linear programming solver (DWR, 2000). The WRESL code is compiled by a special compiler known as WRIMS. The purpose of WRIMS is to convert the WRESL script first into Lahey FORTRAN code, which is utilized to compile the model into an executable program. The executable can then interact directly with the XA solver. WRIMS is under continuous modifications and currently is on two parallel tracks. WRIMS 1.3xx-1.5xx is used for CalSim II and the new WRIMS 2.xx will be used for CalSim III. The new WRIMS will run entirely in Java and can be easily installed without the use of a Lahey FORTRAN compiler. The XA solver is owned by Sunset Software Technology.

2.2 WRESL

2.2.1 Objective

CalSim is a simulation model. However, at its core, it is solved using a mixed integer linear program, which operates to preserve specified operating priorities for each time step individually. Every time step's operation has an objective function that the model tries to maximize. Using a linear combination of decision variables and weights along with soft constraints and penalties, an objective function (DWR, 2000):

$$\max Z = \sum_{i=1}^{nwt} (w_i \cdot X_i) + \sum_{j=1}^{npen} (-p_j \cdot x_j^+ | x_j^-) \quad (1)$$

where,

X is a decision variable

w is a priority weight

x^- is a slack variable

x^+ is a surplus variable

p is the penalty weight for a slack or surplus

2.2.2 Soft Constraints

Sometimes constraints need to be flexible and be allowed to break as long as a penalty is in place. Soft constraints in WRESL are used in such instances by assigning a “left hand side” to one decision variable and a “right hand side” to another decision variable along with the associated penalty:

$$S_A - S_B + x^- + x^+ = 0 \quad (2)$$

Where,

S_A and S_B are decision variables. x^- and x^+ are slack and surplus variables that allow for flexibility in the constraint.

2.2.3 Coding

WRESL code uses a series of “define” and “goal” statements. Define statements declare two types of variables, state and decision. State variables are values that are evaluated before solving the LP problem. Decision variables are unknown values that the LP solver must find. Goal statements specify constraints and decision making procedures. Code can be broken into modules and imported from various sources and relationship tables can be read in by define statements. Other features in WRESL are conditional case statements allowing for different goals or definitions for various conditions and the use of cycles. Cycles are used to run different models in the same time step and are completed sequentially. This allows for some processes to run and then pass decision variables (as state variables) between cycles (DWR, 2000).

2.3 EXISTING LINEAR PROGRAMMING MODELS WITH ROUTING

2.3.1 ModSim

ModSim is a reservoir system network flow simulation model developed at Colorado State University. It is entirely user input driven, but offers many features for long and short-term planning operations along with water rights, environmental and governmental regulations. Modsim’s features are its ease of use (including a GUI), free licensure, and wide array of features for including various routing methods. The model was developed in Microsoft Visual C++.net framework with the GUI written in Visual Basic.net, which brings high portability (Labadie, 2010).

ModSim uses a Muskingum routing scheme based on user defined coefficients as inputs. However, there is also an option for using a time lag as predefined by the user as well. The main implementation of Muskingum routing uses an iterative procedure on each routing link (Labadie, 2010).

$$q'_{kt} = c_0 q_{kt} + c_0 q_{k,t-1} + L \quad (3)$$

q'_{kt} is the ordinate of the outflow hydrograph at time t

$q_{j,t-\tau}$ is the ordinate of the inflow hydrograph at t- τ for $\tau = 0, 1 \dots$

c_0, c_0, K are routing coefficients

L is the remaining products of coefficients and previous inflows.

The routing link is divided into two parts, where the downstream portion of the divided link carries routed flows occurring in the current time step t only. The routed flows appearing at time step t due to flows in the link occur prior to time step t placed back into a return node, which is the original terminal node for the routing link (Labadie, 2010).

This model is also said to use a routing method to combat the problem of allocation priorities of upstream and downstream uses, which they call Backrouting (Labadie, 2010). The Backrouting involves “looking ahead” to predict downstream conditions and have that value “backrouted” upstream to determine the allocations. To do this, the system is divided into regions, which represent the boundary of water flow influence in a single time step. A set of time lag coefficients is assigned to each region, which physically correspond to *what percentage of water will reach the furthest downstream most point on each day?* So a coefficient array of [0.5, 0.5] means that for any amount of water coming from this region, 50% will reach the most downstream node on day one and the remaining (Labadie, 2010). 50% will reach there on day two. By using a series of matrices, the water is thereby routed to and from each region.

2.3.2 HEC FCLP

HEC-FCLP, also known as HEC-ResFloodOpt, is a reservoir operations optimization model for minimizing damages. It was developed by David Ford Consulting for the United States Army Corps Hydrologic Engineering Center (HEC) and uses the same mixed integer linear programming and XA solver as CalSim. However the similarities end there. This discontinued software was used primarily to look at reservoir network operations during flood periods (USACE, 2000). The code was originally developed by David Ford and written entirely in FORTRAN. FCLP uses a coefficient routing scheme based on the Muskingum method. Unlike WRIMS, FCLP interacts with the solver directly so the coefficients are placed directly into the decision making matrix and entered into the XA solver (USACE, 2000).

2.3.3 HFAM-II

A relatively new proprietary model, HFAM-II, is a continuous model for short and long-term studies as well as reservoir operations optimization. HFAM-II is capable of four types of runs: forecast, analysis, probabilistic, and optimization. The hydrological input data is stored in three main databases: historical, real-time, and forecast. The software is developed by Hydrocomp and the software is based on the old Stanford Watershed Model, the Hydrologic Simulation Program (FORTRAN) or HSPF, the Snake River Forecast Model (SRFM) and, the Seattle Forecast Model (SEAFM). HFAM-II was finished in 2006 (HydroComp, 2006). The model uses its own storage routing technique in the form of:

$$\mathbf{VOL} = \mathbf{VOLT} - (\mathbf{KS} * \mathbf{ROS} + \mathbf{COKS} * \mathbf{ROD}) * \mathbf{DELTS} \quad (4)$$

Where,

\mathbf{VOL} is the volume at the end of the time interval

\mathbf{VOLT} is the total volume at the beginning of the time interval

\mathbf{KS} is a weighting factor (0-.99)

COKS is the complement of *KS* (1-*KS*)

ROS is the total rate of outflow from the *RCHRES* at the start of the interval

ROD is the total rate of demanded outflow for the end of the interval

DELTS is the simulation interval in seconds

The two unknowns (bolded) are **VOL** and **ROD**. Using a user-specified Storage-Outflow relationship table and the linear routing equation, both unknowns can be solved through an iterative process (HydroComp, 2006).

2.3.4 *Aquatool*

Aquatool is a decision-support system created in Spain that combines optimization and simulation models. *Aquatool* is broken down into many separate modules that account for various basin management, risk assessment, optimization and simulation modules. There is a graphical user interface where a modeler can place nodes and arcs assembled in a schematic fashion. In the optimization module, *OPTIGES*, the channels and nodes are processed as an internal flow network based on the conservation of mass. The objective is minimizing the total weights of the system. Cycles are used as an iterative process to compute reservoir evaporation and return flows. The optimization is used primarily for exploration and must work in refining its solutions using the simulation models (Andreu, 1995).

The simulation module, *SIMGES*, uses the monthly allocations computed from the optimization as initial values. A simulation of the surface and groundwater interaction is performed iteratively, until convergence is reached. Once these values are found and updated in the network, other non-linear processes such as channel routing are performed in the same iterative way (Andreu, 1995).

2.3.5 *OASIS*

OASIS with *OCL*TM is a generalized program for modeling water system operations. Water is routed through nodes and arcs and accounts for natural and unnatural flows. *Oasis* allows the user to write their own scripts using its Operations Control Language (*OCL*), where constraints, goals, and variables can be declared. Time series databases and external programs can also be accessed using the *OCL* script. Unlike other modeling programs, there is no inherent channel routing feature. Instead routing rules must be set up as constraints similarly as *WRESL* (Hydrologics, 2009).

2.4 LIMITATIONS OF *WRESL*

WRESL script poses many challenges for implementing channel routing. The main obstacle is the inability to perform iterations needed for some channel routing methods. *WRESL* script is a series of define and goal statements nested in case by case conditions. This does not readily lend itself to performing looping operations as traditional programming languages such as *FORTRAN* and *C++* for generating coefficients or checking conditions are met. Iterations are needed in cases of subreaches and sub-time steps where the smaller steps and reaches must be run multiple times and aggregated during a single time step. At this time, *WRIMS* can not handle multi-time step optimization, which would facilitate channel routing

implementation. Further complications involve system setup to ensure stability in the formulations. Modelers often use cycles, which are models that are run sequentially each time step, to separate different processes. When using the cycling method, only a small finite number of cycles are allowed per run and with each increasing cycle comes increasing run time. Furthermore, when using cycles, each model must then be rewritten for every iteration. That assumes that the number of iterations needed is predetermined and not solved during the run time. Another problem arises because the solver solves each time step as an independent problem. This means that decision variables can only rely on past time steps values and not future values, which in some cases may be needed, specifically in regards to forecasting.

In the past, DWR and the Bureau have used workarounds for some of these problems. For example, ANN processes in CalSim use an external dll and some partially compiled object files to run specific functions. A strict set of rules apply when using external subroutines. Only one value may be passed to the function at a time and the return value can only be used as a state value. This means that arrays and time series cannot be passed at once nor stored. Given these sets of limitations, this study will attempt to implement channel routing methods with the goals of simplicity, speed, and accuracy.

Chapter 3
REVIEW OF ROUTING METHODS

3.1. HYDROLOGIC VERSUS HYDRAULIC ROUTING

Channel routing is commonly divided into two categories, hydrologic and hydraulic. Both routing types are widely used and accepted. Determining which type of routing technique is suitable for a model depends on the purpose, the accuracy required, and the physical system being modeled. Hydrologic methods tend to be simpler, linear, less demanding of data, and less accurate than hydraulic methods. Hydraulic methods are based on the full dynamic St. Venants equations and are sets of nonlinear equations. Finite difference methods can closely approximate hydraulic routing schemes using linear equations (McCuen, 2001).

3.1.1 Hydraulic Routing Methods

Hydraulic routing combines the continuity and momentum equations.

Continuity equation

Conservation form
$$\frac{\partial Q}{\partial x} + \frac{\partial A}{\partial t} = 0 \tag{5}$$

Nonconservation form
$$V \frac{\partial y}{\partial x} + \frac{\partial V}{\partial x} + \frac{\partial y}{\partial t} = 0 \tag{6}$$

Momentum equation

Conservation form

$$\frac{1}{A} \frac{\partial Q}{\partial t} + \frac{1}{A} \frac{\partial}{\partial x} \left(\frac{Q^2}{A} \right) + g \frac{\partial y}{\partial x} - g(s_0 - s_f) = 0 \tag{7}$$

Local	Conservative	Pressure	Gravity	Friction
acceleration	acceleration	force	force	force
term	term	term	term	term

Nonconservation form (unit with element)

$$\frac{\partial V}{\partial t} + V \frac{\partial y}{\partial x} + g \frac{\partial y}{\partial x} - g(S_0 - S_f) = 0 \tag{8}$$

	Kinematic wave
	Diffusion wave
	Dynamic wave

These equations are the St. Venant's equations. The St. Venant's equations are believed to be the most comprehensive and accurate equations used to approximate one dimensional unsteady wave flow. Often, simplifications can be made to these equations with the kinematic wave approximation, where the pressure and gravity forces are considered negligible. This can lead to linear equations that can be solved through discretized finite-difference grids. To apply these equations, the bathymetry of each channel must be known.

Due to the high complexity, long computation times, and high degree of inputs needed, hydraulic routing methods will not be used in this study (Mays, 2001).

3.1.2 Hydrologic Routing Methods

The two important forms of the storage equation are the ordinary differential equation and the centered discretization forms.

$$\frac{dS}{dt} = I(t) - O(t) \quad (9)$$

$$\frac{1}{2}(I_1 + I_2) - \frac{1}{2}(O_1 + O_2) = \frac{S_2 - S_1}{\Delta t} \quad (10)$$

A relationship between storage outflow and/or inflow is required in order to solve equation 10. For example, the discretized storage equation can be simplified using the following equations:

$$S_0 = b \left[\left(\frac{O}{a} \right)^{1/d} \right]^m = b \left(\frac{O}{a} \right)^{m/d} = \left[b \left(\frac{1}{a} \right)^{m/d} \right] O^{m/d} = KO^{m/d} \quad (11)$$

$$S = xKI^{m/d} + (1-x)KO^{m/d} \quad (12)$$

where,

a and d are constants for stream reach properties; b and m are constants for log-log relationship between storage and depth (McCuen, 2001).

All routing methods in ModSim, HEC-FCLP, and HFAM II are hydrologic methods. Due to the simpler parameters necessary for implementation, hydrologic methods are better suited for complex linear programming problems. When calibrated correctly, hydrologic routing methods can give a fairly accurate depiction of a system despite its formulation shortcomings compared to the St. Venants based equations. One study on the Illinois watershed conducted by NOAA using the NEXRAD model found that under certain circumstances that for small time increments, a hydrologic method yielded more accurate results than hydraulic routing (NOAA, 1999). Within hydrologic routing are a few broad subcategories of methods. Those methods include, coefficient routing, storage routing, and lag routing all of which were used in the other linear programming models in some form. The next sections describe these methods to see how they can be used for WRIMS application.

3.2. COEFFICIENT AND MUSKINGUM ROUTING

3.2.1 Storage and Routing Equations

Flow Routing is a procedure to estimate the time and magnitude of flow at a point on a watercourse from hydrographs at one or more points upstream. In hydrologic routing, flow is calculated as a function of time with no spatial variability and is governed by the continuity equation (Mays, 2001).

Many coefficient type routing methods were examined including Convex, Modified At-Kin, Modified-Puls, Working R&D, Successive average (Tatum), Progressive Average (SSAR), and Lag and K, but due to overlapping similarities and popular acceptance, the Muskingum method will be primarily discussed.

3.2.2 General Muskingum Method

The Muskingum method is based on the routing equations 9 and 10, and storage equation 11 and 12. By setting $m/d = 1$ and $K = b/a$, the storage equation becomes

$$S = K[xI + (1-x)O] \quad (13)$$

When it is plugged into equation 9 and rearranged, the routing equation becomes

$$O_2 = C_0 I_2 + C_1 I_1 + C_2 O_1 \quad (14)$$

where,

$$C_0 = -\frac{Kx - .5\Delta t}{K - Kx + .5\Delta t} \quad (15)$$

$$C_2 = \frac{K - Kx - .5\Delta t}{K - Kx + .5\Delta t} \quad (16)$$

$$C_0 + C_1 + C_2 = 1 \quad (17)$$

To apply the method, the upstream hydrograph O_1 , routing interval Δt , and estimates for routing coefficients K and x must be used. K is the time through the reach and x is a parameter between 0 and 0.5 representing physical features of the channel. A value of 0 indicates that the wave exhibits only attenuation (dampening of the wave) and a value of 0.5 indicate that the wave is subject to translation with little or no attenuation. Figure 2 shows the feasible range of values for the variables. In some cases, using a derivation of the Manning's equation, K and x can be estimated assuming the $K = b/a$ and x as discussed before can be set to:

$$x = \frac{1.49S^{1/2}}{nP^{2/3}} \quad (18)$$

where S is the slope, n is Manning's coefficient, and P is the wetted perimeter (McCuen, 2001).

3.2.3 Coefficient Muskingum Method

A common variant on the general Muskingum method parlays the three coefficients into an array of coefficients each multiplied by the past inflows.

$$O_t = C_0 I_t + C_1 I_{t-1} + C_2 I_{t-2} \dots C_n I_{t-n} \quad (19)$$

Equations were taken from Army Corps manual EM 1110-2-1417 for Muskingum method. The constraints for X and K are given by the Muskingum-Cunge formulas.

$$C' = \frac{((2K(1-X) + \Delta t) - 2\Delta t)}{2K(1-X) + \Delta t} \quad (20)$$

$$C_1 = C_0 \cdot C' + \frac{(\Delta t + 2KX)}{2K(1-X) + \Delta t} \quad (21)$$

$$C_i = C_{i-1} \cdot C' \quad (22)$$

for $i \geq 2$

$$K = \frac{L}{V_w} \quad (23)$$

$$V_w = \frac{1}{B} \frac{dQ}{dy} = 1.5 * V_n \quad (24)$$

$$X = \frac{1}{2} \left(1 - \frac{Q_0}{BS_0 c \Delta x} \right) \quad (25)$$

where,

O_2 = Outflow at current time step

O_1 = Outflow at previous time step

X = Muskingum Coefficient (representing of physical properties of channel)

K = time through reach

Δt = time step

C_{1-3} = Muskingum Routing Coefficients

V_w = floodwave velocity [ft/s]

V_n = Average Velocity (from manning's equation)

Q_0 = reference flow

B = base width of channel (for a given flow)

S_0 = slope of channel

c = celerity or floodwave speed

Δx = length of routing subreach

Parameters can be estimated through other means, the most common being trial and error. Other ways include using least squares regression, fitting to a storage curve and iterating. The “Mupers” software package uses nonlinear and linear methods and rapidly yields coefficients and tests them for accuracy (Yoon, 1993).

When the K coefficient is much larger than the time step, an alternative strategy is then used, which divides long reaches into smaller sub reaches.

$$\# \text{subreaches} = \frac{K}{\Delta t} \quad (26)$$

Also it is recommended that parameters, K , X , and Δt are chosen such that

$$2KX < \Delta t \leq K \quad (27)$$

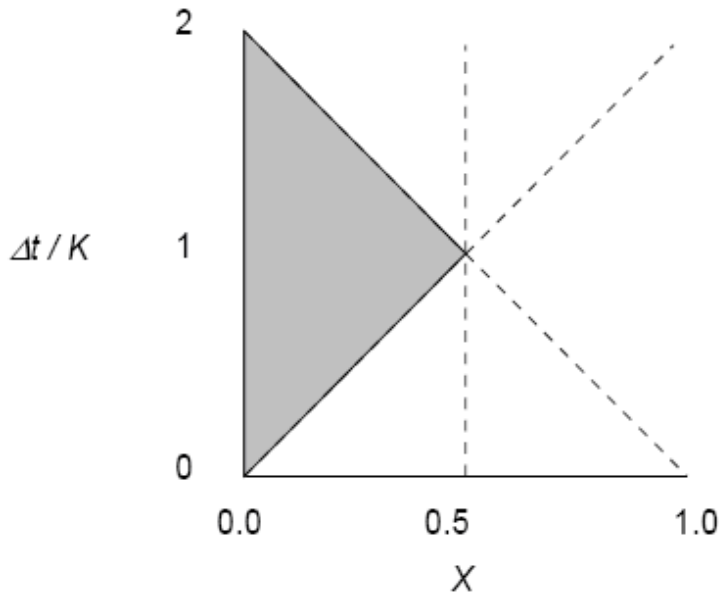


Figure 2. Feasible region for Muskingum model parameters (USACE, 200)

This ensures that the routing coefficients generated will be positive and lead to stable solutions.

The Muskingum method can produce outflow results similar to those of kinematic wave methods (Smith, 1999). However, the method has been criticized for yielding negative results, being derived from Lag and K method, and having an unreliable storage equation (Can, 1985). The negative outflows can be prevented by using lag and k routing (setting x equal to 0). The storage equation used in the Muskingum method applies only to the channel with bank storage being implied. In reality, this may not be the case and a modification to the Muskingum equations may be needed to account for the bank storage (Gill, 1979). Another issue occurs when the inflow hydrograph starts to change to when the outflow hydrograph begins to change, a time lapse that occurs. The Muskingum method assumes that both begin

changing at the same time. The Muskingum method should be used for steep slopes where backwater effects will have little influence on the outflow. Overall though, when compared to the kinematic wave, the consensus is that it has similar results (Choudhury, 2007).

3.2.4 *Other Coefficient-Based Methods*

Many other routing methods are similar to the Muskingum method and are classified as coefficient methods. The Convex and Modified At-Kin are coefficient routing methods that use a single coefficient as opposed to the Muskingum, which uses two coefficients. The main differences in the coefficient routing methods lie in the storage equation that is used. Each coefficient routing method makes certain assumptions or simplifications to the generic storage equation (equations 9, 10) and derives a corresponding outflow routing equation. The equations are summarized in Table 1.

3.3. STORAGE ROUTING

Storage routing methods also have a wide range of forms. Storage routing is generally used for reservoir routing purposes, but can be applied to channel routing as well. However, channel outflow is not dependent on storage alone, so storage routing should be applied cautiously to channels. A basic form of storage routing is use of Manning's equation in conjunction with the continuity equation.

$$V = \frac{k}{n} R_h^{2/3} \cdot S^{1/2} \quad \text{eq. 28}$$

V is velocity, k is 1 or 1.486 (English units), R_h is wetted perimeter, and S is slope.

Variations of storage based routing exist such as the Modified-Puls, Working R&D, and HFAM II. These methods use the storage equation to derive storage to outflow rating curves and are used with weighted coefficients. The rating curves can be a fixed look up table or a varying function of inflow and outflow.

Storage routing was used in a study on the Colorado River, which looks at developing a release schedule that would maximize hydropower and profits. The study used the storage as a determining factor for reservoir releases upstream based on the current storage. A negative storage implies that there is not enough water in the system and the solution is infeasible under the current run settings (Chow, 1964).

3.4. LAG ROUTING

This is the most basic type of routing where an inflow hydrograph is lagged a specified number of time steps. There is generally no attenuation in the outflow; however methods exist to combine lag routing with K attenuation. The Successive Average method developed by F.E. Tatum for the U.S. Army Corps of Engineers is used in most HEC programs (Chow, 1964). It assumes that discharge-storage relation varies uniformly across a channel; the average of inflows at routing periods 1 and 2 will be experienced at some point downstream at period 2, which apply to all routing periods of the same time interval; the change in shape of a hydrograph between two points results from the cumulative effects of all the storage characteristics of the reach, so the routing can be repeated for as many subreaches as desired to find the change in shape of a hydrograph due to storage.

$$O_{n+1} = C_1 I_1 + C_2 I_2 + C_3 I_3 + \dots + C_{n+1} I_{n+1} \cdot$$
$$C_n = \frac{n(n-1)(n-2)\dots}{2^n (n-1)!} \quad (29), (30), (31)$$
$$C_{n+1} = \frac{n!}{2^n n!} = \frac{1}{2^n}$$

where,

O is outflow for the current time step, C is the lag time coefficient, n is the number of subreaches, and I is the inflows. The lag method is empirical and has limited applicability. It is typically used on long slowly varying flows and channels (Chow, 1964). The Progressive Average method also averages inflow values but lags them by the travel time of the flood wave. The inflow period of the flood wave can be varied and adjusted to match an observed outflow hydrograph.

3.5. ROUTING APPLIED TO WRIMS

When sub reaches or smaller time steps are involved, channel routing becomes an iterative process. When applying these methods to a non-iterative LP environment, problems may arise. HEC-FCLP and ModSim use coefficient routing along with a user option of lag routing whereas HFAM-II uses a storage routing scheme. Since lag, storage, and Muskingum methods have been implemented successfully, it is worth pursuing for WRIMS application. However, the problem of not being able to use looping methods or multi-step optimization in WRIMS poses a big challenge. CalLite and CalSim are already fixed systems, but introducing channel routing may require changes in the schematic. This study explores these methods for the feasibility for large scale use.

3.6. ROUTING METHODS SUMMARY

The routing methods researched are summarized in Table 1. This does not include popular hydraulic models or full dynamic wave routing methods. Three general categories of hydrologic methods were considered: coefficient routing, storage, routing, and lag routing. Coefficient routing is a general term that can encompass many types of routing including lag and storage routing. However, for this study we will refer to it as a generic form of Muskingum routing and separate it from storage coefficient and lag coefficient routing.

The Convex, Modified At-Kin, and Muskingum methods are typical coefficient based routing procedures. Modified-Puls, Working R&D, HFAM II, and storage coefficient routing are storage based routing methods due to the use of a rating curve (Chow, 1964). Successive, progressive and lag and K are lag methods based on empirical formulas with limited applicability. This study focuses on Muskingum, Successive lag, and coefficient storage routing for simplicity and reliability, but many other options also exist (Shaw, 2005).

Table 1. Channel Routing Methods Summary Table Compilation

Routing Method	Routing Equation	Routing Parameters	Major Software	Pros	Cons
<i>Hydrologic</i>					
Convex	$O_2 = C I_1 + (1-C) * O_1$	$C = \Delta t / K$	None	<ul style="list-style-type: none"> requires fitting 1 parameter 	<ul style="list-style-type: none"> Less flexible storage equation Assumption $x = 0$ Same coefficient to weigh inflow hydrograph ordinate (C, 0) -> I1, I2
Modified At-Kin	$O_2 = I_1 C_m + (1-C_m) * O_1$	$C_m = L / mV$	None	<ul style="list-style-type: none"> See Convex 	<ul style="list-style-type: none"> See Convex
Modified Puls	$(I_1 + I_2) + \left(\frac{2S_1}{\Delta t} - O_1 \right) = \frac{2S_2}{\Delta t} + O_2$	S_2, O_2	HEC-1 ²⁹ , ResSim ³² , HMS ³⁰	<ul style="list-style-type: none"> Simplified routing and basis for other storage discharge relationships 	<ul style="list-style-type: none"> Attenuation depends on river reach lengths Stages produced are limited value because downstream effects are not taken into account Invariable discharge storage relationship Neglects variable slope during passage of a wave
Working R&D	$O_2 = D_2 - \frac{X}{1-X} (I_2 - D_2)$	$R = .5D\Delta t + S(1-X)$ $D = XI + (1-X)O$ K, X	ResSim ³² , HEC-1 ²⁹	<ul style="list-style-type: none"> More advantageous than Muskingum if independent variable such as inflow or controlled discharge through a gated low dam is involved 	<ul style="list-style-type: none"> More complex and intricate to implement
Coefficient Storage	$O_2 = O_1 + C(I_1 - O_1) + .5C(I_2 - I_1)$	$C = \frac{\Delta t_2}{K + .5\Delta t}$	None	<ul style="list-style-type: none"> Generic Storage Equation Can be used with or without rating curve 	<ul style="list-style-type: none"> assumes a linear storage with only 1 estimated parameter
Muskingum Method	$O_2 = C_0 I_2 + C_1 I_1 + C_2 O_1$	$X = \frac{C_1 - C_0}{(1 - C_0)}$ $K = \frac{\Delta t(1 - C_0)}{C_0 + C_1}$	All: HMS ³⁰ , ResSim ³² , HEC-1 ²⁹ , NWSRFS ²⁷	<ul style="list-style-type: none"> general storage equation X may vary Different coefficients to weigh inflow <ul style="list-style-type: none"> C0, C1 -> I1, I2 Adequate for flood control and multi purpose projects 	<ul style="list-style-type: none"> Must fit 2 parameters Routing period must be restricted otherwise could have negative outflow due to great inflow slope

Routing Method	Routing Equation	Routing Parameters	Software Implemented	Pros	Cons
Lag Methods:					
Tatum (successive avg)	$O_2 = .5(I_1 + I_2)$ $O_{n+1} = C_1 I_1 + C_2 I_2 + \dots + C_{n+1} I_{n+1}$	$C_{n+1} = 1/(2^n)$	HMS ³⁰ , NWSRFS ²⁷	<ul style="list-style-type: none"> • Simpler than Muskingum • Avoids negative outflows 	<ul style="list-style-type: none"> • Long reaches and slowly fluctuating streams • Not based on mathematical relationships of motion or channel storage • Developed from intuitive & empirical processes • Reliability and applicability are limited
SSAR (progressive avg)	$T_s = \frac{KIS}{Q^n}$	KTS	All: HMS ³⁰ , ResSim ³² , HEC-1 ²⁹ , NWSRFS ²⁷	<ul style="list-style-type: none"> • Length of period does not necessarily relate to the flood-wave travel time 	<ul style="list-style-type: none"> • Length of inflow period is determined by trial until a satisfactory agreement is obtained between the computed and observed peak outflows
Lag and K	Any Lag Method with K attenuation	Varies	NWSRFS ²⁷	<ul style="list-style-type: none"> • Flexible routing method – lag and k can be constant or variable 	<ul style="list-style-type: none"> • Multiple Intercept Errors – graph may double back and can be cumbersome to account for • Occasional volume errors • Peak attenuation • Complicated implementation
<i>Semi-Hydraulic</i>					
Kinematic Wave	NA	NA	All: HMS ³⁰ , ResSim ³² , HEC-1 ²⁹ , NWSRFS ²⁷	NA	NA
Muskingum-Cunge	NA	NA	NA	NA	NA
HFAM II	$Vol_{Reach} = Vol_0 + Vol_I + Vol_{Rain} - Vol_{Evap} - Vol_{Out} - diversion demands$	KS & physical parameters	HFFAM II ¹⁶	NA	NA
<i>Hydraulic</i>					
St. Venant's Equations	NA	NA	NA	NA	NA

Chapter 4
MODEL APPLICATION AND NETWORK SYSTEM

4.1. GENERAL APPROACH

This chapter compares routing options for suitability in WRIMS and eventually in CalLite. A simple network model idea is used to test the various methods. Since CalLite is the model where routing will be implemented, a section of the CalLite schematic is used from Shasta Reservoir and to Hood, incorporating 6 channels: C_Shsta, C_Kswck, C_RedBlf, C_Wilkns, C_SacFea, and C_SacAme. They are circled in red in Figure 3. Figure 4 shows the geographic locations of each of the nodes and channels.

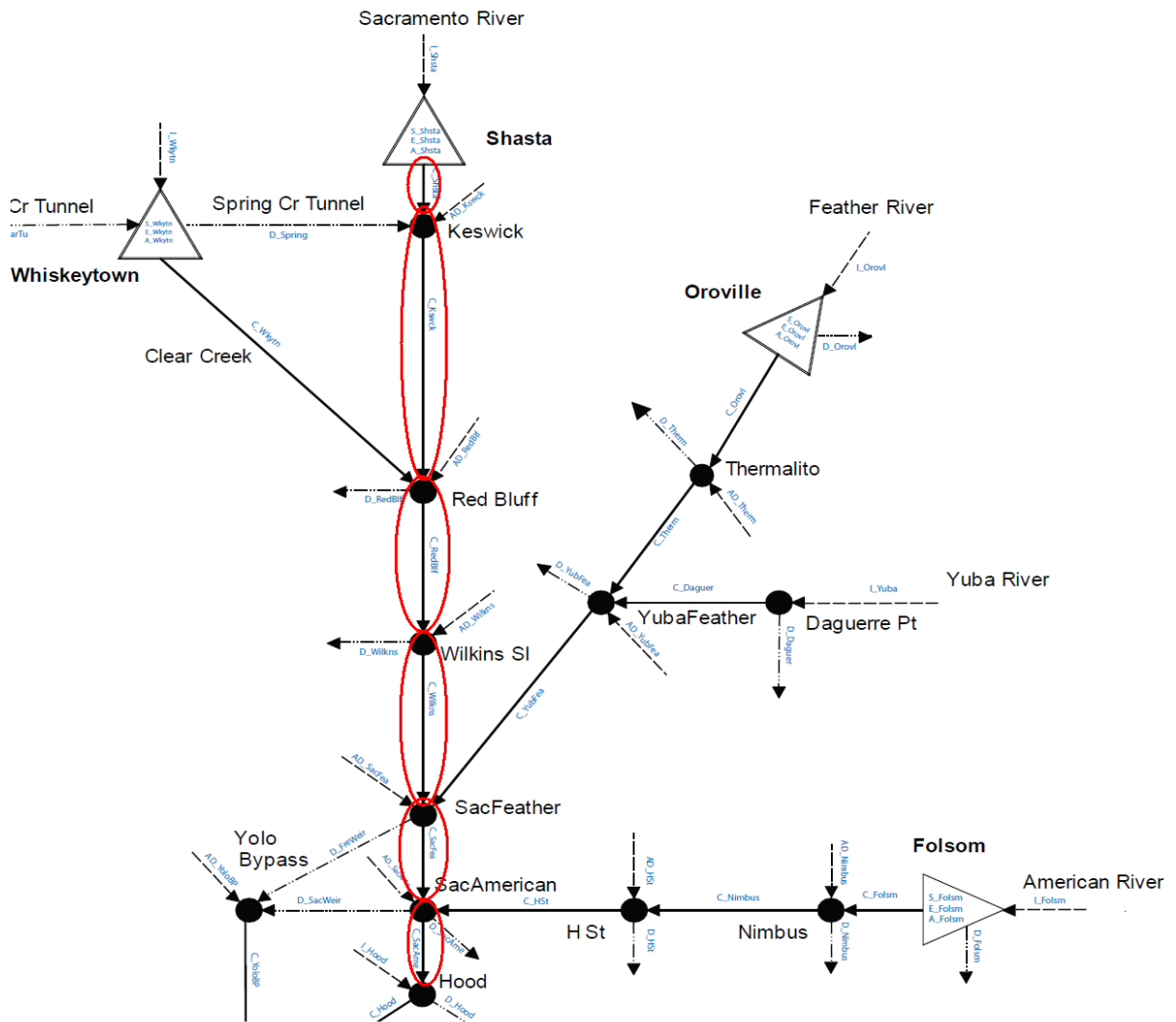


Figure 3. Study area of Sacramento River in CalLite. Channels circled in red.

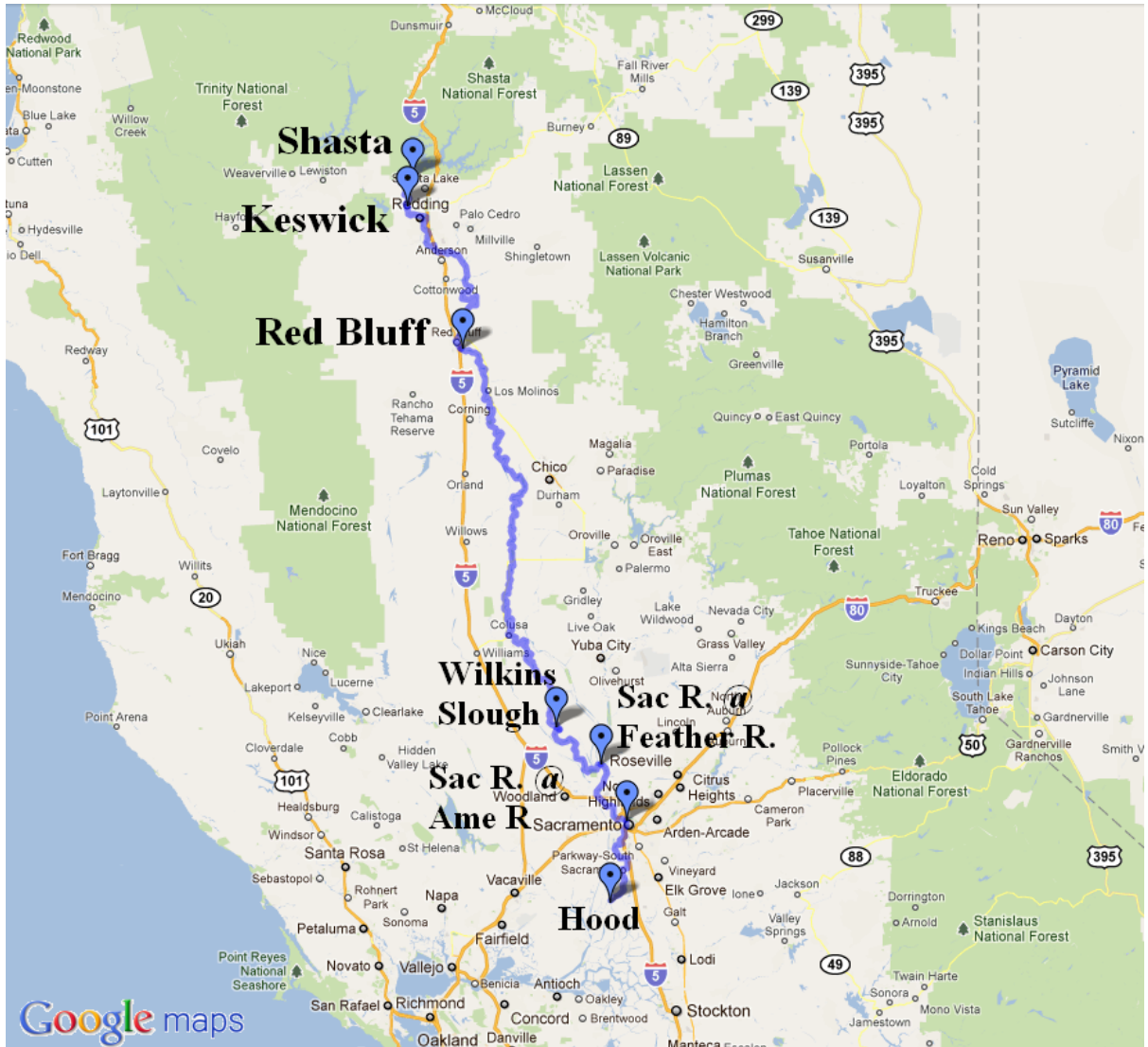


Figure 4. Study area of Sacramento River on Northern California Map from Google Maps

4.2. DATA COLLECTION AND WARMF MODEL

Daily outputs for the 72 year time period that CalLite simulates are desired. However, CalSim and CalLite are monthly models so all the hydrologic inputs cannot be easily disaggregated to a daily basis. Observed data from sources such as CDEC, Reclamation's dam operation reports, and USGS gage stations are incomplete in some areas and nonexistent for important nodes north of Red Bluff. Also there is a problem of mass balance in determining flow's origins above gage stations. A simulation model with water accounting and routing flows for all areas in the Sacramento basin for a historical dataset at a daily time step is needed. Few such models exist. The Army Corps' UNET model and DWR and National Weather Service's NWSRFS models are designed primarily for floods at much smaller time scales and reaches. The WARMF model has the appropriate duration and scale (Figure 5).

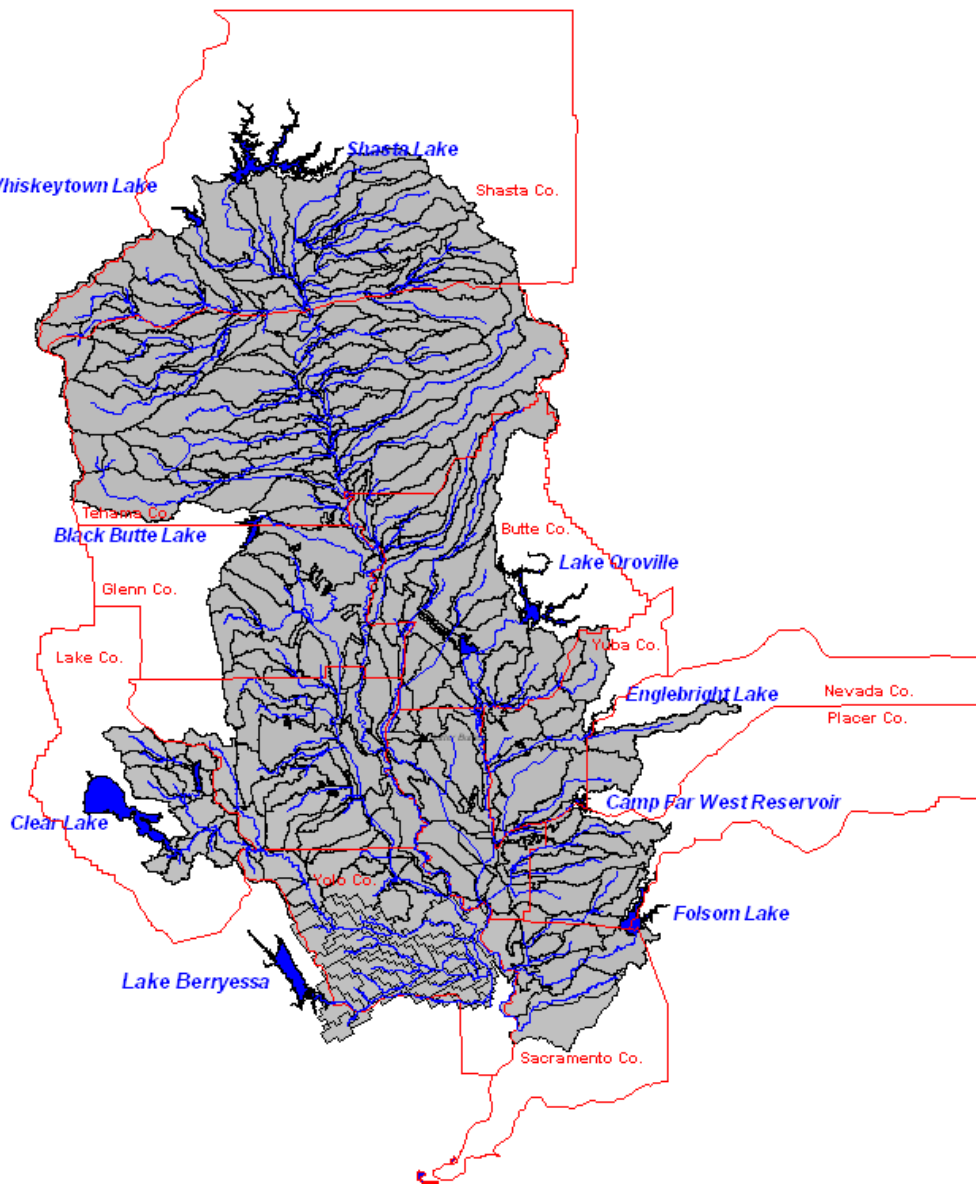


Figure 5. WARMF Interface

4.2.1 *WARMF Background and Routing Procedure*

WARMF is a model developed by Systech for satisfying the Environmental Protection Agency's (EPA) Total Maximum Daily Load (TMDL) allocation and analyses (Goldstein, 2001). It uses a watershed approach to model pollutants for water quality limitation sections (WQLS). The model can include point and nonpoint source discharges throughout a watershed system. In addition to pollutant tracking, WARMF has its own hydrology developed for each of its watersheds. For this study, the Sacramento WARMF Watershed will be used.

The creators of WARMF claim that for every reach in its watershed a kinematic wave approach is used to route the flows. Upon closer inspection, WARMF actually uses a derived form of Manning's equation combined with the mass balance equation (see section 3.2) and solves the two equations iteratively (Goldstein, 2001).

$$O_m = \frac{D^{2/3} \cdot S^{1/2} \cdot A_s}{n} \quad \text{eq. 32}$$

O_m is the Manning's outflow, D is the depth (Area/Wetted Perimeter [L]), S is the slope, A_s is the surface area of the river segment, and n is Manning's roughness coefficient. For English units, a multiplication factor of 1.49 is used.

4.2.2 *Data Collection from WARMF Model*

Every stream segment in WARMF is based on the mass balance continuity equation; changes in storage equal inflows minus the outflows. Inflows to a stream segment include outflow from upstream river segments, outflow from upstream reservoirs, local inflow from surrounding land catchments, and inflow from point sources. Local inflows include both subsurface (groundwater infiltration) and overland flow. Input parameters for WARMF include elevation change, Manning's n , reach profile, point sources, and diversions as flow time series. Output from WARMF includes stream flow for every reach as a time series, corresponding velocities and depth, and catchment runoff. Unfortunately storage change and channel inflows are computed internally and are unavailable for viewing (Goldstein, 2001). Using all of these data, a time series for accretions and depletions can be calculated for each reach to account for gains and loss of water.

4.2.3 *Data Compilation from WARMF Model*

Watershed hydrology is a primary part of a watershed network model. WARMF may have simulated stream flow results for every reach river segment, but the model itself may be incomplete. However, due to lack of available data and time constraints for collecting data, this study assumes that the WARMF hydrology is generally correct for the Sacramento watershed. Even with knowledge of how the general system is supposed to behave, there are many uncertainties in its computation and use of stream flows. This issue will be addressed further in the discussion section.

Since reaches in WARMF do not correspond to the CalLite schematic, simplifications to the WARMF data are needed to represent longer reaches in a channel. Each reach in WARMF along the Sacramento River from Shasta to the most southern channel (assumed to be near Hood and the Delta Cross Channel) were compiled into a spreadsheet with corresponding reach properties. Using a Visual Basic 6 (VB6) script, the

reach properties were combined by weighted average to create a representative CalLite channel (Appendix A). A second FORTRAN script creates relationship tables based on Manning's equation and Muskingum coefficients from the Muskingum-Cunge equations. Median flow values taken from WARMF simulations are used for the reference flows. Delta t values were chosen such that they would yield single reaches or few subreaches for routing and were divisible evenly by 24 hours for easier calculations.

Table 2. Channel characteristics

Channel	Qref (cfs)	Length (ft)	Width (ft)	Area (sq ft)	K (hrs)	X	Δt (hrs)
C_Shsta	10,431	123,270	93	889	2.32	0.43	2
C_Kswck	10,737	232,476	197	1,577	7.63	0.46	8
C_RedBlf	10,737	811,467	322	3,295	56.22	0.43	24
C_Wilkns	10,737	53,210	350	3,406	3.86	0.30	4
C_SacFea	19,791	107,878	547	7,486	9.84	0.24	8
C_SacAme	23,795	76,961	753	13,140	10.1	0.20	12

The remaining hydrology is a combination of rim inflows and accretion and depletion time series. Rim flows are taken from USGS gage stations and are used as reservoir releases. Flow accretions and depletions (AD) are calculated manually by adding the upstream inflows into a reach, point sources, and catchment inflows and subtracting any diversions. Each CalLite reach has a corresponding AD time series that is added at the beginning of the reach. Weir flows are included as time series integrated into the AD terms for simplification.

4.3. MODELLING APPROACH

There are many approaches to consider when implementing channel routing in a linear programming network operations model. Two issues need to be addressed, routing and optimization. Routing is the application of formulas to simulate an outflow hydrograph in a channel. Optimization involves the use of linear equations and solving an objective function for the maximum or minimum value. Also included in the formulation of linear equations is the issue of minimum inflow regulations. The general question is *how does an upstream reservoir to release the appropriate amount of water days before the water is needed for a downstream requirement?*

Two general ideas are linking to an external dll or using WRESL code while optimizing over multiple time steps. The idea of the dll is that the routing can be done iteratively outside of the WRIMS software and have those values relayed back in. No optimization occurs in a dll and coupled with the restrictive nature of passing and receiving large datasets, this idea may not be easy to implement. The second idea would use WRESL code without iterative processes. To do this, a channel will be defined to have inflow and outflow decision variables. The storage can be calculated from the change in outflow and inflow added to the previous day's storage level. The code will address the issues of flood routing, meeting delta salinity flows, and meeting minimum in-stream flows discussed at the beginning of the paper. A similar implementation of optimizing over multiple time steps is used in FCLP, but uses iterative processes (Jones, 1997).

4.3.1 *Scenarios and Hydrology*

Three categories of routing methods will be assessed: coefficient routing, storage routing and lag routing. For each routing scheme, three sets of tests are performed: a flood wave test, delta outflows test, and minimum in stream flow test. For the Muskingum and storage routing methods, two sets of coefficients will be used, one based on the equations from HEC's hydraulic manual (USACE, 1993) and the other based on optimum coefficient values described in the next section.

The initial test involves an input pulse flood wave from January 1980 Shasta Reservoir outflow, in the wet season. The pulse is routed using WRIMS for all the methods as well as a separate HEC-RAS model using the same bathymetry (USACE, 2010). HEC-RAS is a hydrodynamic 1-D model. It uses hydraulic routing to compute flows, depths, and velocities for channels given user defined bathymetry. To test the routing methods using WRIMS model, a comparison study will be the first test. The RAS model uses the same channel inputs as the WARMF model including cross section, channel length, and elevation data. The flow at each of the corresponding Callite locations can be measured and used as a reference value. The upstream boundary condition consists of a 5 day pulse flow hydrograph. The inflow hydrograph period is for two months with the base flow set at 10,000 cfs. At the beginning of the second month the flow increases to 20,000 cfs for 5 days and then recesses back to 10,000 cfs for the remainder of the run to isolate the flood wave. WARMF output using the same conditions are also presented for comparison.

The delta outflows portion focuses on using rim inflows, accretion/depletion inputs from WARMF, and an allocation based script in WRESL to assess how well each method makes allocations for future demands. The Delta has strict guidelines for specific times of the year to manage salinity. To simulate this type of regulation, a downstream time series acts as a demand. It is required to be met with releases from previous days from Shasta, which will be routed along the Sacramento River channels.

The last part deals with minimum in-stream flows. These apply to many streams in the upper portion of the Sacramento River. The hydrology inputs are the same as the delta outflow test. Minimum in-stream flows must be kept for environmental factors and are regulated by reservoir releases. Like the delta salinity test, a second demand time series is added at for the Keswick channel outflow. In this case, two competing demands must be met, one downstream to the Delta and the other upstream near Red Bluff.

4.4. MODEL CALIBRATION

4.4.1 *Muskingum, Coefficient Routing Application and Sensitivity*

Muskingum coefficients are derived from the Muskingum-Cunge equation. This follows the Army Corps manual for implementing Muskingum routing in HEC FCLP (USACE, 2000). Using the observed rim flows as reference flow values, the coefficients for K, X as well as the number of subreach and time steps are necessary. In some cases reaches that did not meet the constraints in the Muskingum coefficient guidelines were disaggregated to find suitable number of subreaches, time step interval, and K values (Tables 2 & 3).

Table 3. K, X, and Δt coefficients from HEC Manual based Formulas

Channel	Muskingum Parameters					
	K (hrs)	X	Δt (hrs)	C0	C1	C2
Shasta	2.19	0.456	2.00	0.000	0.912	0.088
Keswick	7.13	0.439	8.00	0.109	0.891	0.000
Red Bluff	26.00	0.462	24.00	0.000	0.923	0.077
Wilkins	3.53	0.433	4.00	0.119	0.881	0.000
SacFea	8.52	0.178	8.00	0.225	0.502	0.273
SacAme	8.88	0.000	8.00	0.311	0.311	0.379

The use of subreaches involves using iterations to loop through the subreaches, route flows through the reaches and averages them to find the final outflow through the entire reach. However, since iterations of this sort are not possible in WRIMS, values for dt are chosen that yield the fewest subreaches. Only Red Bluff was broken into two subreaches with the time interval being the same as the model time step of one day. The remaining channels used only a single reach. For channels with time steps less than one day, multiple iterations are run, which are written out as separate decision variables explicitly. The iterations run the required number of times to be the equivalent of 24 hours time elapse with the inflows being held constant and the outflows averaged for daily aggregation. Mass balance calculations and were done to ensure that the routing application was sound.

Two other sets of variable values were also chosen using WARMF and HEC-RAS output for calibration (Tables 4 & 5). The values were constrained to fall within the bounds of the Muskingum parameters and found using solver in Excel.

Table 4. K, X, and Δt coefficients from WARMF calibration

Reach	K(hrs)	X	Δt (hrs)	C0	C1	C2
Shasta	5.92	0.17	2	0.000	0.338	0.662
Keswick	9.44	0.03	8	0.283	0.325	0.392
Red Bluff	33.54	0.00	24	0.264	0.264	0.473
Wilkins	7.65	0.00	4	0.207	0.207	0.585
Sac Fea.	9.46	0.00	8	0.297	0.297	0.406
Sac Ame.	4.82	0.00	8	0.453	0.453	0.093

Table 5. K, X, and Δt coefficients from HEC-RAS calibration

Reach	K(hrs)	X	Δt (hrs)	C0	C1	C2
Shasta	5.23	0.00	2	0.161	0.161	0.679
Keswick	11.67	0.06	8	0.220	0.315	0.465
Red Bluff	40.73	0.11	24	0.156	0.342	0.502
Wilkins	6.70	0.00	4	0.230	0.230	0.540
Sac Fea.	12.50	0.00	8	0.242	0.242	0.515
Sac Ame.	4.00	0.00	8	0.500	0.500	0.000

To better understand the effects of the three sets of variables, a simple sensitivity analysis was performed on the Muskingum variables K, X, and Δt. Tables 6 through 8 use the first channel, Shasta, as a base, the variables were varied one by one and the effect on the outflows compared. K and Δt were varied from 1 to 24 and X from 0.1 to 0.5. The previous flows are set at 10,000 cfs and the current inflow is at 20,000 cfs. The percent

change in the variable is compared to the base values of Shasta in table 3. The percent error is the difference in the changed variable output to the output value from using the base. Figure 9 compares the percent change to error for each variable. The variable X has the most drastic effect on the outflow compared to Δt and K. When K and Δt are changed by 100%, the effect on the outflow is around 30% as opposed to the 80% difference caused by changing X by that same amount. A ratio exists between K to Δt . If the ratio and value of X are kept constant, K and Δt can be changed such that output value will not change.

Table 6. Muskingum sensitivity by varying K

K (hrs)	X	Δt (hrs)	C0	C1	C2	Peak Outflow	% Change	% Error
2.19	0.456	2.00	0.000	0.912	0.088	10,000	-	-
1.00	0.456	2.00	0.352	0.943	-0.295	13,524	54%	35%
2.00	0.456	2.00	0.042	0.915	0.042	10,423	9%	4%
3.00	0.456	2.00	-0.140	0.899	0.240	8,604	37%	14%
4.00	0.456	2.00	-0.259	0.889	0.370	7,408	82%	26%
6.00	0.456	2.00	-0.407	0.876	0.531	5,932	174%	41%
8.00	0.456	2.00	-0.494	0.868	0.626	5,056	265%	49%
12.00	0.456	2.00	-0.594	0.859	0.734	4,064	447%	59%
24.00	0.456	2.00	-0.707	0.849	0.858	2,930	994%	71%

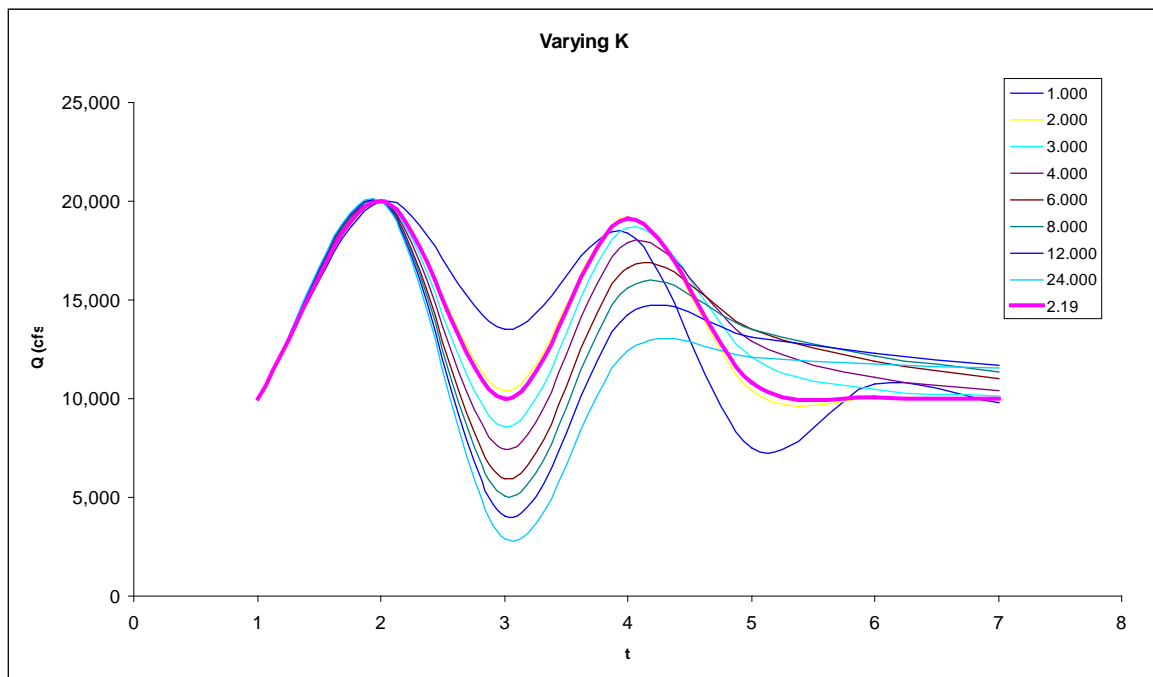


Figure 6. Plot of Muskingum sensitivity by varying K. The bolded pink line is the base case.

Table 7. Muskingum sensitivity by varying X

K (hrs)	X	Δt (hrs)	C0	C1	C2	Peak Outflow	% Change	% Error
2.19	0.456	2.00	0.000	0.912	0.088	10,000	-	-
2.19	0.100	2.00	0.262	0.410	0.328	12,624	78%	26.24%
2.19	0.200	2.00	0.204	0.522	0.274	12,037	56%	20.37%
2.19	0.300	2.00	0.135	0.654	0.211	11,348	34%	13.48%
2.19	0.400	2.00	0.053	0.811	0.137	10,529	12%	5.29%
2.19	0.500	2.00	-0.046	1.000	0.046	9,538	10%	4.62%

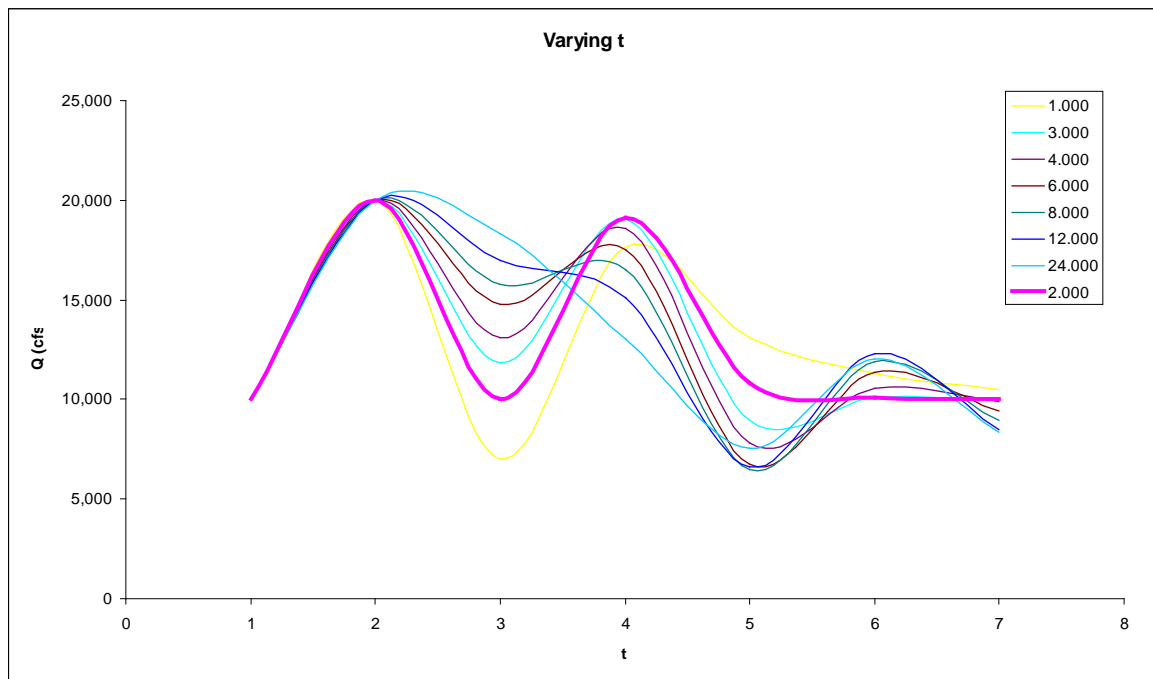


Figure 7. Plot of Muskingum sensitivity by varying Δt . The bolded pink line is the base case.

Table 8. Muskingum Sensitivity by varying Δt

K (hrs)	X	Δt (hrs)	C0	C1	C2	Peak Outflow	% Change	% Error
2.19	0.456	2.00	0.000	0.912	0.088	10,000	-	-
2.19	0.456	1.00	-0.295	0.886	0.410	7,048	50%	29.52%
2.19	0.456	3.00	0.186	0.928	-0.114	11,856	50%	18.56%
2.19	0.456	4.00	0.313	0.939	-0.252	13,131	100%	31.31%
2.19	0.456	6.00	0.477	0.954	-0.431	14,769	200%	47.69%
2.19	0.456	8.00	0.578	0.963	-0.540	15,776	300%	57.76%
2.19	0.456	12.00	0.695	0.973	-0.668	16,950	500%	69.50%
2.19	0.456	24.00	0.834	0.985	-0.819	18,337	1100%	83.37%

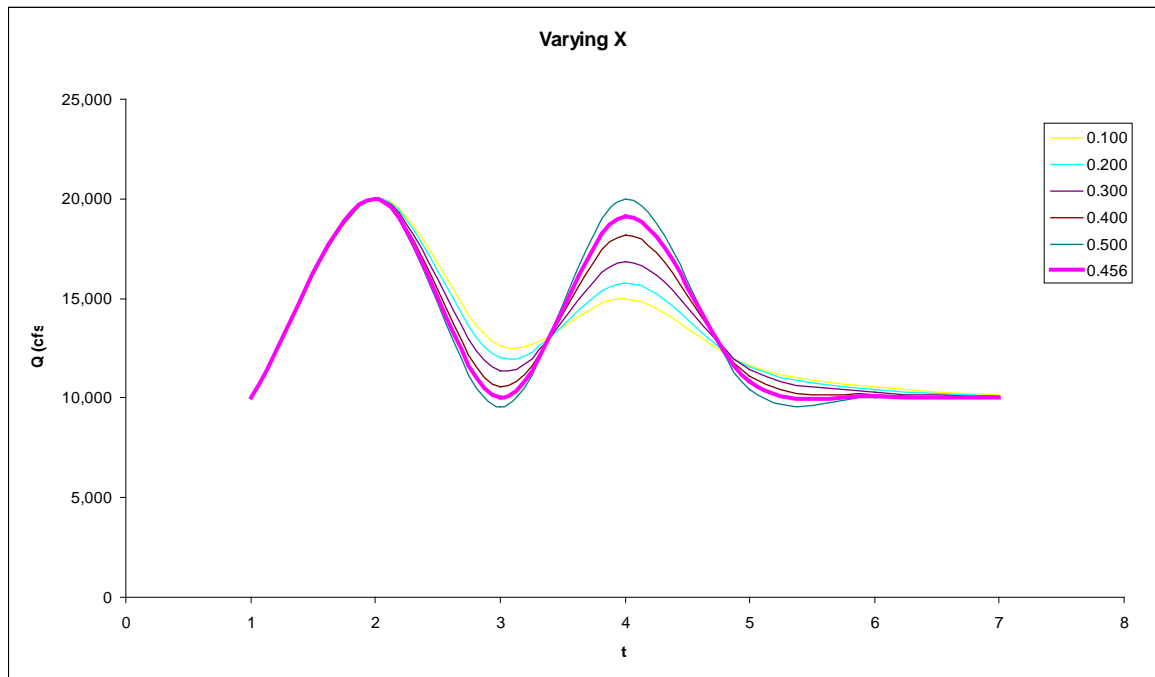


Figure 8. Plot of Muskingum sensitivity by varying X. The bolded pink line is the base case.

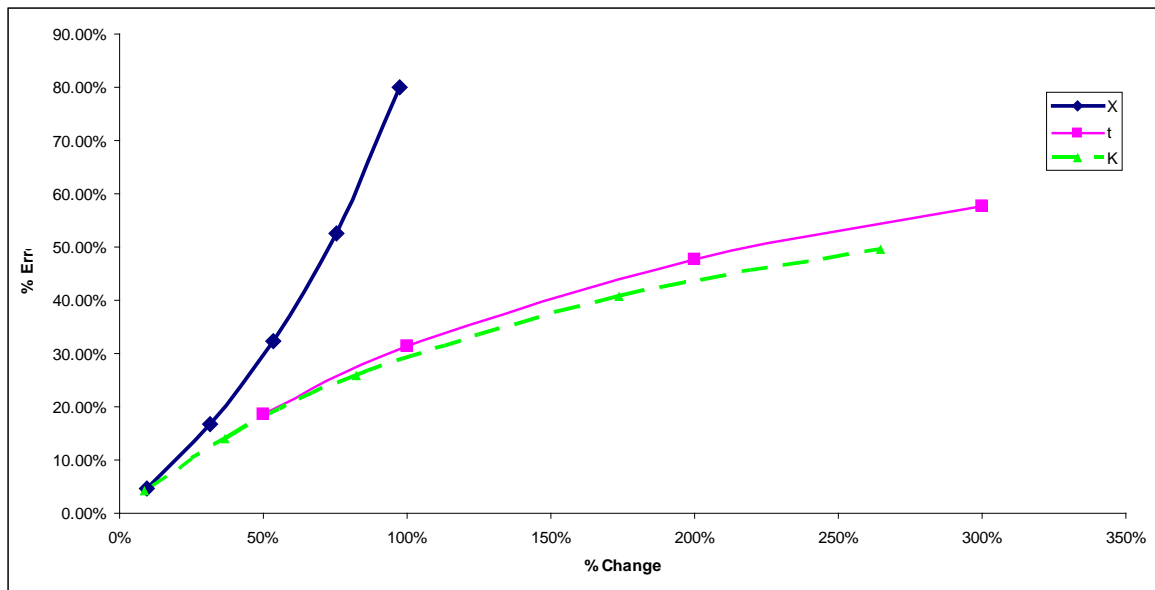


Figure 9. Muskingum variable error for X, t, and K

4.4.3 Storage Routing Application and Sensitivity

Storage routing relationships were derived from the Manning's equation with physical parameters taken from WARMF. The reaches were assumed to be triangular for simplification and due to the high flows in every reach. The same Δt parameter is used for the Muskingum method are used for coefficient storage routing for consistency (Table 9). This reduces the number of necessary iterations, which originally was thought to have decreased accuracy, but discovered later to have little effect except to make the model run faster. By having a fixed C, it is assumed that no rating curve will be used meaning that

the storage outflow relationship is constant and not variable. This simplification was necessary due to the lack of time to develop accurate rating curves for each channel.

Table 9. K, Δt , and C coefficients from HEC Manual based Formulas

Channel	Storage		
	K	Δt	C
Shasta	2.37	2	0.593
Keswick	9.69	8	0.585
Red Bluff	34.05	24	0.521
Wilkins	5.29	4	0.548
SacFea	13.34	8	0.461
SacAme	8.52	8	0.639

Similarly with the Muskingum scenario, two sets of variables based off of WARMF and HEC-RAS output was tested using storage routing (Tables 10 & 11).

Table 10. K, Δt , and C coefficients from WARMF calibration

WARMF	K	Δt (hrs)	C
Shasta	5.98	2.00	0.286
Keswick	10.59	8.00	0.548
Red Bluff	34.05	24.00	0.521
Wilkins	7.65	4.00	0.414
Sac Fea.	9.63	8.00	0.587
Sac Ame.	4.82	8.00	0.907

Table 11. K, Δt , and C coefficients from HEC-RAS calibration

WARMF	K	Δt (hrs)	C
Shasta	2.37	2.00	0.593
Keswick	9.69	8.00	0.585
Red Bluff	34.05	24.00	0.521
Wilkins	5.29	4.00	0.548
Sac Fea.	13.34	8.00	0.461
Sac Ame.	8.52	8.00	0.639

A sensitivity analysis was performed on K and Δt variables based on the Shasta variable values in Table 9. The previous flows are set at 10,000 cfs and the current inflow is at 20,000 cfs. Tables 12 and 13 vary K and Δt from 1 to 24. The new routing coefficient is calculated and the effects on the outputs are measured.

Table 12. Storage Routing Sensitivity by varying K

K	Δt	C	Output	% Change	% Error
2.19	2	0.626	13,131	-	-
1.00	2	1.000	15,000	54%	14%
2.00	2	0.667	13,333	9%	2%
3.00	2	0.500	12,500	37%	5%
4.00	2	0.400	12,000	82%	9%
6.00	2	0.286	11,429	174%	13%
8.00	2	0.222	11,111	265%	15%
12.00	2	0.154	10,769	447%	18%
24.00	2	0.080	10,400	994%	21%

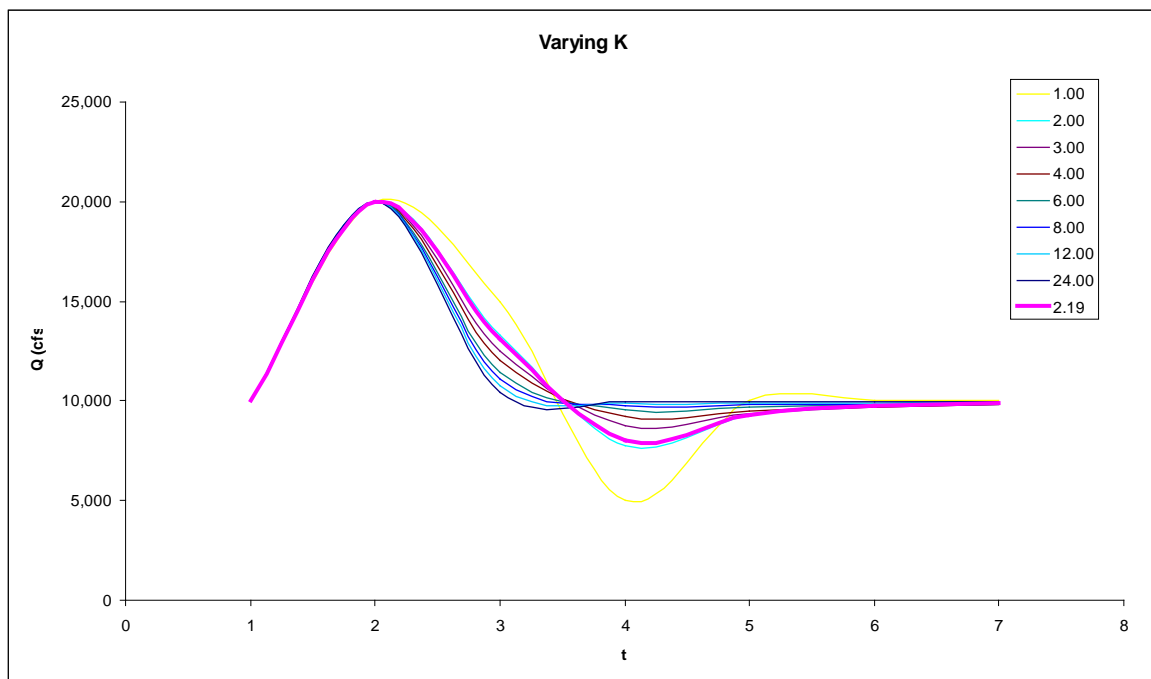


Figure 10. Plot of storage routing sensitivity by varying K. The bolded pink line is the base case.

Table 13. Muskingum Sensitivity by varying Δt

K	Δt	C	Output	% Change	% Error
2.19	2	0.626	13,131	-	-
2.19	1	0.371	11,856	50%	10%
2.19	3	0.812	14,061	50%	7%
2.19	4	0.954	14,769	100%	12%
2.19	6	1.155	15,776	200%	20%
2.19	8	1.292	16,458	300%	25%
2.19	12	1.465	17,323	500%	32%
2.19	24	1.691	18,454	1100%	41%

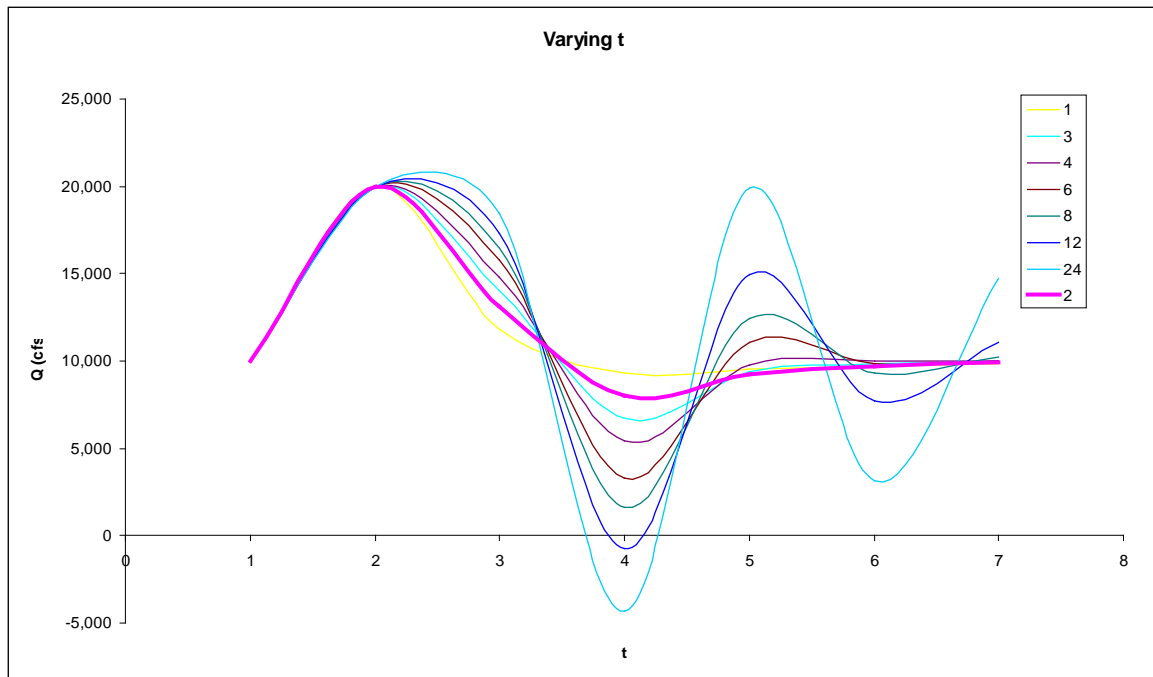


Figure 11. Plot of storage routing sensitivity by varying K. The bolded pink line is the base case.

In Figure 12, the percent change in the variable is plotted against the error of the output. The Δt variable has the larger effect on the outflow than the K variable. However, the range of the error is very similar for small changes in either of the variables and it takes a drastic change in either variable to alter the outflow by 25%. In comparison to the Muskingum variables, the storage variables are less sensitive to changes in its variables. This implies that the range of outputs is smaller for the storage routing method than the Muskingum method.

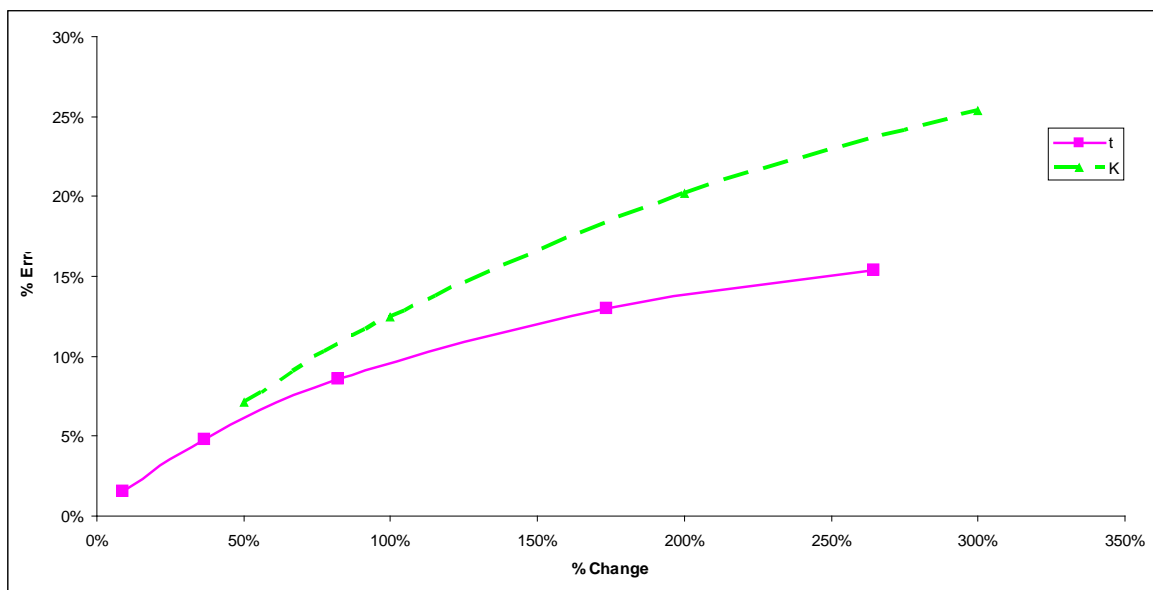


Figure 12. Storage variable error for t and K

4.4.4 Lag Routing Application

The lag coefficients, estimated using the successive average-lag method, are simple when each channel contains at most one or two subreaches. The coefficients used are listed (Table 14) and are averages of the current and previous day inflows. Generally there is little attenuation and translation effects are the biggest factor in the producing the outflow hydrograph.

This study only looks at the successive average-lag method, although many variations of Lag type routing exist. This method will serve as a general baseline routing method for the more complex Muskingum and storage routing methods due to being a more empirically based routing method.

Table 14. Lag Reach parameters

Channel	Lag		
	C0	C1	C2
Shasta	0.5	0.5	0
Keswick	0.5	0.5	0
Red Bluff	0.25	0.5	0.25
Wilkins	0.5	0.5	0
SacFea	0.5	0.5	0
SacAme	0.5	0.5	0

4.4.4 Forecasting

The delta flows and minimum in-stream flows part of this study involve forecasting. Forecasting is needed to predict downstream conditions ahead of time to make release decisions. Channel routing is an upstream to downstream process, but the upstream reservoir releases are governed by downstream predictions. Using the flood routing portion of this study by matching the peak flow downstream of a single upstream pulse, a 2-3 day forecast was found to be needed. The basic idea is for every time step, there is a main routing that occurs in real time for every reach. In addition, parallel systems of releases occur using the values of the main routing system as inputs (Figure 13). This creates the illusion of multiple time steps occurring in a single time step to determine the downstream conditions for a window of time. WRIMS is unable to use multiple time steps and can use only a daily or monthly time step. To do routing at the hourly scale, all iterations must be written out explicitly along with separate decision variables, which can then be aggregated and averaged (Figure 14). The last outflow from the last day parallel system is used to control release from the main system. In this way there are actually multiple releases occurring on a given day, each assigned the same value to represent equal weighting for current and future releases. However, only the release from the main routing system is important since the remaining parallel releases are recalculated at the next time step.

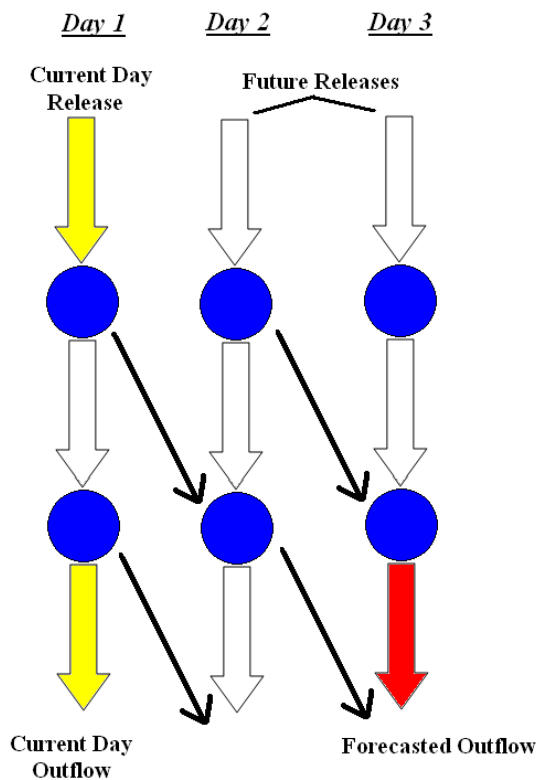


Figure 13. Example parallel system of releases. The red forecasted outflow is computed based on the yellow current day release value. Using a known time series for perfect foresight, the forecasted outflow is set to be greater than the corresponding time series value that is 3 days later. The solver backtracks to find the optimal current day release on day 1.

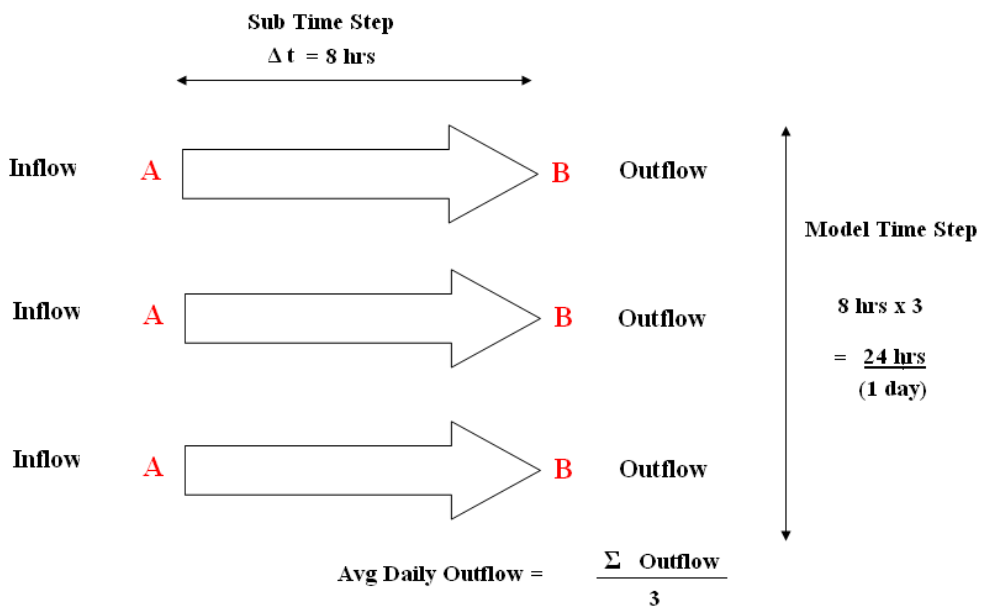


Figure 14. Example aggregation and averaged daily flow for a single channel of $\Delta t = 8$ hours from point A to B. The routing is performed 3 times using the same inflow value and previous (arrow above) outflow value.

Chapter 5 RESULTS AND DISCUSSION

5.1. OVERVIEW

This chapter is organized into the four sections. Sections 2 through 4 present the findings from the three test cases for flood channel routing, outflows to delta optimization, and minimum inflows optimization. A select few graphs are presented in the results section and the remainder can be found in Appendix C. Section 5 discusses and summarizes the findings as well as problems encountered in this study. Finally there is a brief word about model run time pertaining to expanding the methods used here to a larger scale model.

5.2. FLOOD CHANNEL ROUTING TEST

The first test is to see what a single “pulse” inflow hydrograph would look like when routed downstream. This helps assess an appropriate forecast length for each routing method. The test also allows for some general insight as to how each routing method will behave when using the linear solver. The pulse is a five day continuous release of 20,000 from Shasta Reservoir and then drops abruptly to the base flow of 10,000 cfs for the remainder of the testing period.

A summary of the statistics of the Shasta channel is shown in Table 15. The total volume begins at 3074 taf over 7 days. The peak flow day is based on using the WARMF calibrated coefficients. At first it seems there is some variation in the peak flow date, but this is the furthest upstream channel so it simply reflects tiny changes in the initial pulse flow. This can be seen in Figure 15, Figure 16, and Figure 17, which show inflow and outflow hydrographs for the Shasta reach under WARMF, RAS, and theoretical calibrated variable settings respectively. The Input, WARMF outflow, HEC-RAS outflow, and lag outflow are the same in the three figures and are present for baseline comparisons. The Muskingum and storage routing methods can be closely fit to both the WARMF and HEC-RAS hydrographs using arbitrary coefficients. However, when applying the HEC hydraulics based equations for K , X and Δt , the outflows lie in between the WARMF and HEC-RAS outflows.

The statistic summary table for the Sacramento River at American River channel (SacAme) is presented in Table 16 with the peak flow day based off of the WARMF calibrated coefficients. The volume at the end is the same for the Muskingum, storage, and lag routing methods as the volume of the inflow at Shasta. This is expected because they are all based off the continuity equation. The final volume of HEC-RAS outflow is lower by 159 cfs, about 5%. This can be attributed to it being a hydraulic model and includes bathymetry information for each reach whereas the other methods, including WARMF, are hydrologic based and simply lump the bathymetry as part of the routing coefficient. This means that water is stored in the river due to dips in elevation and profile differences, but hydrologic routing assumes that all the water eventually passes through each channel. Figure 18, Figure 19, and Figure 20 are the hydrographs for SacAme reach under WARMF, RAS, and theoretical calibrated variable settings respectively. The outflows are closely matched up to the WARMF and HEC-RAS outflow when the coefficients are calibrated to them. When using the HEC hydraulics based equations, the outflows are much tougher to match to either WARMF or HEC-RAS outflows. This is

because of the reliance of many variables and also choosing an appropriate reference flow, which is arbitrary. The reference flows used in this study are all based off the average flows for the respective channels, which is typical in many cases. However, the outflow is significantly different

Table 15. Flood routing test for Shasta channel summary table

	RAS	MUSK	STOR	LAG	WARMF
Avg (cfs)	15,556	15,555	15,555	15,556	15,555
Min (cfs)	10,000	10,010	10,011	10,000	10,010
Max (cfs)	20,000	19,998	19,998	20,000	19,998
Range (cfs)	10,000	9,988	9,987	10,000	9,988
Total Volume (taf)	3,074	3,074	3,074	3,074	3,074
Peak Flow Day	2	5	6	6	3

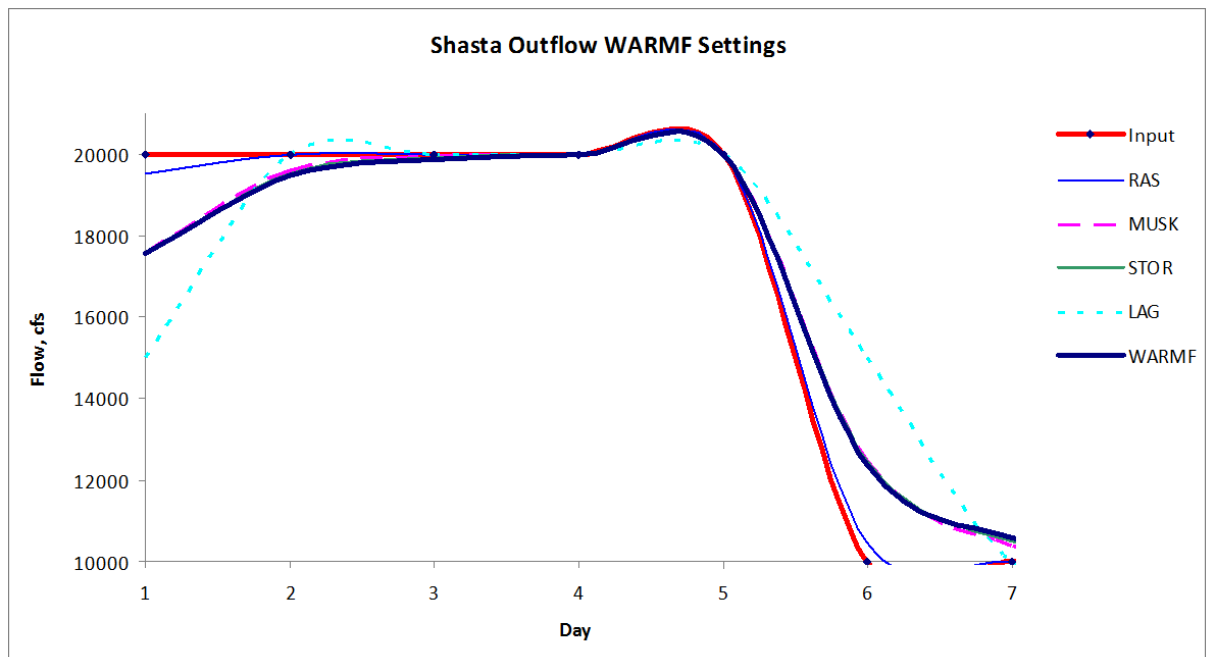


Figure 15. Outflow at Shasta for a 5 day release from Shasta Reservoir using WARMF calibrated coefficients

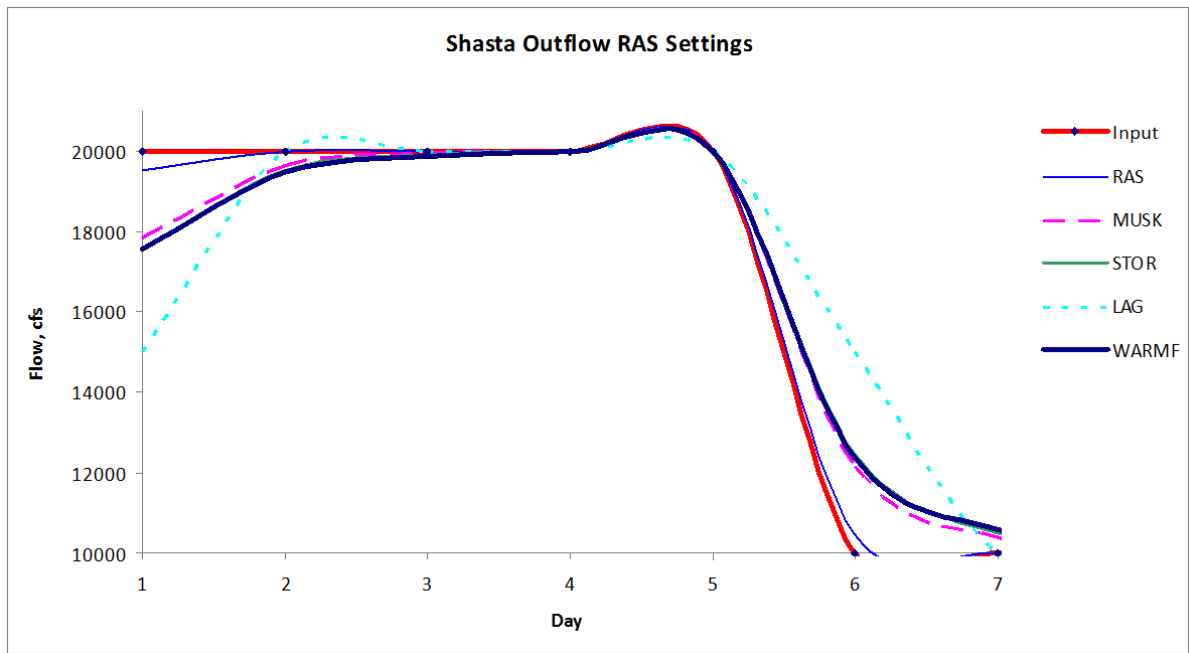


Figure 16. Outflow at Shasta for a 5 day release from Shasta Reservoir using HEC-RAS calibrated coefficients

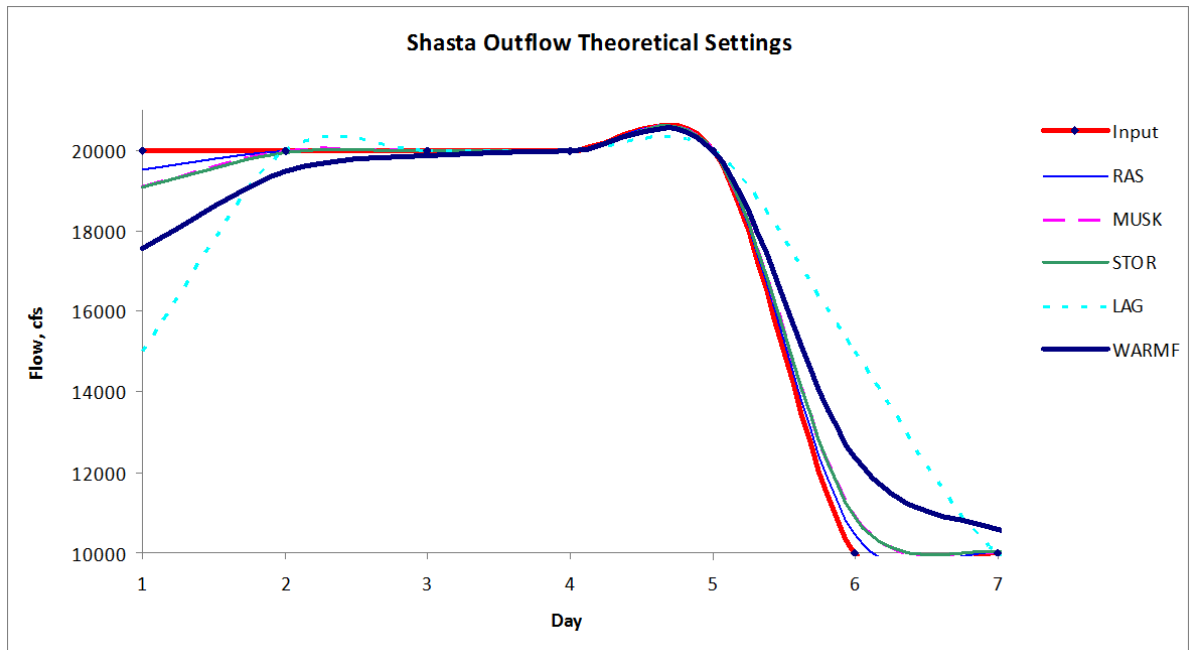


Figure 17. Outflow at Shasta for a 5 day release from Shasta Reservoir using HEC Hydraulics Manual calibrated coefficients

Table 16. Flood routing test for SacAme channel summary table

	RAS	MUSK	STOR	LAG	WARMF
Avg (cfs)	12,778	14,051	15,392	14,900	13,576
Min (cfs)	10,039	10,000	10,464	10,078	10,132
Max (cfs)	16,707	19,296	18,631	19,297	17,166
Range (cfs)	6,668	9,296	8,168	9,219	7,034
Total Volume (taf)	2,915	3,074	3,074	3,074	3,071
Peak Flow Day	8	7	7	6	7

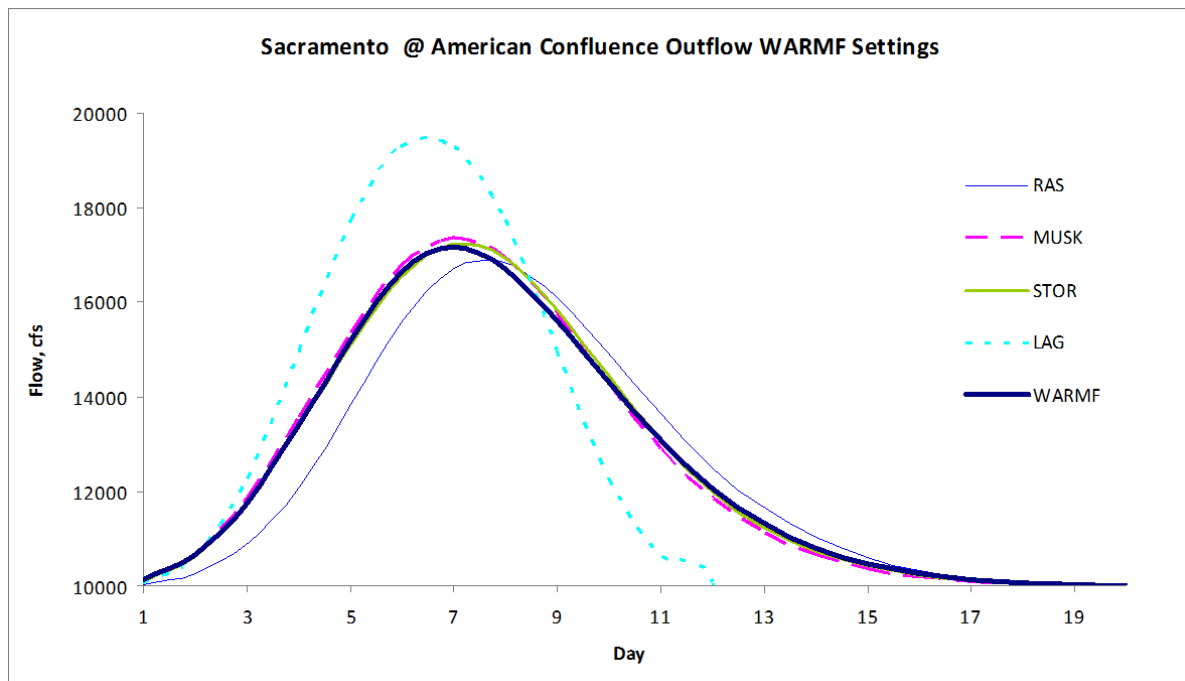


Figure 18. Outflow at Hood for a 5 day release from Sacramento River at American Confluence Channel using WARMF calibrated coefficients

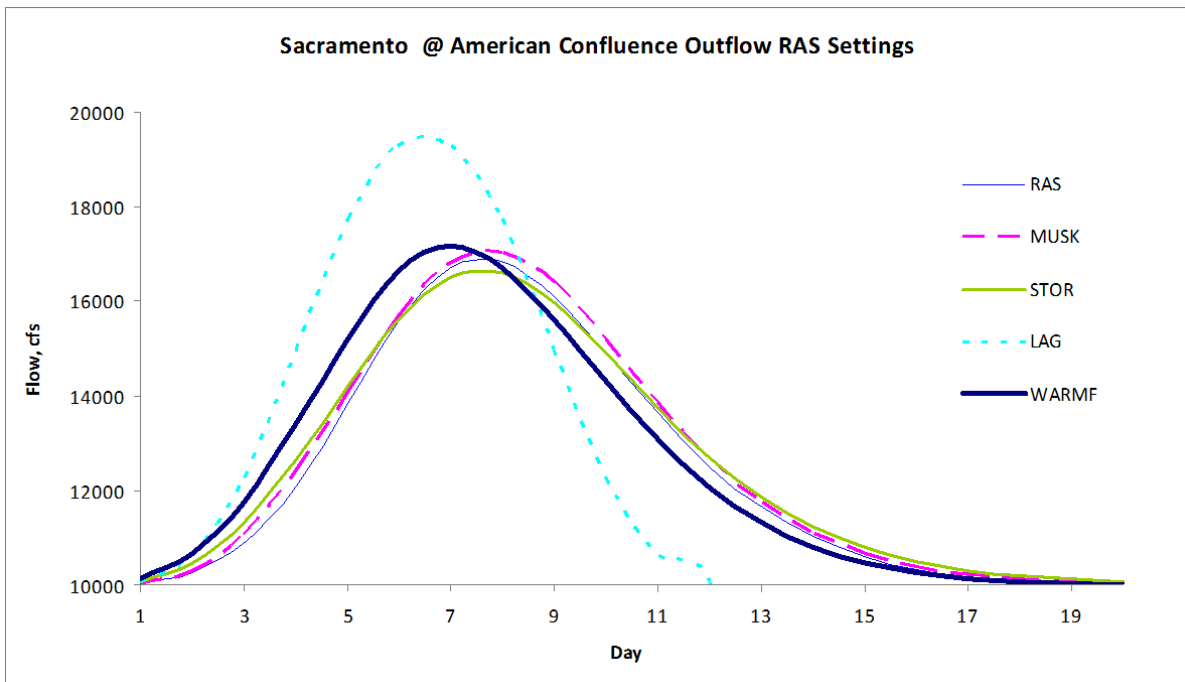


Figure 19. Outflow at Hood for a 5 day release from Sacramento River at American Confluence Channel using HEC-RAS calibrated coefficients

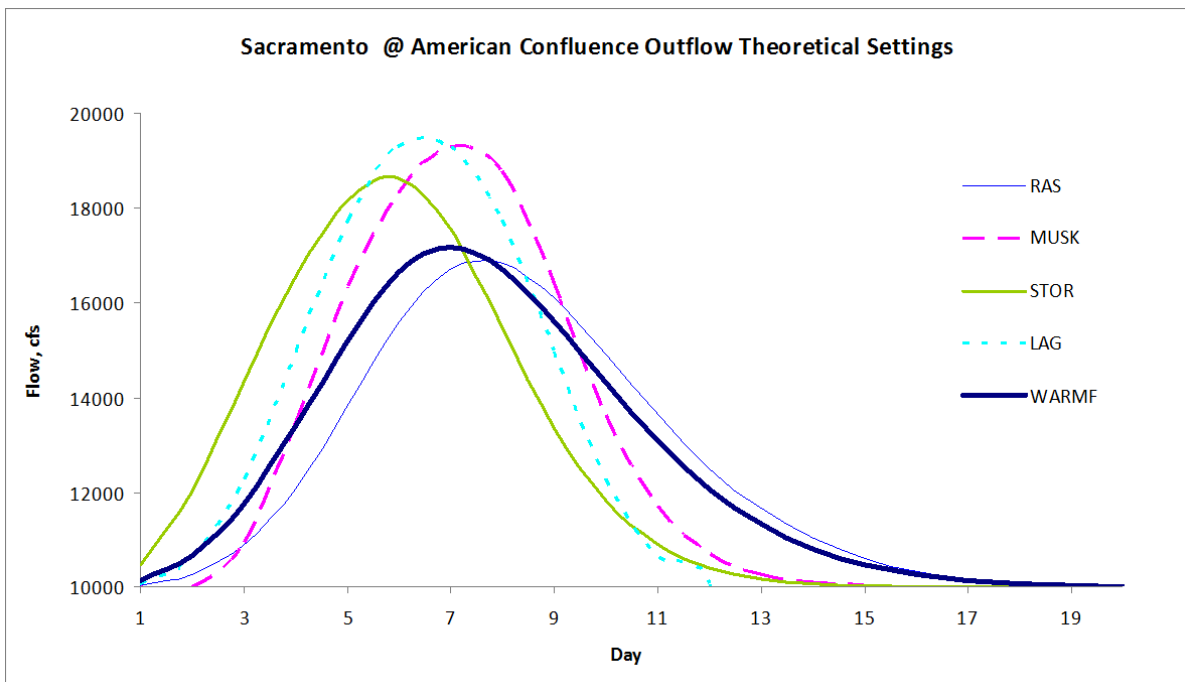


Figure 20. Outflow at Hood for a 5 day release from Sacramento River at American Confluence Channel using HEC Hydraulics Manual calibrated coefficients

5.3 OUTFLOWS TO DELTA OPTIMIZATION

Combining routing with the optimization solver using WRESL script is the main goal of this study. The solver will have to compute releases to meet a continuous downstream demand time series and is constrained by the routing rules. The models use a look-ahead forecast to see the demands for the next 2-3 days, depending on the model. Next they calculate the release for the next 2-3 days plus the current day to meet all demands and give equal weight to all releases. By incorporating runoff and diversions in accretion/depletion terms, the decision variable releases can be analyzed to learn more about the behavior of each routing method since outflows are expected to be similar. The objective of this test case is to be as close to the WARMF values as possible at the outflow to the Delta. In this way the models will be tested for how well it can match a fluctuating demand, which is typical of many minimum in-stream flow regulations. Since the downstream conditions are set the same for each model, it is useful to compare the releases from Shasta upstream. There is a lot of variation in the release amounts for all of the models.

The statistics for the downstream-most channel are shown in Table 19 and Table 20 for WARMF and theoretical calibrated coefficients respectively. The statistics, Figure 23 and Figure 24 yield similar numbers with the theoretically calibrated peak outflow slightly above that of the WARMF calibrated model. All the routing methods are able to reproduce similar target outflows downstream at the Delta based on a single constraint. The differences lie in the amount of water needed to be released to achieve the downstream target. This is accomplished by looking at the most upstream channel and seeing the pattern of flows coming down from Shasta in Figure 21 and Figure 22.

Using the WARMF flow as a baseline for comparison shows that there is a significant difference in the amount of water released from Shasta for each routing method and calibrations. There is a lot of fluctuation and no discernable trends can be drawn at first glance. However, in the entire model only one constraint drives the reservoir releases, which leaves the set of possible solutions very open ended. The ideal solution would emulate the WARMF flows and have steady releases of 10,000 cfs and 30,000 cfs. When the flows fluctuate, it means that the solver is choosing a solution where a large amount of water is released upstream, which may satisfy the downstream demand for a few days. In those next few days, a low flow is needed to meet the new demand because a large amount was released prior. Then when all the water is fully routed and exits the system a new large pulse is needed to repeat the process. Although the hydrographs are not ideal, they are correct solutions.

There are a many ways to correct for fluctuating decision variables including setting weights on the objective function, changing the coefficients, the time step, or the forecasting period. Another way is to set more constraints on the upstream reaches. Since not all these ideas can be pursued at this time, only the latter is pursued in the next section discussing an additional set of constraints upstream on the Keswick channel.

Table 17. WARMF calibrated Delta outflow routing test for Shasta channel

	WARMF	Musk	Stor	Lag
Avg (cfs)	17,810	18,639	20,327	21,349
Min (cfs)	6,405	1,419	134	1,421
Max (cfs)	36,465	39,668	64,111	57,033
Range (cfs)	30,060	38,249	63,977	55,612
Total Vol (taf)	33,948	35,528	38,745	40,695
Peak Day	17	22	23	12

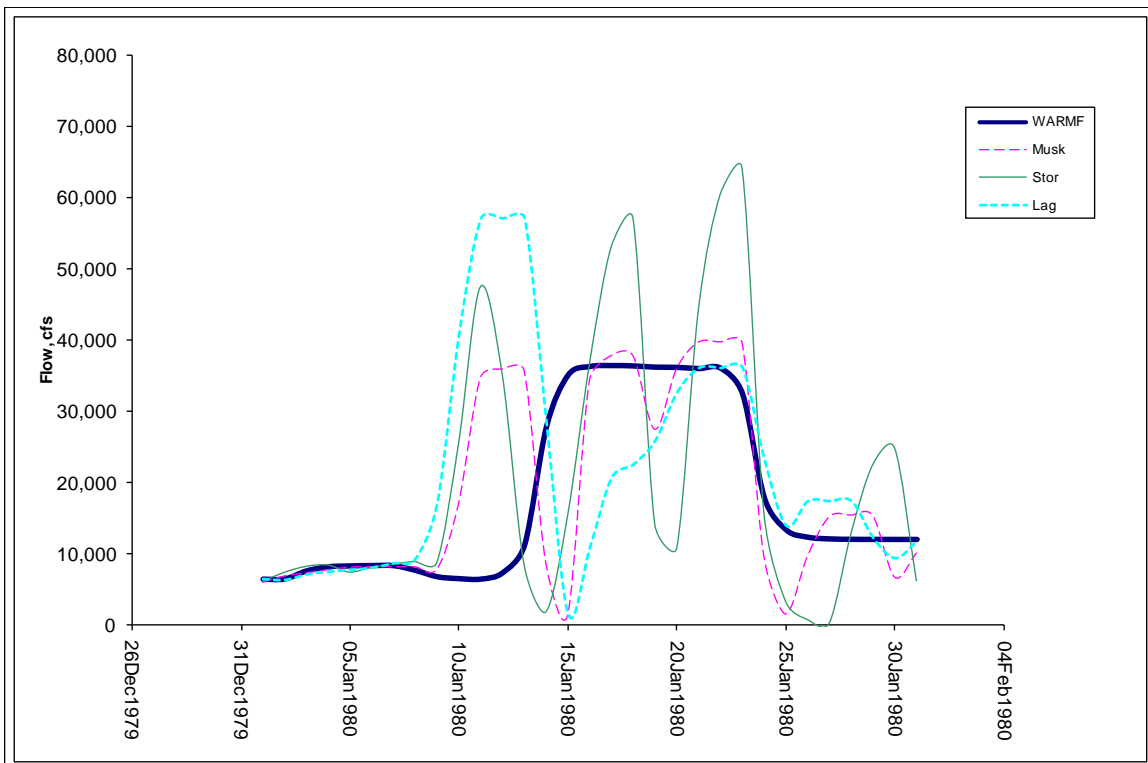


Figure 21. Outflow at Shasta channel for time series demand at the Hood using WARMF calibrated coefficients

Table 18. HEC hydraulics manual calibrated Delta outflow routing test for Shasta channel

	WARMF	Musk	Stor	Lag
Avg (cfs)	17,810	19,228	20,075	21,349
Min (cfs)	6,405	34	196	1,421
Max (cfs)	36,465	46,010	72,744	57,033
Range (cfs)	30,060	45,976	72,548	55,612
Total Vol (taf)	33,948	36,650	38,265	40,695
Peak Day	17	11	11	12

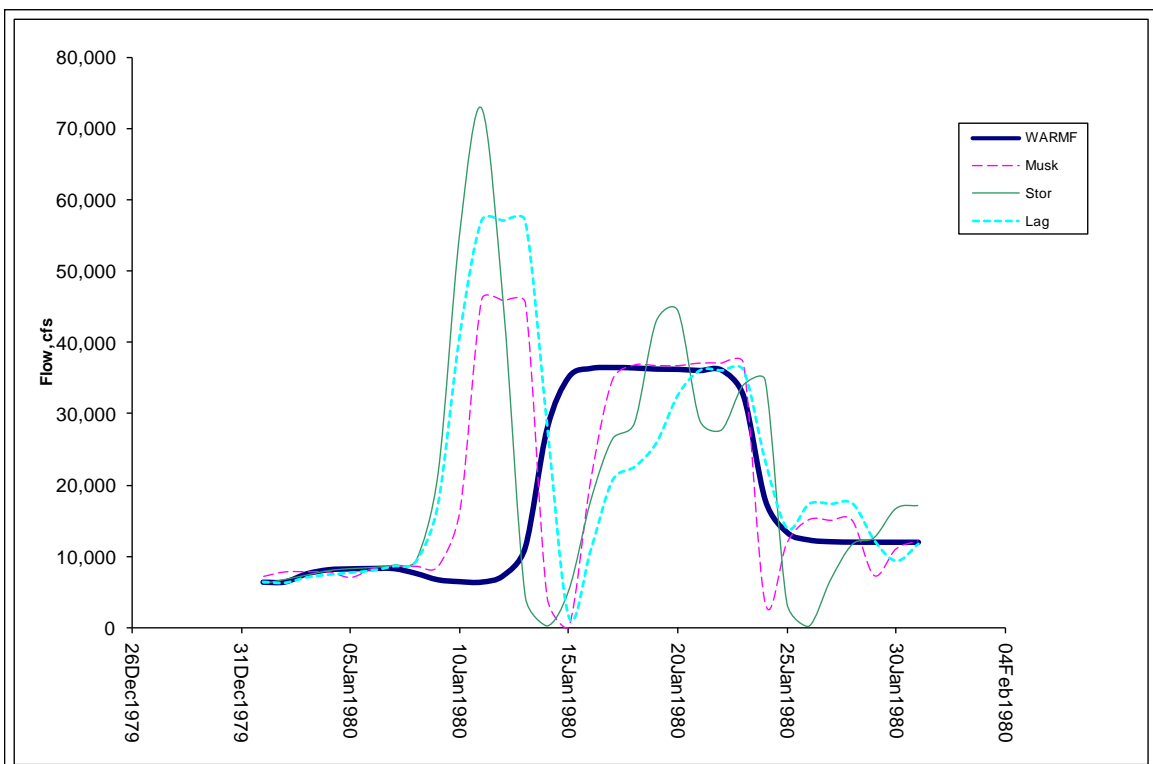


Figure 22. Outflow at Shasta channel for time series demand at the Hood using HEC Hydraulics Manual calibrated coefficients

Table 19. WARMF calibrated Delta outflow routing test for SacAme channel

	WARMF	Musk	Stor	Lag
Avg (cfs)	66,618	67,533	68,824	70,424
Min (cfs)	18,186	18,197	18,269	18,239
Max (cfs)	179,898	185,537	183,148	210,178
Range (cfs)	161,713	167,340	164,879	191,939
Total Vol (taf)	126,981	128,725	131,187	134,236
Peak Day	15	16	16	16

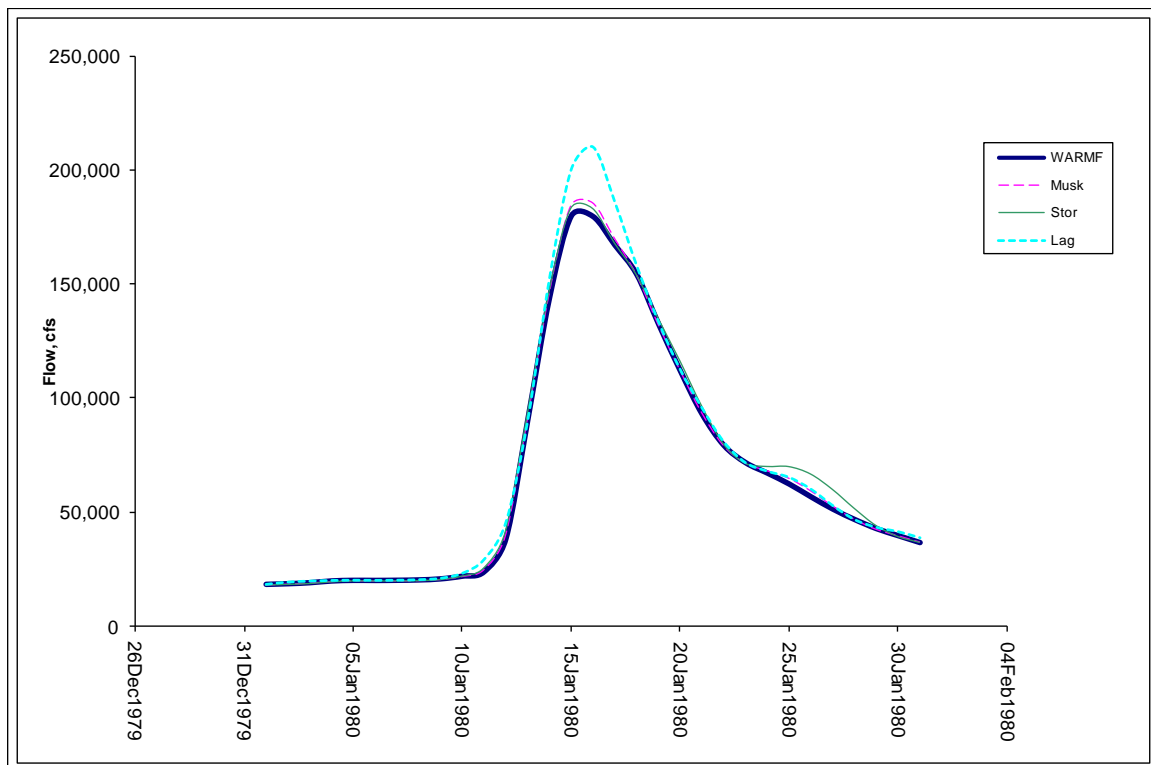


Figure 23. Outflow at Hood for a time series demand using WARMF calibrated coefficients

Table 20. HEC hydraulics manual calibrated Delta outflow routing test for SacAme channel

	WARMF	Musk	Stor	Lag
Avg (cfs)	66,618	68,123	68,537	70,424
Min (cfs)	18,186	18,207	18,256	18,239
Max (cfs)	179,898	192,737	189,385	210,178
Range (cfs)	161,713	174,529	171,129	191,939
Total Vol (taf)	126,981	129,850	130,639	134,236
Peak Day	15	16	16	16

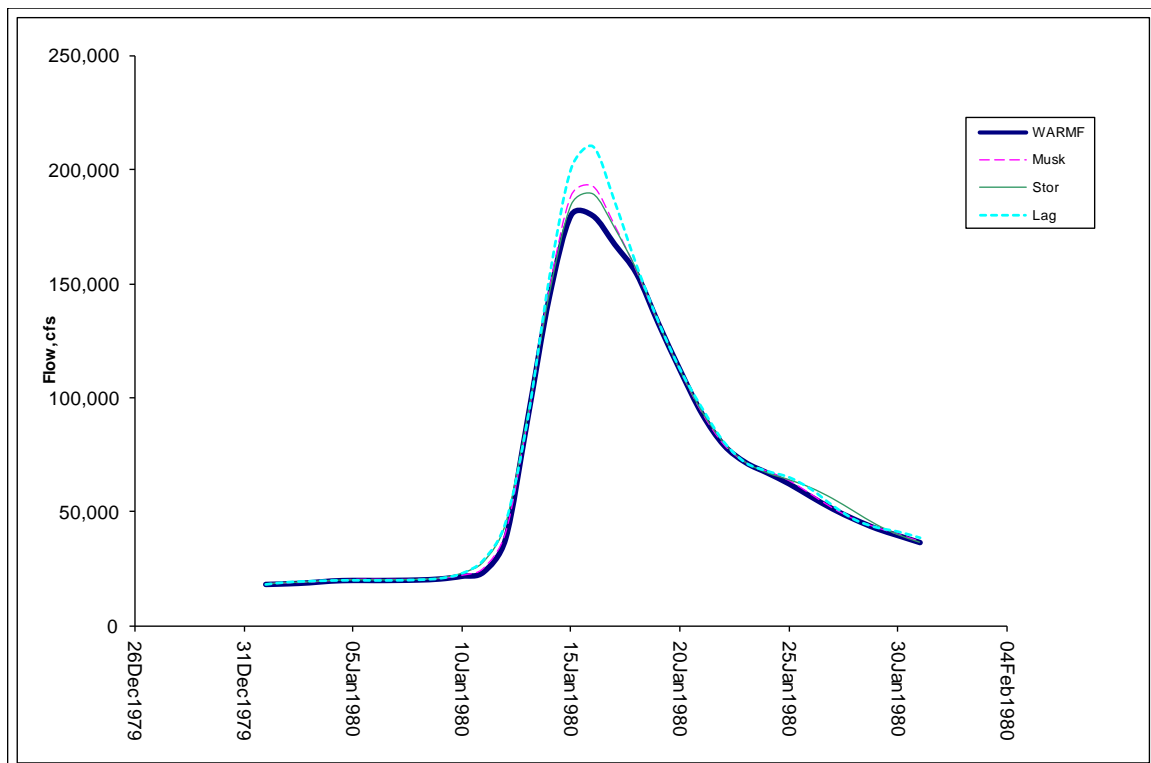


Figure 24. Outflow at Hood for a time series demand using HEC Hydraulics Manual calibrated coefficients

5.4. MULTIPLE MINIMUM INFLOWS TEST

The previous section shows that all the models respond well to a single downstream demand. However, there are usually multiple demands along the river at any given time. This test is to see how the models respond to multiple downstream demands at the Delta and Keswick.

The models respond well and have considerably less fluctuation at the most upstream channel (Figure 25 and Figure 26). There is a large spike prior to leveling out for all the routing methods and the peak days are displayed in Table 21 and Table 22. The peak is most likely in response to an initial sudden change in either the demand or amount of water available in the system on that day. The peak is less pronounced when using the WARMF calibrated coefficients, which suggests that changing the coefficient values can be one way to dampen further spiking. A similar trend occurs for all reaches where the routed flows start to match the WARMF flows closer when an additional upstream constraint is set. The remaining graphs can be found in Appendix C. This makes sense because when further outflows are constrained to those of WARMF, the remaining reaches upstream will begin to take the form of the upstream WARMF hydrographs. This also explains the nature of the high fluctuations seen before since having more constraints will lead to fewer possible solutions.

There is not much change in the downstream flows compared to the downstream flows (Figure 27 and Figure 28) with a single downstream constraint. The average volume in the system increases slightly by about 3000 cfs due to the extra constraint (Table 23 and Table 24). This could lead to a compounding problem, where adding an upstream constraints leads to increasing over allocations. It may be due to the differences in routing methods between WARMF and other hydrologic routing schemes. In practice, constraints on flows are used typically as a floor or ceiling and not necessarily having the goal of matching up.

The Muskingum method appears to yield the more accurate results compared to the storage and lag methods. The Muskingum simply over allocates the least amount of water compared to the other two routing methods. This trend occurs for both the WARMF and theoretical calibrated models. For the WARMF calibrated model, the average flow is 17,810 cfs. The Muskingum method has an average flow of 21,158 cfs, which is closely followed by storage routing with 21,639 cfs. Both routing methods over allocate roughly 3,000 cfs to 4,000 cfs worth of water. The totals are reflected in the total volume over the month with WARMF having a volume of 33,948 taf whereas the Muskingum and storage routing have volumes of 40,330 taf and 41,246 taf respectively. There is an extra 8,000 taf worth of water in the system over the month. The Muskingum method, however, resembles the shape of the WARMF hydrograph better and is reflected in the day in which the peak flow occurs on. For the WARMF model, the peak flow occurs on the 17th day of the month, the Muskingum on the 18th day, storage routing on the 11th day, and lag routing on the 13th day. The Muskingum method is only a day off the ideal peak flow day, but when the coefficients are changed to those calculated using equations 20 through 25 as found in the HEC hydraulics manual (USACE, 1994), the peak flow day is on the 11th day. The peak flow for the storage routing remains the same, but the magnitude of the peak flow changes by almost 25,000 cfs.

Table 21. WARMF calibrated minimum in-stream flows routing test for Shasta channel

	WARMF	Musk	Stor	Lag
Avg (cfs)	17,810	21,158	21,639	25,477
Min (cfs)	6,405	6,951	6,964	7,053
Max (cfs)	36,465	36,407	47,556	57,017
Range (cfs)	30,060	29,455	40,592	49,964
Total Vol (taf)	33,948	40,330	41,246	48,562
Peak Day	17	18	11	13

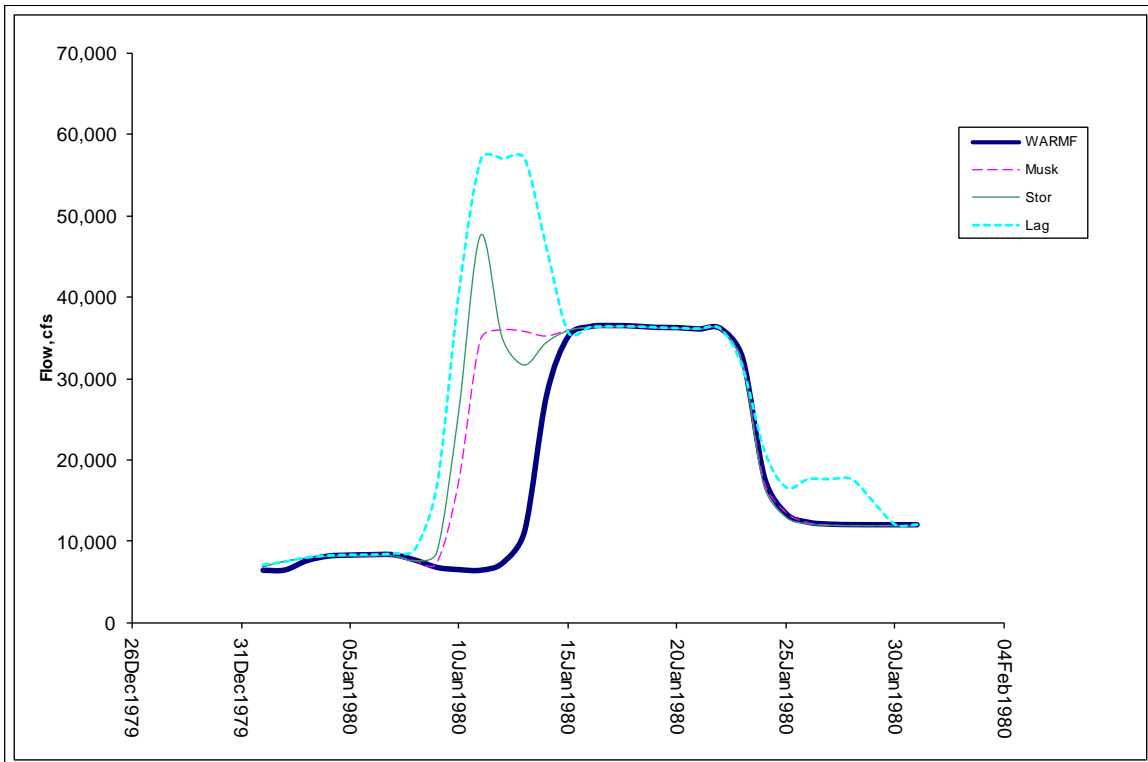


Figure 25. Outflow at Shasta channel for time series demands at Hood and Keswick using WARMF calibrated coefficients

Table 22. HEC hydraulics manual calibrated minimum in-stream flows routing test for Shasta channel

	WARMF	Musk	Stor	Lag
Avg (cfs)	17,810	22,338	24,383	25,477
Min (cfs)	6,405	7,035	7,712	7,053
Max (cfs)	36,465	46,213	72,960	57,017
Range (cfs)	30,060	39,178	65,248	49,964
Total Vol (taf)	33,948	42,580	46,476	48,562
Peak Day	17	11	11	13

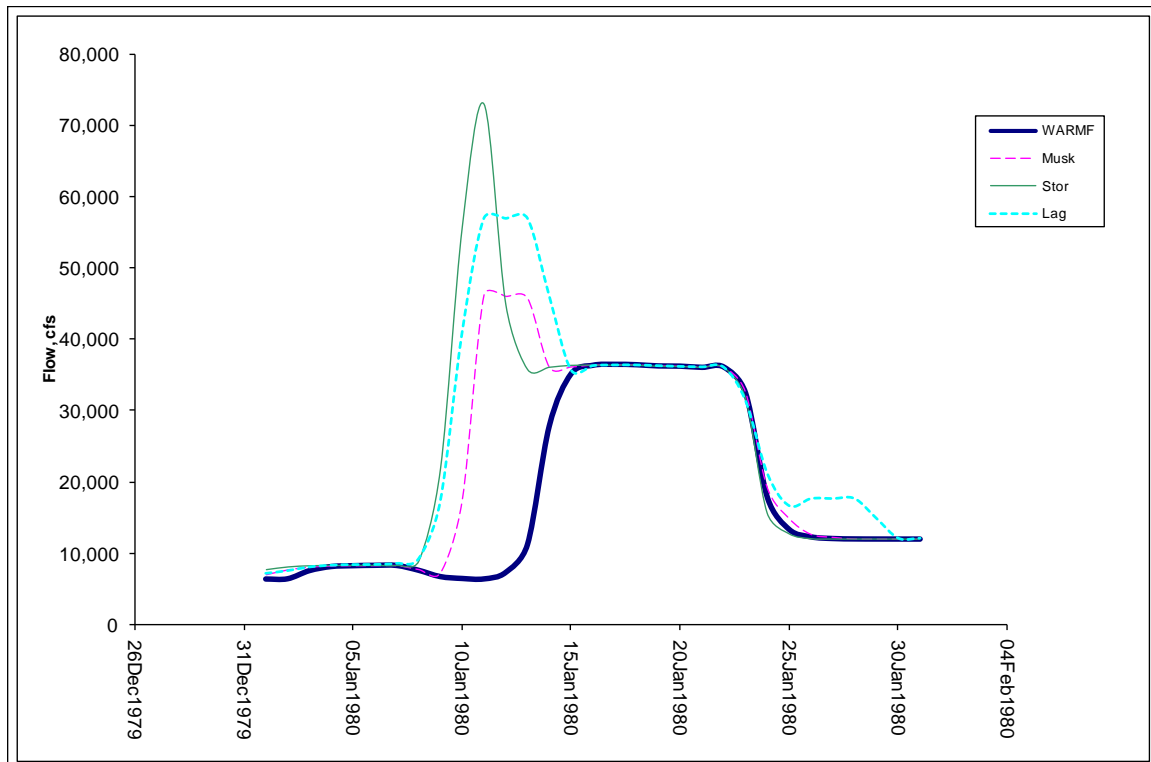


Figure 26. Outflow at Shasta channel for time series demands at Hood and Keswick using HEC hydraulics manual calibrated coefficients

Table 23. WARMF calibrated minimum in-stream flows routing test for SacAme channel

	WARMF	Musk	Stor	Lag
Avg (cfs)	66,618	69,941	70,394	74,396
Min (cfs)	18,186	18,325	18,341	18,186
Max (cfs)	179,898	191,713	192,941	217,890
Range (cfs)	161,713	173,388	174,600	199,704
Total Vol (taf)	126,981	133,315	134,180	141,808
Peak Day	15	16	16	16

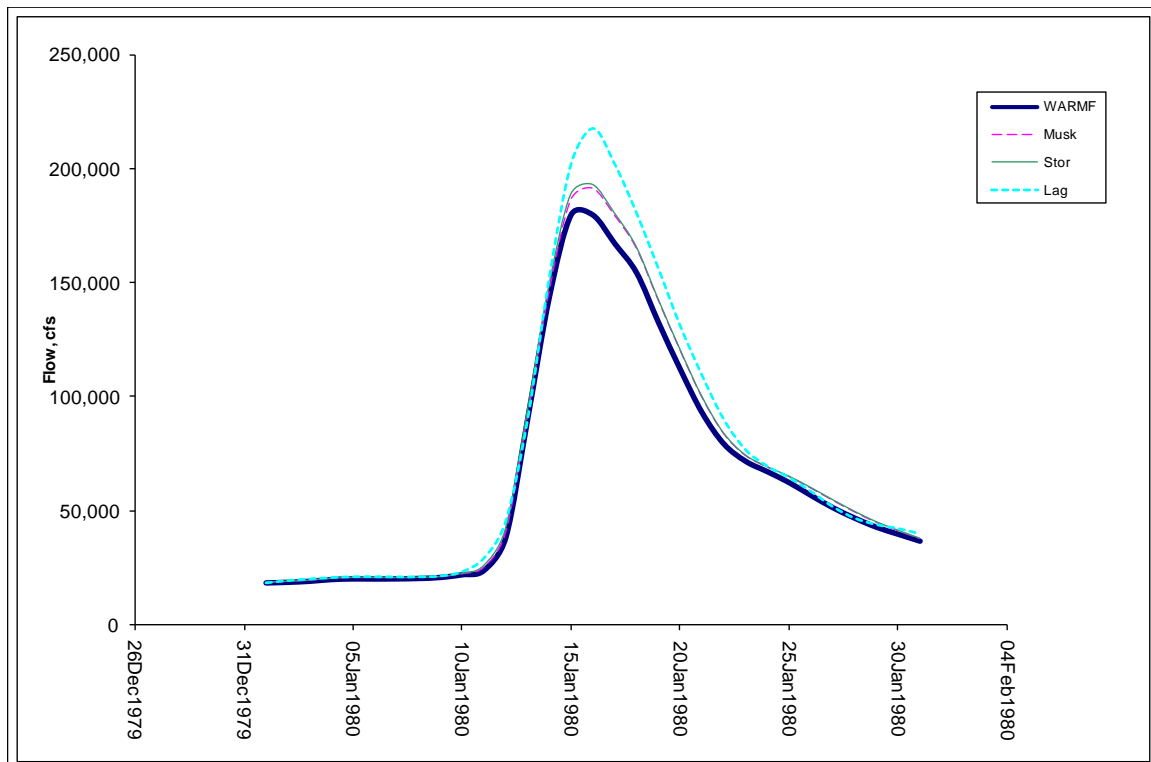


Figure 27. Outflow at Hood for time series demands at Hood and Keswick using WARMF calibrated coefficients

Table 24. HEC hydraulics manual calibrated minimum in-stream flows routing test for SacAme channel

	WARMF	Musk	Stor	Lag
Avg (cfs)	66,618	71,185	72,990	74,396
Min (cfs)	18,186	18,430	18,339	18,186
Max (cfs)	179,898	201,002	200,161	217,890
Range (cfs)	161,713	182,572	181,822	199,704
Total Vol (taf)	126,981	135,686	139,127	141,808
Peak Day	15	16	16	16

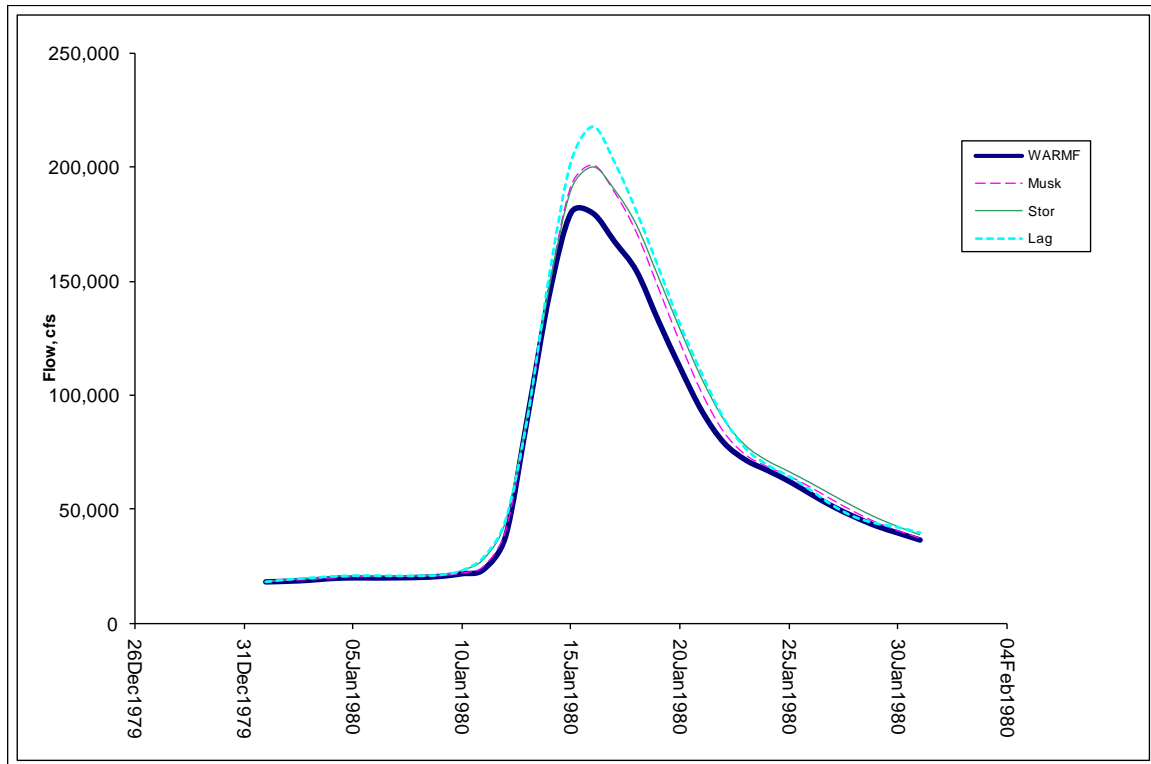


Figure 28. Outflow at Hood for time series demands at Hood and Keswick using HEC Hydraulics Manual calibrated coefficients

5.5. COMPARISON OF ROUTING METHODS AND LIMITATIONS

5.5.1 *Comparison of Routing Methods*

Table 25 summarizes the three routing methods for a range of criteria including accuracy, sensitivity, range, number of routing coefficients, number of decision variables used, and average approximate run time. The results from this study support that lag and coefficient storage routing methods as more accurate compared to the Muskingum routing method. This is not necessarily true. Each routing method has its list of pros and cons, but each is capable of accurate routing.

Muskingum uses three parameters, K , Δt , and X , to perform channel routing, which is one more than for coefficient based storage routing. The added flexibility allows the Muskingum method to take on a larger range of possible solutions by tweaking one of the variables. Consequently it is also highly sensitive to changes in variables especially the X term. The Muskingum method can be highly accurate as shown in the previous tests. The drawback is in the difficulty of calibrating the coefficients. For small time periods a constant set of coefficients is sufficient in accurately routing the stream flow. When hydraulic conditions change over time in a channel, the same set of coefficients may not work and could yield divergent results.

Storage routing is sensitive to problems of bad storage-outflow relationship data. Storage coefficient routing is susceptible to high fluctuations and uses two parameters, which is also difficult to predict the outcome and must be delicately calibrated. The storage routing method is less sensitive than the Muskingum parameters, but can still be susceptible to large fluctuations in upstream releases. Storage routing is simple to implement and requires fewer decision variables for larger systems. However, the accuracy can be as good as that of the Muskingum method despite having fewer decision variables and a quicker run time.

The lag routing is the simplest and the least susceptible to large fluctuations. However, attenuation is limited and so this should not be the first method applied to a new model, but would make for a good comparative method as the outflow is easily predicted. It is the easiest method to implement and predict the forecasted outflows. It is also the quickest and uses the fewest decision variables. When used in conjunction with fulfilling a downstream constraint, the lag method is able to match the target fairly well. However, all points upstream of the target point have hydrographs that are inconsistent with the Muskingum and storage routing methods.

Table 25. Comparison of routing methods tested

Criteria	Muskingum	Storage	Lag
Accuracy	· Accurate for short time frames subject to calibration	· Accurate for short time frames subject to calibration	· Low
Sensitivity	· Highly sensitive to large changes in parameters	· Less sensitive to large changes in parameters	· N/A
Range of Possible Solutions	· Largest range	· Modest range	· Small range
Number of Coefficients	3	2	· Varies
Number of Decision Variables Used in WRESL	352	266	65
Average Run Time	~ 3 mins	~ 2.5 mins	~ 1.5 mins

5.5.2 Model Limitations

A model is only as accurate as the data that is available and due to the high reliance on WARMF model, many simplifications were made. The toughest part of coefficient based routing techniques is deriving accurate coefficients. Ideally a model would have different sets of coefficients to account for different types of hydrology experienced. This would lead to more precise outflows, but is potentially susceptible to mass balance problems. Using hourly routing aggregated to daily average flows can also lead to some mass loss, which needs to be tracked in the storage of each channel.

The problem in this study is really a two part problem, routing and optimization in WRIMS environment. The optimization part necessitates a good forecasting scheme. Forecasting is another problem because many routing methods rely on past, present, or future values, but are subject to change when the next time step is reached. Future releases will have effects on the current day's projected outflow, which can not always be accounted for. By setting constraints on each of the forecasted outflows to meet future demands is a good way to work around the problem. Also the flows released from Shasta drastically depending on the number of days used to look ahead.

5.5.3 Run Time

Model run time has not been discussed up until now, but is primarily affected by the number of decision variables needed. For this simplified model, run times were not a big issue in that all runs took less than 3 minutes for 82 years worth of daily data. However, the lag model used far fewer decision variables since it did not require sub time steps, since the coefficients are empirical. A limitation with WRIMS in the current state is that there is no way to reuse variables, nor are there loop functions like a typical programming language. This means that if sub reaches and multiple time steps are to be used, each sub reach must be assigned a whole new set of decision variables for each sub time step, which can increase run time dramatically for a larger model.

Chapter 6 CONCLUSION

CalLite is becoming more user friendly and is trying to make the jump from a comparative model to a decision making tool. The users have demanded that more features be added to accommodate a larger number of scenarios. To accomplish this, a daily model is needed with channel routing. Few models of such a large scale have made this type of change in time step, but some models already have these types of capabilities. Routing and optimization inspired techniques from ModSim, HEC-FCLP, OASIS, Aquatool, and HSFM HFAM-II were used to compile this study. Although this is a simplified study in comparison, many useful conclusions can be drawn using the criteria of ease of implementation, accuracy, and applicability:

- 1) *A coefficient based routing with multiple time steps can be calibrated to represent a single wave with acceptable results.* The problem with the lag method is the simplicity and empirical basis. Storage routing is extremely sensitive to having good data available, requires more decision variable thereby slowing down the run time, and may have inconsistent forecasting methods. Muskingum method requires precise calibration and may need its coefficients by dynamically adjusted during run time to be precise. A semi-dynamic routing method is not needed for a planning model to be accurate nor is the need for individual rating curves for each channel, both of which become difficult to implement.
- 2) *All routing methods can be optimized for a single downstream demand. The differences are illustrated at the most upstream channel.* Since coefficient methods are simple in theory and implementation, the results are easily understood. Using any set of coefficients that fit the Muskingum criteria will yield results that can be generally accurate. However, when the required demand is routed back upwards to the release point, many possible solutions exist. Variation in the upstream hydrograph that depends on the routing method, the coefficients, and constraints used.
- 3) *When additional flow constraints are added, the number of possible solutions becomes more limited and flows can be made to resemble ideal flow conditions.* A drawback to adding more constraints is it may lead to over allocation of water depending on the type of constraint being added. Care should be taken to take into account of other factors when trying to calibrate and match flow values. Constraining the problem may initially lead to a less fluctuating results, but the magnitudes of the flows may be much greater than expected.
- 4) *Muskingum method is the recommended first choice for most of systems.* The Muskingum method uses the most parameters so it can fit a corresponding pair of upstream and downstream hydrographs the best. The modeler will have to make assumptions to specify the period of study, channel lengths, and time steps that will be used. Calibration requires more work than either the storage or lag methods, but once calibrated, the Muskingum method is relatively easy to implement and can be used in most water systems. Muskingum is a generally accepted routing method in the water resources community whereas the storage and lag methods may raise questions with resolution and derivation basis.

- 5) *There are many ways to implement channel routing. Using the current native WRESL language version 1, poses challenges that other similar models work around.* The method of implementation proposed here is one of many ways of coupling channel routing and optimization. Even within the WRIMS environment there are alternatives that may be a bit more complex, such as the use of external dll functions, and could possibly be easier to implement for larger systems. Many models are able to utilize some form of an iterative scheme to test for convergence of routing equations, but this can not be done in the current version of WRESL. Writing out all the equations used for forecasting in a single time step can become cumbersome and future versions of WRESL language may address these issues in the future.

REFERENCES

- 1) Andreu, J., J. Capilla, and E. Sanchis. "AQUATOOL, a generalized decision-support system for water-resources planning and operational management." *Journal of Hydrology*. 177. (1995): 269-291.
- 2) Birkhead, A.L. "Muskingum river routing with dynamic bank storage." *Journal of Hydrology*. 264. (2002): 113-132.
- 3) Bokun, Luo. "Some Problems with the Muskingum Method." *Hydrological Sciences Journal*. 32.4 (1987):
- 4) CA. Department of Water Resources (2002). *Benchmark Studies Assumptions*. Sacramento, Calif.
- 5) CA. Department of Water Resources (2009). *CalLite User's Guide*. Sacramento, CA
- 6) CA. Department of Water Resources (2003). *CalSim II Simulation of Historical SWP/CVP Operations: Technical Memorandum Report*, Bay-Delta Office, Sacramento, Calif.
- 7) CA. Department of Water Resources (2000). *CalSim Water Resources Simulation Model Manual*. Sacramento, Calif.
- 8) CA. Department of Water Resources (2010). *DWR NEW: People*, Bay-Delta Office, Sacramento, Calif.
- 9) California Data Exchange Center. 2011. <http://cdec.water.ca.gov/>
- 10) Can, Emre K. "Problems with Modeling Real-Time Reservoir Operations." *Journal of Water Resources Planning and Management*. 111.4 (1985): Print.
- 11) Choudhury, Parthasarathi. "Multiple Inflows Muskingum Routing Model." *ASCE*. 12.5 (2007): 473.
- 12) Chow, Ven Te. *Handbook of Applied Hydrology A Compendium of Water-resources Technology*. New York, NY: McGraw-Hill Book Company, 1964.
- 13) DWR Website. 2011. <http://www.water.ca.gov>
- 14) Gill, Mohammad. "Critical Examination of the Muskingum Method." *Nordic Hydrology*. 10. (1979): 261-270.
- 15) Goldstein, Robert A. EPRI. *Watershed Analysis Risk Management Framework (WARMF): Update One A Decision Support System for Watershed Analysis and Total Maximum Daily Load Calculation, Allocation and Implementation*. Palo Alto, CA: 2001.

- 16) "HFAMII Help File." HydroComp, 2006.
- 17) Hydrologics (2009). *User Manual for OASIS WITH OCL™* Columbia, MD
- 18) Jones, Dustin Jon. (1997). Application of Mixed-Integer Programming for Flood Control in the Sacramento Valley: Insights & Limitations. Unpublished master's thesis, University of California, Davis.
- 19) Labadie, John W. Colorado State University. *MODSIM 8.1: River Basin Management Decision Support System User Manual and Documentation*. Ft. Collins, CO: 2010.
- 20) Martin, Quentin. Texas Department of Water Resources. (1982). *MULTIRESERVOIR SIMULATION AND OPTIMIZATION MODEL SIM-V: Program Documentation and User's Manual, UM-38*. Austin, Texas.
- 21) Martin, Quentin W. "Optimal Reservoir Control For Hydropower on Colorado River, Texas." *Journal of Water Resources Planning and Management*. 121.6 (1995)
- 22) Mays, Larry W. *Water Resources Engineering*. 1st. New York, NY: John Wiley & Sons, Inc., 2001.
- 23) McCuen, Richard H. *Hydrologic Analysis and Design*. 2nd. Upper Saddle River, NJ: Prentice Hall, 2001.
- 24) Northern California Map. retrieved on July 2011 from website <maps.google.com>
- 25) Shaw, Dean. "Flow routing in large-scale models using vector addition." *Journal of Hydrology*. 307. (2005): 38-47.
- 26) Smith, Michael, Victor Koren, and Bryce Finnerty. NOAA. *Distributed Modeling: Phase 1 Results*. 1999.
- 27) United States. *NWSRFS Overview*. <<http://www.weather.gov/iao/pdf/Manual.pdf>>
- 28) U.S. Department of Commerce (1999). NOAA Technical Report NWS 44. *Distributed Modeling: Phase 1 Results*
- 29) U.S. Army Corps of Engineers (1998). *Hydrologic Engineering Center's HEC-1 Flood Hydrograph Package User's Manual*. Davis, Calif
- 30) U.S. Army Corps of Engineers (2000). *Hydrologic Engineering Center's Hydrologic Modeling System HEC HMS Technical Reference Manual Regulation*. Davis, Calif
- 31) U.S. Army Corps of Engineers (2000). *Hydrologic Engineering Center's Reservoir Flood Control Optimization Program HEC-ResFloodOpt Technical Reference Manual Regulation for Flood Control*, Sacramento District, Sacramento, Calif

- 32) U.S. Army Corps of Engineers (2007). *Hydrologic Engineering Center's HEC ResSim Reservoir System Simulation*, Davis, Calif
- 33) U.S. Army Corps of Engineers (2010). *Hydrologic Engineering Center's River Analysis System HEC-RAS Hydraulic Reference Manual*, Sacramento District, Sacramento, Calif.
- 34) U.S. Army Corps of Engineers (1993). EM 1110-2-1416:*Engineering and Design River Hydraulics*, Department of the Army, Washington DC.
- 35) U.S. Army Corps of Engineers (1994). EM 1110-2-1417:*Engineering and Design FLOOD-RUNOFF ANALYSIS*, Department of the Army, Washington DC.
- 36) USGS Website. 2011. <http://waterdata.usgs.gov>
- 37) Yoon, Jaewan, and G. Padmanabhan. "Parameter Estimation of Linear and Nonlinear Muskingum Models." (1993) ASCE.

APPENDIX

APPENDIX A WARMF STREAM PROPERTIES

Table 26. Channel Properties from WARMF model

Warmf Reach	Stream ID	Callite Reach	L (m) [warmf]	Upstream (m)	Downs (m)	Stage (m)	Width (m)	N	S
Sacramento River at Shasta Lake	423	C_Shasta	970.624	0.1	0	2	40	0.04	0.0001
Sacramento River at Keswick	118	C_Shasta	36600	183	130	1.21	37	0.04	0.0014
Sacramento River 22	122	C_Kswck	8128.98	130	119.5	2.01	79	0.04	0.0013
Sacramento River 24	124	C_Kswck	4772.24	119.5	115.5	2.11	84	0.04	0.0008
Sacramento River 26	126	C_Kswck	1536.82	115.5	114.91	2.24	92	0.04	0.0004
Sacramento River 31	131	C_Kswck	4246.48	114.91	110	2.91	137	0.04	0.0012
Sacramento River 33	133	C_Kswck	889.74	110	109.4	3.06	147	0.04	0.0007
Sacramento River 50	150	C_Kswck	5500.2	109.4	106.4	3.1	151	0.04	0.0005
Sacramento River 56	156	C_Kswck	768.411	106.4	106.1	3.14	153	0.04	0.0004
Sacramento River 59	159	C_Kswck	3356.74	106.1	102.9	4.04	223	0.04	0.0010
Sacramento River 65	165	C_Kswck	11647.5	102.9	93.7	4.32	248	0.04	0.0008
Sacramento River at Bend Bridge	176	C_Kswck	19372	93.7	78.7	4.36	251	0.04	0.0008
Sacramento River near Red Bluff	188	C_Kswck	10636.4	78.7	72.9	4.45	258	0.04	0.0005
Sacramento River at Red Bluff	190	C_RedBlf	3114.09	75.9	75.6	4.47	260	0.04	0.0001
Sacramento River at Diversion Dam	193	C_RedBlf	1900.81	75.6	73.2	4.53	265	0.04	0.0013
Sacramento River 96	196	C_RedBlf	4853.12	73.2	71	4.61	272	0.04	0.0005
Sacramento River 97	197	C_RedBlf	137.05	71	70.1	4.71	282	0.04	0.0066
Sacramento River 104	204	C_RedBlf	7279.68	70.1	64.6	4.74	284	0.04	0.0008
Sacramento River 105	205	C_RedBlf	566.198	64.6	64.3	4.76	286	0.04	0.0005
Sacramento River 110	210	C_RedBlf	3194.97	64.3	62.5	4.79	289	0.04	0.0006
Sacramento River 116	216	C_RedBlf	2345.68	62.5	60.7	4.83	292	0.04	0.0008
Sacramento River 121	221	C_RedBlf	4731.79	60.7	60	4.91	299	0.04	0.0001
Sacramento River 128	228	C_RedBlf	1415.49	60	56.7	4.99	307	0.04	0.0023
Sacramento River 132	232	C_RedBlf	2264.79	56.7	56.1	5.01	309	0.04	0.0003
Sacramento River 143	243	C_RedBlf	4650.91	56.1	53.3	5.24	330	0.04	0.0006
Sacramento River 151	251	C_RedBlf	4853.12	53.3	51.8	5.28	334	0.04	0.0003
Sacramento River at Vina Bridge	260	C_RedBlf	8735.62	51.8	47.2	5.41	346	0.04	0.0005
Sacramento River 171	271	C_RedBlf	7239.24	47.2	45.7	5.47	352	0.04	0.0002
Sacramento River near Hamilton City	299	C_RedBlf	20828	45.7	37	5.53	358	0.04	0.0004
Sacramento River 137	237	C_RedBlf	5338.43	37	34.4	5.53	358	0.04	0.0005
Sacramento River 212	312	C_RedBlf	7037.03	34.4	32	5.66	370	0.04	0.0003
Sacramento River at Ord Ferry	335	C_RedBlf	22162.6	32	25.6	6.07	412	0.04	0.0003
Sacramento River at Butte City	360	C_RedBlf	16824.2	25.6	19.2	6.11	416	0.04	0.0004
Sacramento River at Colusa	415	C_RedBlf	40119.1	19.2	16.2	6.14	419	0.04	0.0001
Sacramento near Grimes	510	C_RedBlf	45942.9	16.2	10	6.49	455	0.04	0.0001
Sacramento River 301	301	C_RedBlf	31787.9	10	5.3	6.49	455	0.04	0.0001
Sacramento River at Fremont Weir	520	C_Wilkns	16217.5	5.3	4.9	7.48	563	0.04	0.0000
Sacramento River at Verona	521	C_SacFea	1779.48	4.9	4.8	9.13	759	0.04	0.0001
Sacramento River at Verona	318	C_SacFea	4731.79	4.8	4.5	9.23	772	0.04	0.0001
Sacramento River 547	547	C_SacFea	26368.6	4.5	1.2	9.23	772	0.04	0.0001
Sacramento River at I Street Bridge	551	C_SacAme	1981.69	1.2	1	9.69	831	0.04	0.0001
Sacramento River near Freeport	428	C_SacAme	21475	1	-10	9.23	772	0.04	0.0005

APPENDIX B WATER TRAVEL TIMES



Figure 29. Water travel times during flood seasons (DWR, 2011)

APPENDIX C

ESTIMATING THE NUMBER OF FORECASTING DAYS

In order to determine the number of days to look ahead for each model a series of tests were performed. Using the one flow constraint setup at the Delta, each model was run with varying forecasting days. The difference in the outflow at Hood was compared to the WARMF output time series. Simple statistical parameters were taken of these differences including: the greatest (max) difference, the number of times it was over 1,000 cfs (roughly 10% of the total flow), and the sum of all the differences over 1,000 cfs. These criteria along with the results from the flood routing test in section 5.2 were used to determine the best suited number of routing days for each model.

Muskingum

Table 27. Muskingum routing with WARMF based coefficients number of days Summary

Parameter	No. of Days					
	0	1	2	3	4	5
Max (cfs)	376,871	99,140	63,041	59,160	59,160	56,067
#>1000 (cfs)	9,775	6,725	365	683	683	889
sum>1000 (cfs)	196,152,067	25,711,178	1,594,796	2,292,972	2,292,972	3,222,388

Table 28. Muskingum routing with theoretical based coefficients number of days Summary

Parameter	No. of Days					
	0	1	2	3	4	5
Max (cfs)	267,025	102,992	80,456	70,642	64,356	65
#>1000 (cfs)	9,403	2,905	365	532	733	942
sum>1000 (cfs)	145,077,148	9,765,848	1,765,861	1,908,225	2,677,683	3,724,178

Storage

Table 29. Storage routing with WARMF based coefficients number of days Summary

Parameters	No. of Days					
	0	1	2	3	4	5
Max (cfs)	366,797	95,112	50,032	48,178	47,513	48,327
#>1000 (cfs)	9,891	7,206	529	546	751	990
sum>1000 (cfs)	196,200,146	29,322,084	1,571,697	1,580,388	2,328,579	3,427,887

Table 30. Storage routing with theoretical based coefficients number of days Summary

Parameters	No. of Days					
	0	1	2	3	4	5
Max (cfs)	704,945	180,768	81,028	76,783	72,179	68,859
#>1000 (cfs)	9,976	7,804	683	676	840	1,074
sum>1000 (cfs)	224,548,453	38,036,760	3,180,754	2,399,371	3,048,357	4,260,362

Lag

Table 31. Lag routing with theoretical based coefficients number of days Summary

Parameter	No. of Days				
	0	1	2	3	4
Max (cfs)	1,577,408	445,804	209,939	157,449	142,083
#>1000 (cfs)	10,113	9,708	8,369	1,006	1,148
sum>1000 (cfs)	1,078,035,214	216,600,827	39,612,276	5,536,964	5,798,714

APPENDIX D
ALL ROUTING FIGURES

5 Day Pulse Test Results

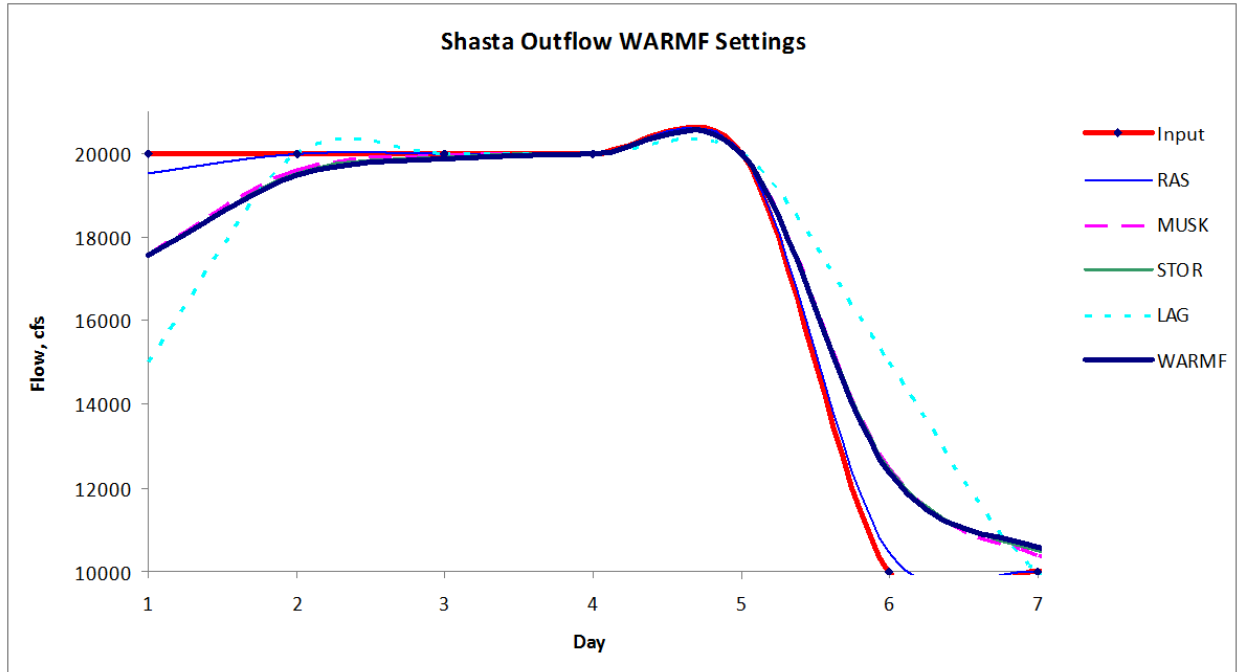


Figure 30. Outflow from C_Shsta at Keswick with WARMF calibrated coefficients

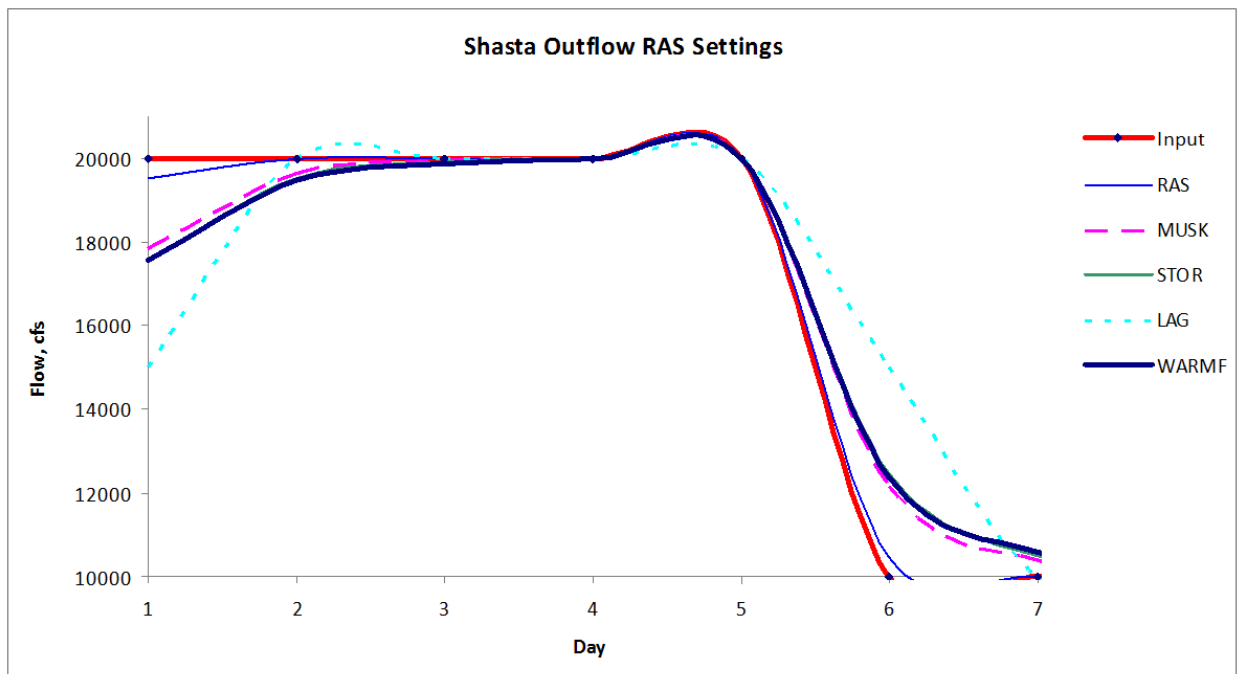


Figure 31. Outflow from C_Shsta at Keswick with HEC-RAS calibrated coefficients

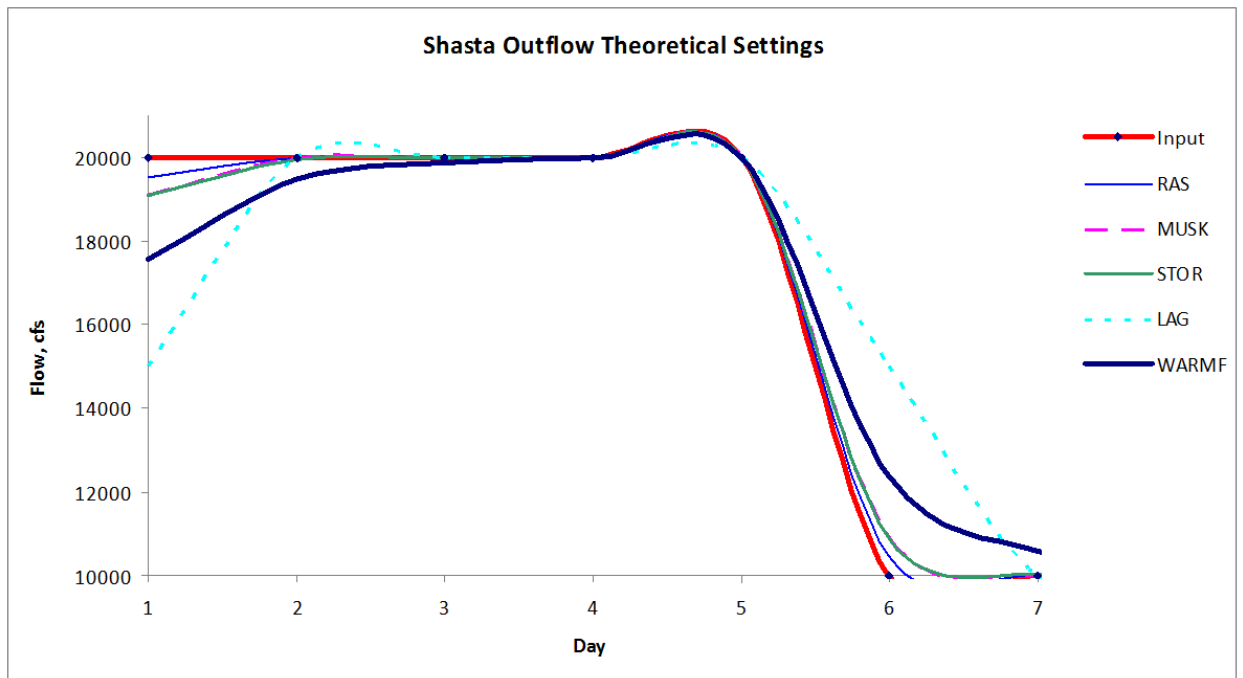


Figure 32. Outflow from C_Shsta at Keswick with theoretically calibrated coefficients

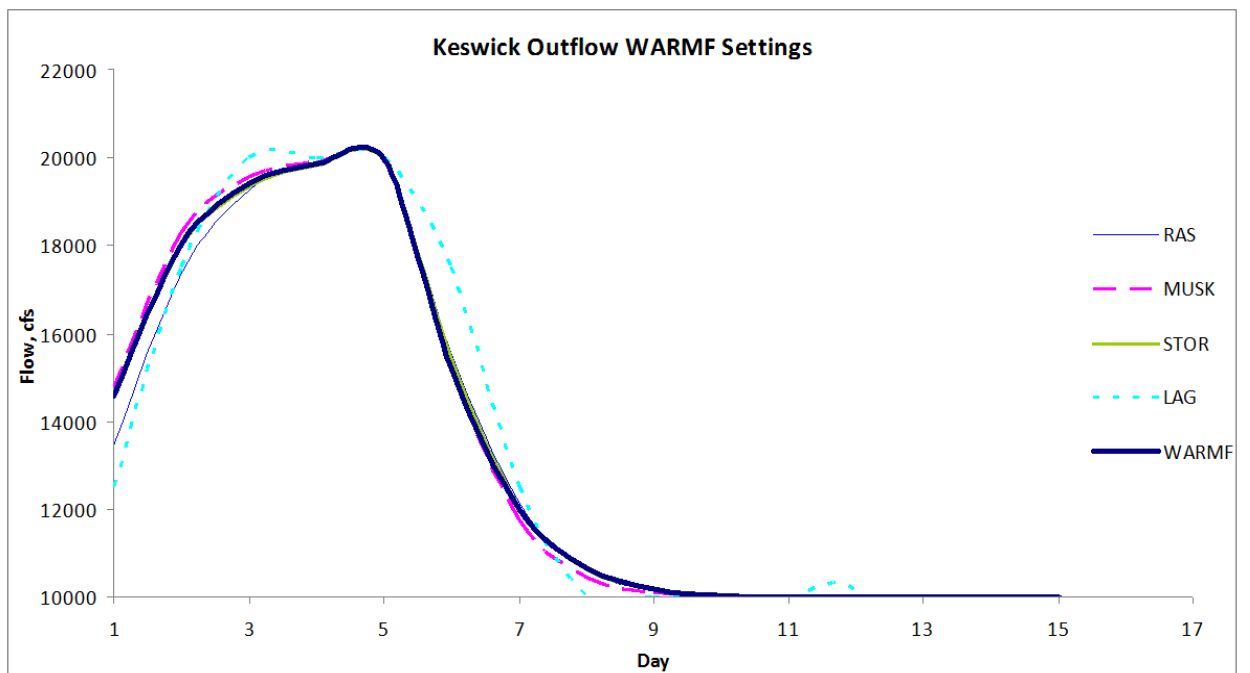


Figure 33. Outflow from C_Kswck at Red Bluff with WARMF calibrated coefficients

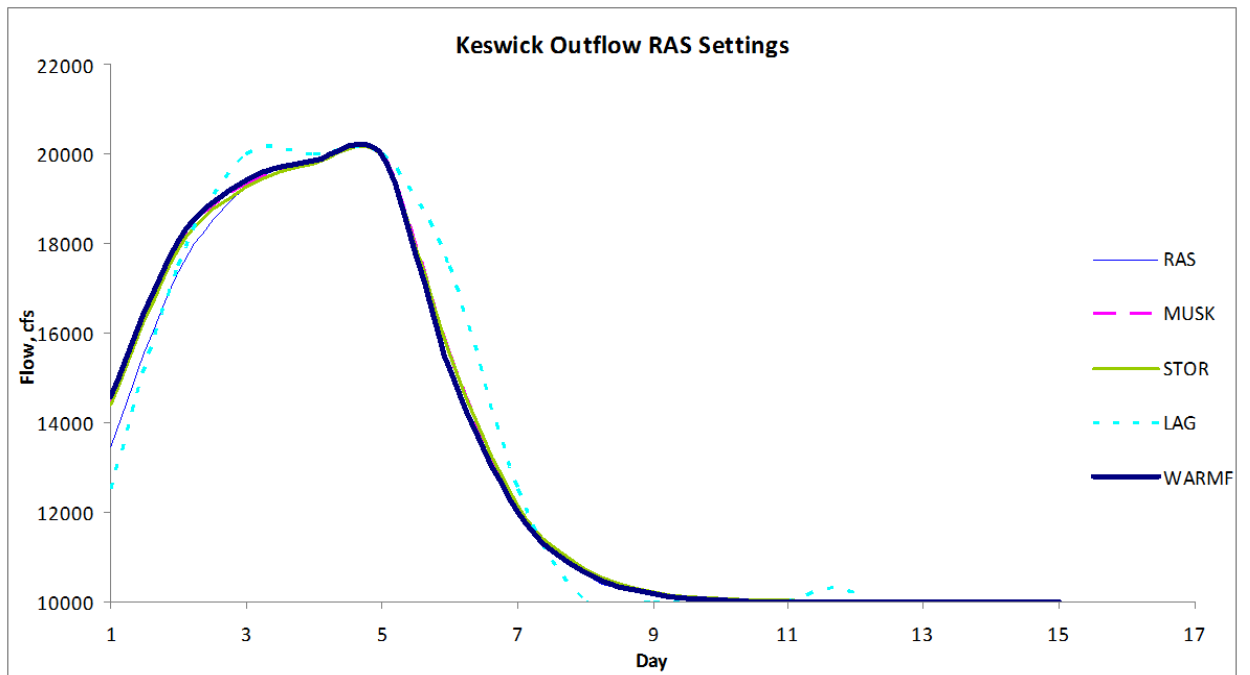


Figure 34 Outflow from C_Kswck at Red Bluff with HEC-RAS calibrated coefficients

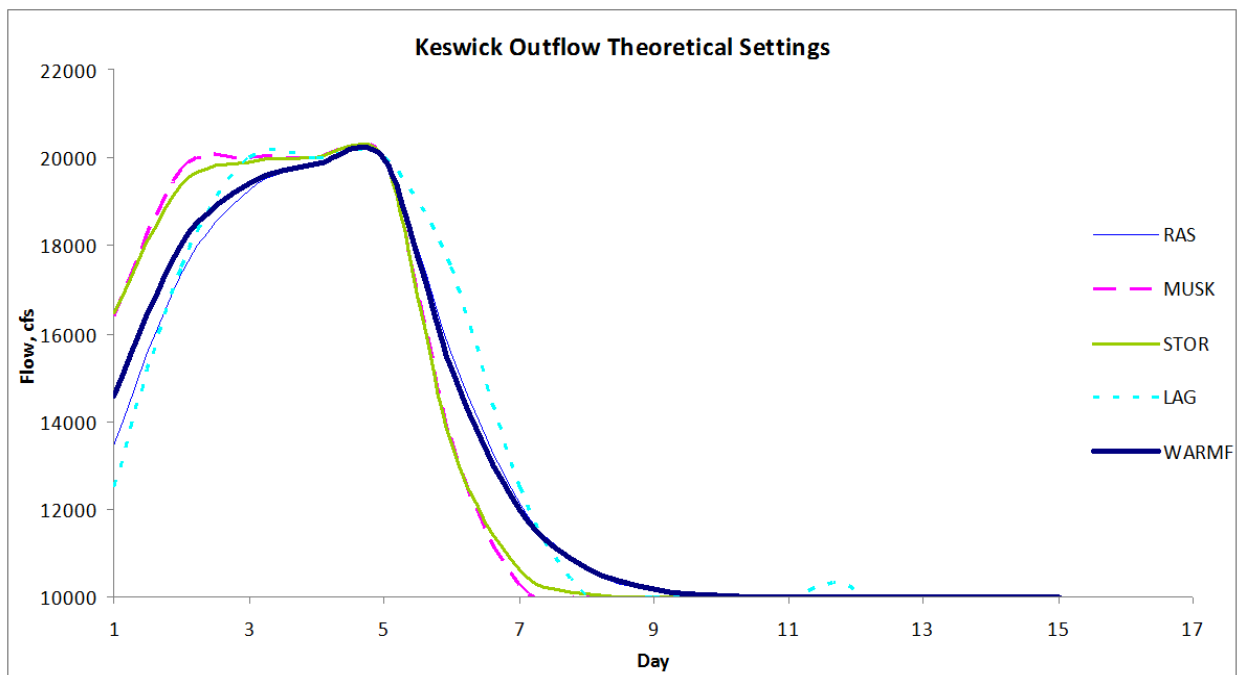


Figure 35. Outflow from C_Kswck at Red Bluff with theoretically calibrated coefficients

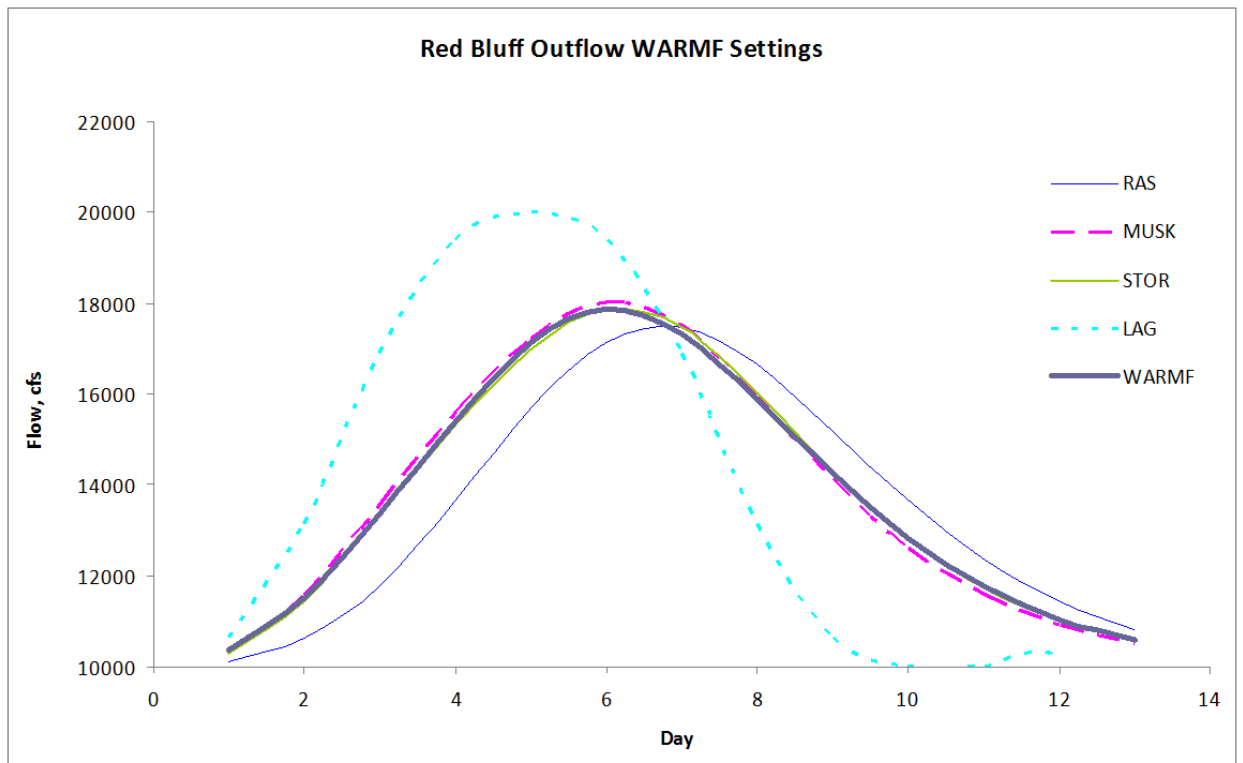


Figure 36. Outflow from C_RedBlf at Wilkins Slough with WARMF calibrated coefficients

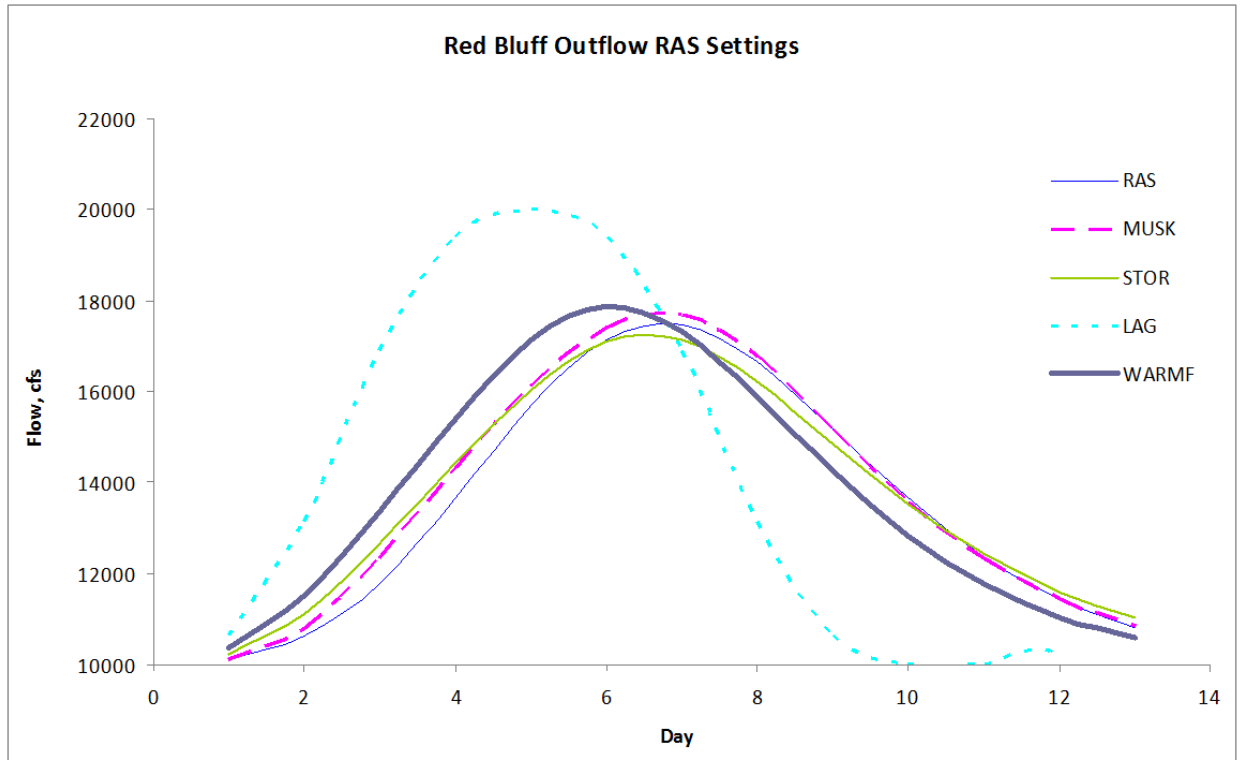


Figure 37. Outflow from C_RedBlf at Wilkins Slough with HEC-RAS calibrated coefficients

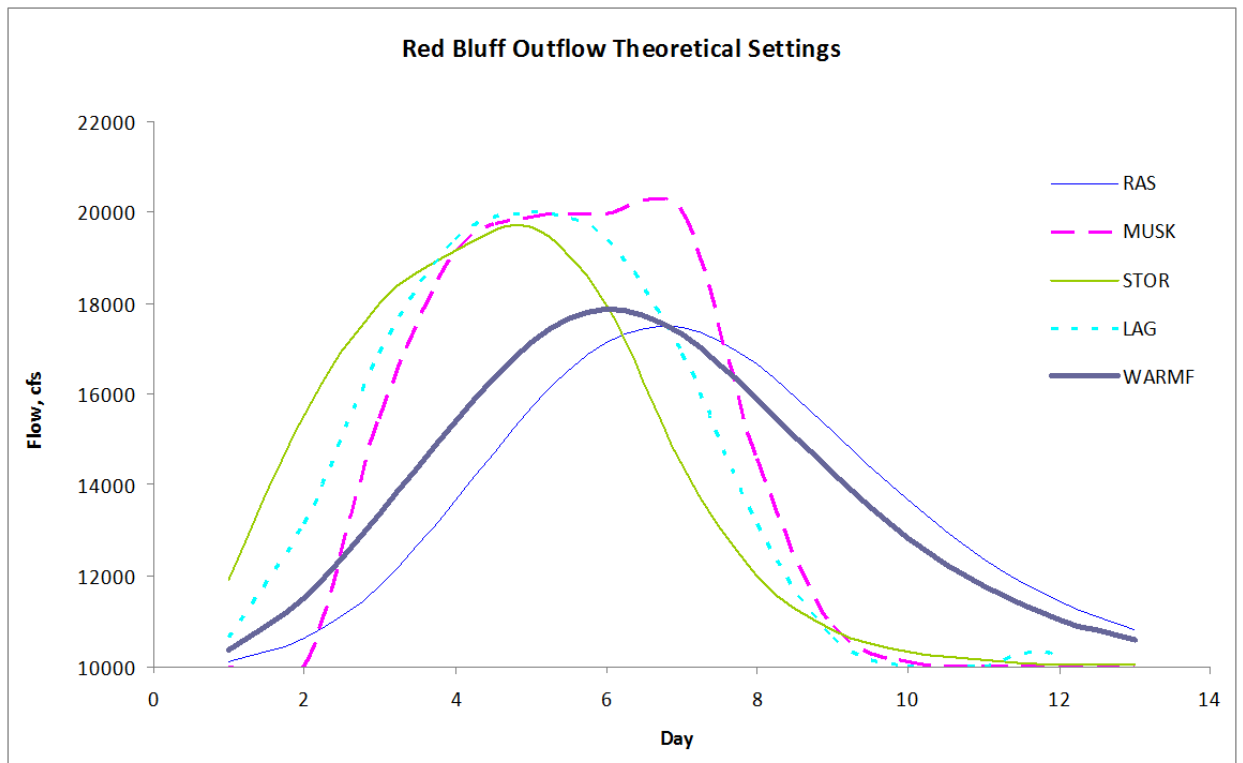


Figure 38. Outflow from C_RedBlf at Wilkins Slough with theoretically calibrated coefficients

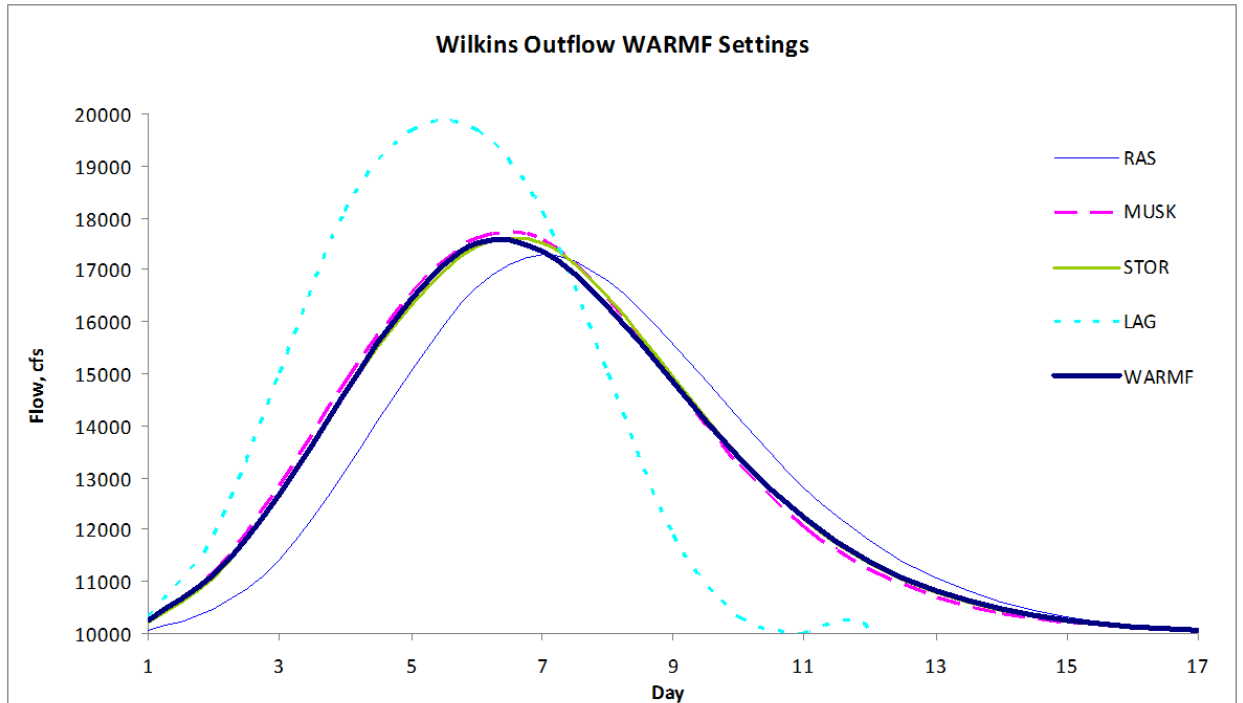


Figure 39. Outflow from C_Wilksn at Sacramento R. and Feather R. confluence with WARMF calibrated coefficients

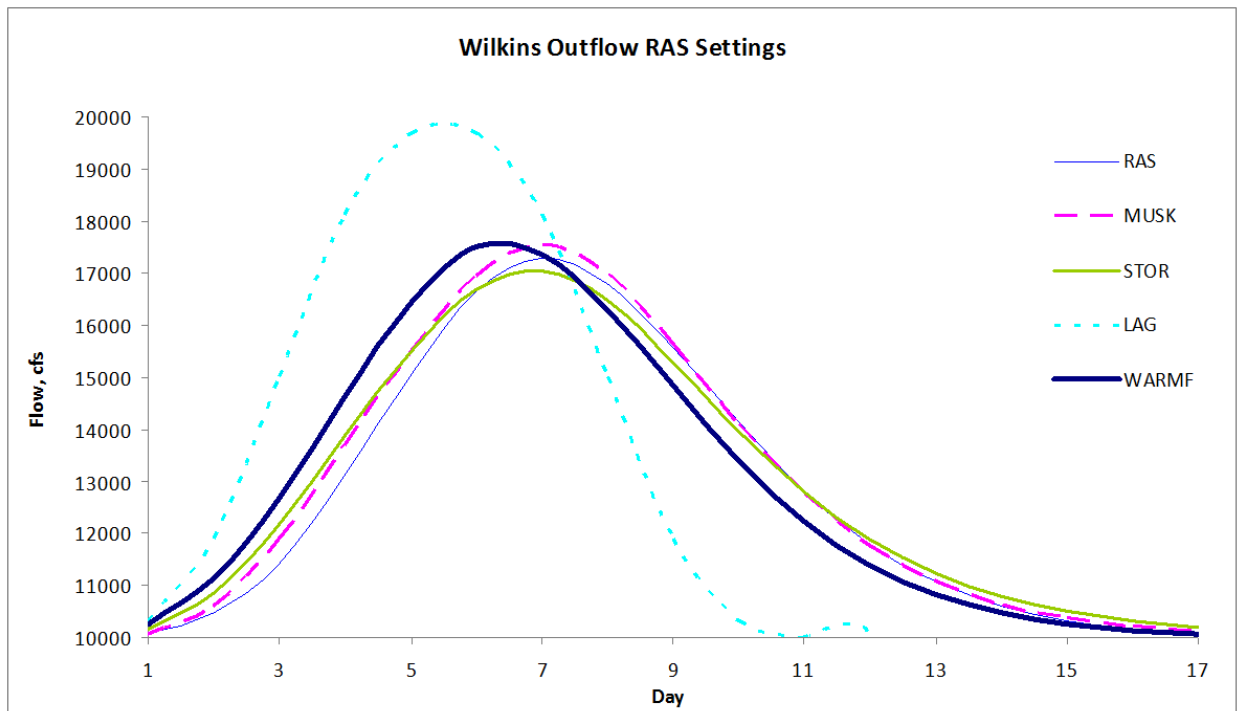


Figure 40. Outflow from C_Wilkins at Sacramento R. and Feather R. confluence with HEC-RAS calibrated coefficients

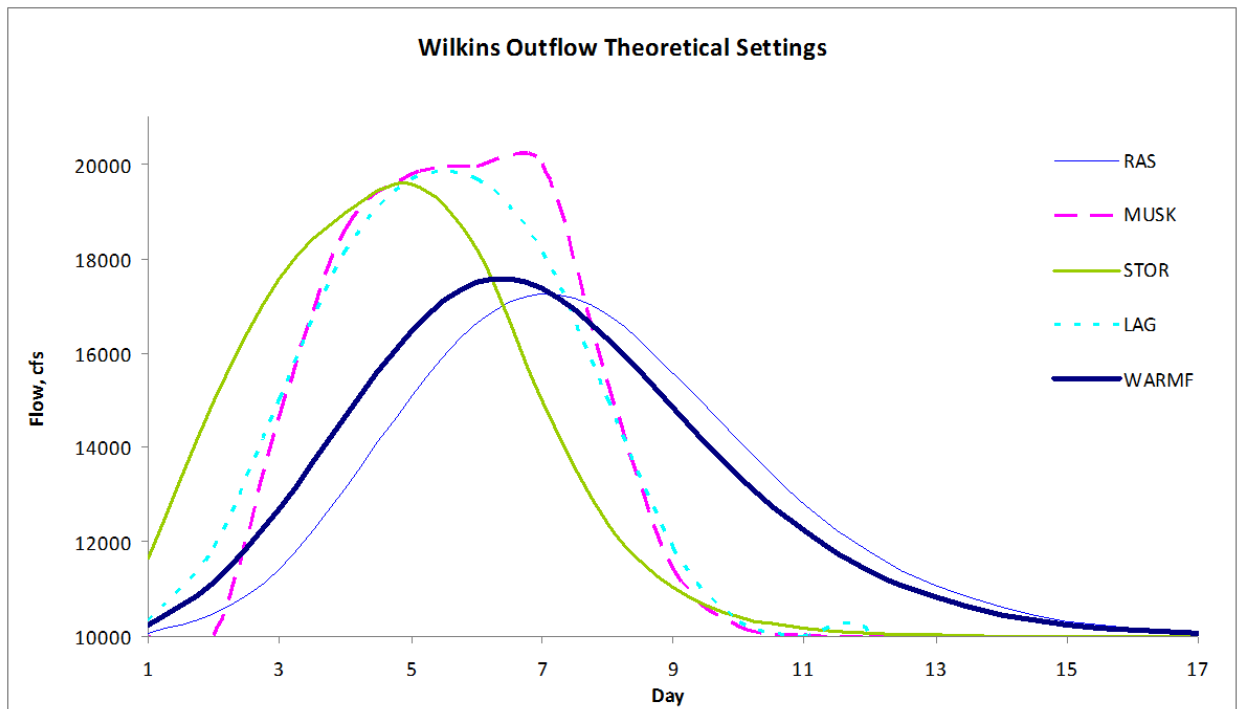


Figure 41. Outflow from C_Wilkins at Sacramento R. and Feather R. confluence with theoretically calibrated coefficients

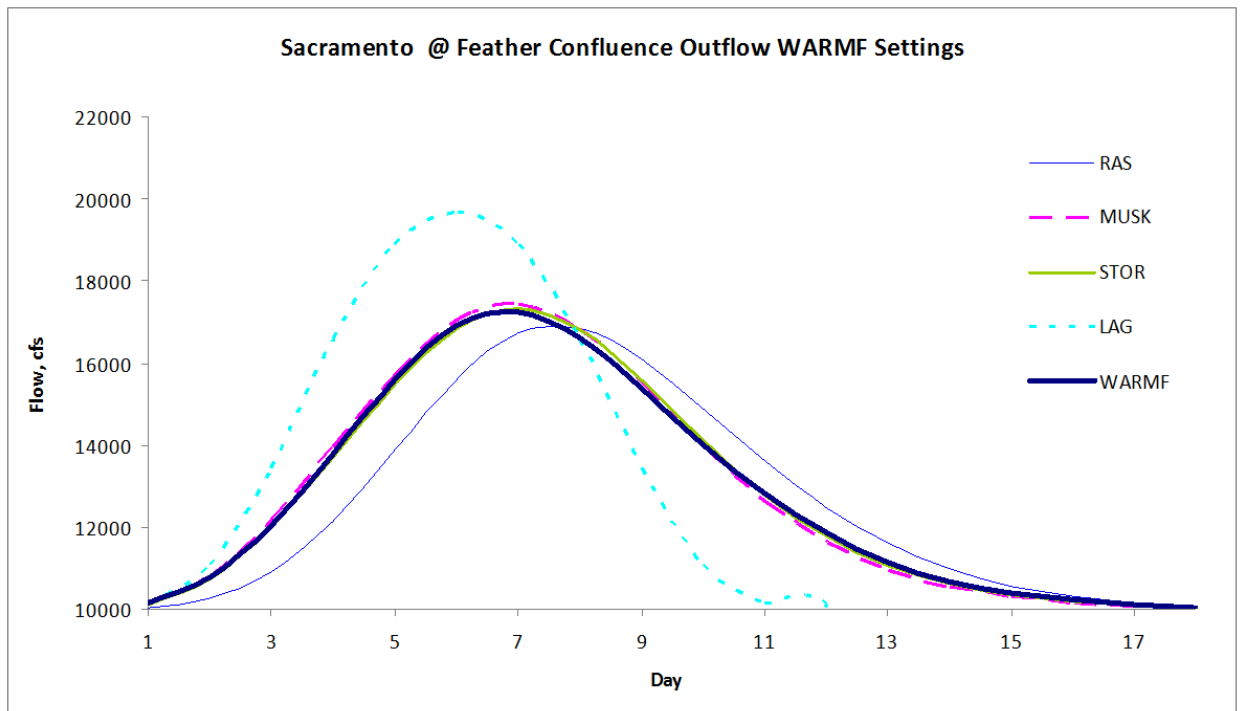


Figure 42. Outflow from C_SacFea at Sacramento R. and American R. confluence with WARMF calibrated coefficients

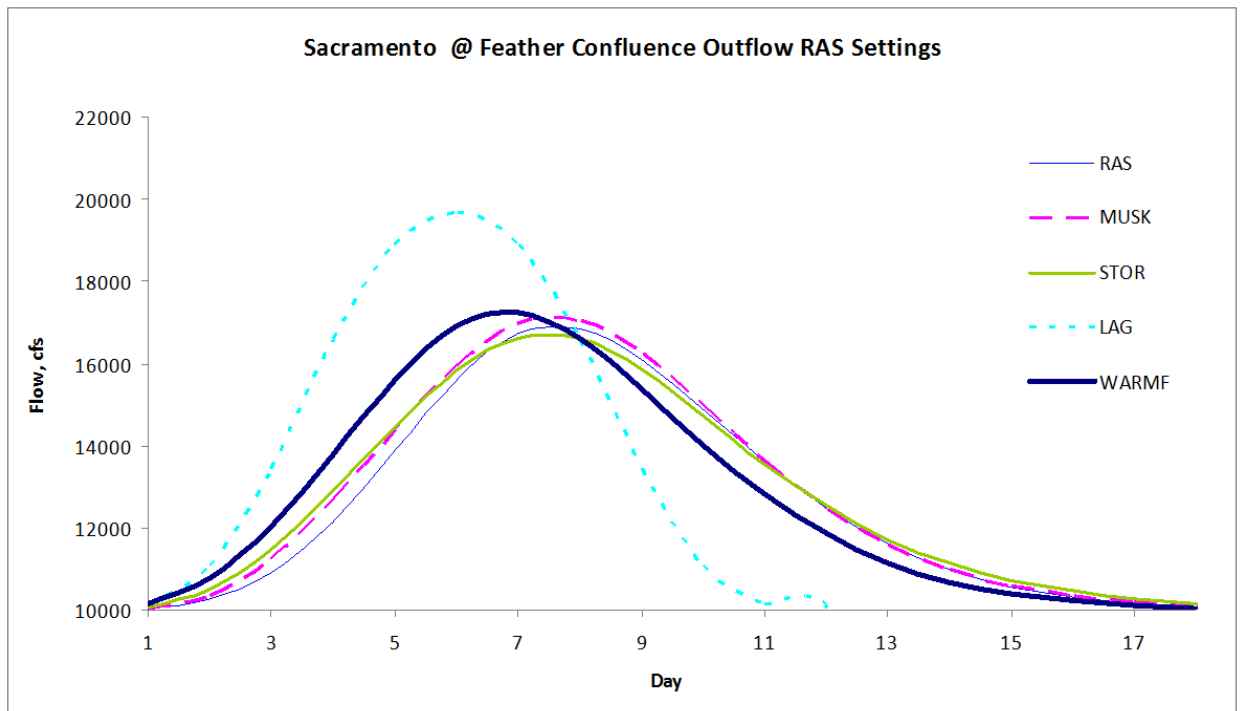


Figure 43. Outflow from C_SacFea at Sacramento R. and American R. confluence with HEC-RAS calibrated coefficients

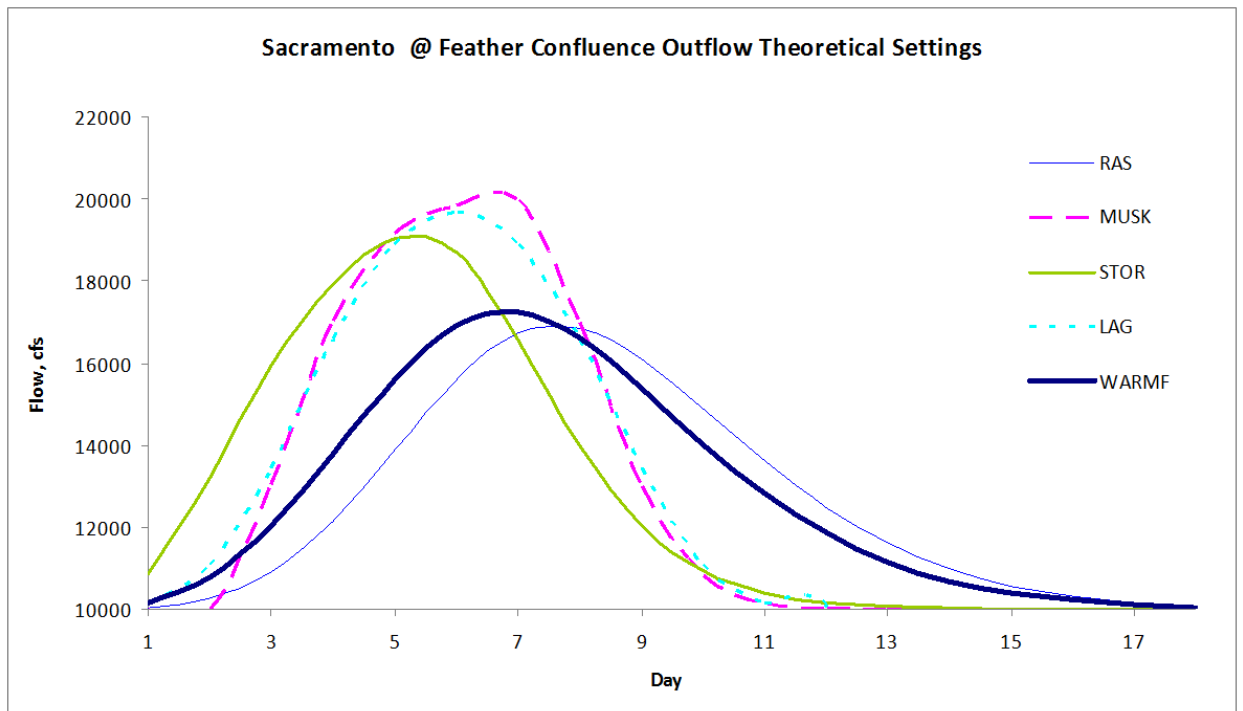


Figure 44. Outflow from C_SacFea at Sacramento R. and American R. confluence with theoretically calibrated coefficients

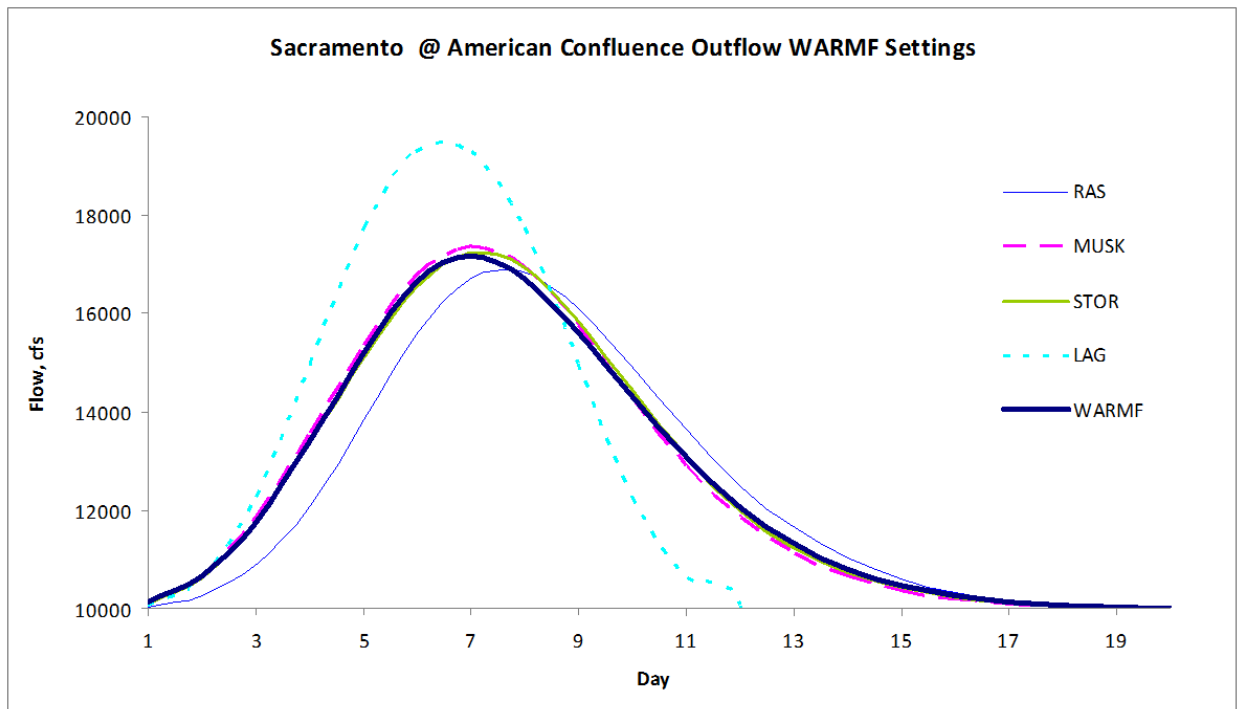


Figure 45. Outflow from C_SacAme at Hood with WARMF calibrated coefficients

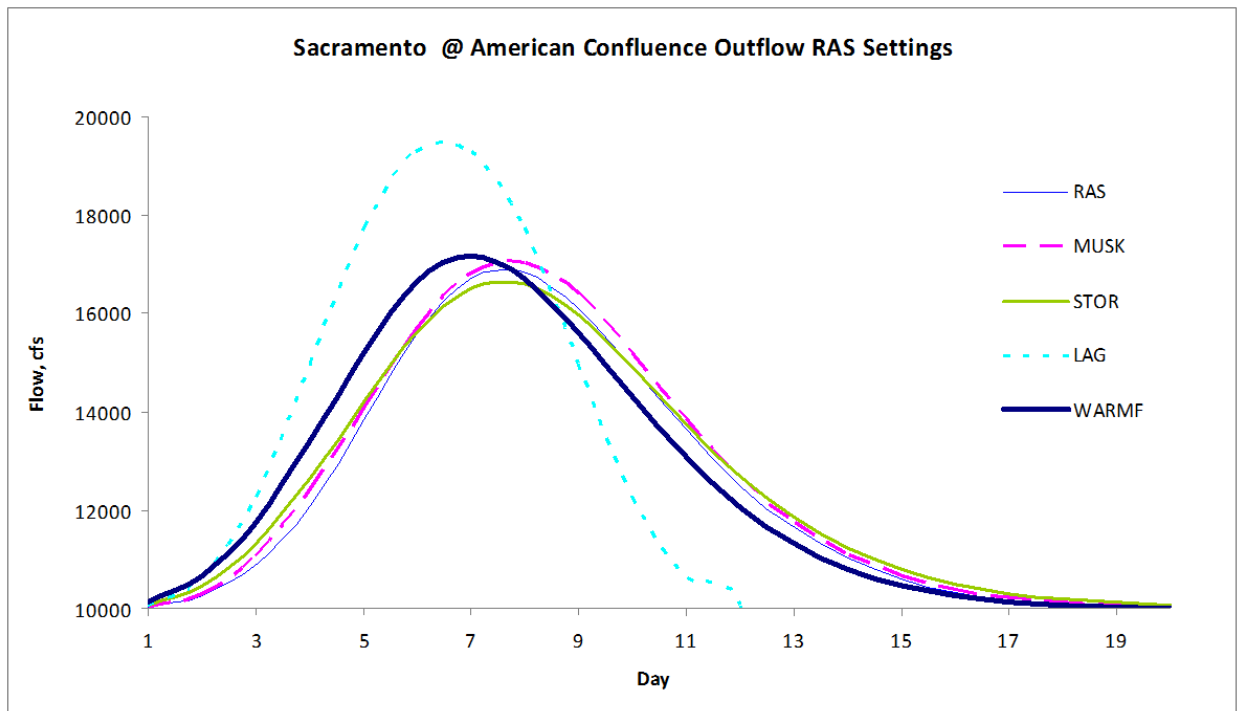


Figure 46. Outflow from C_SacAme at Hood with HEC-RAS calibrated coefficients

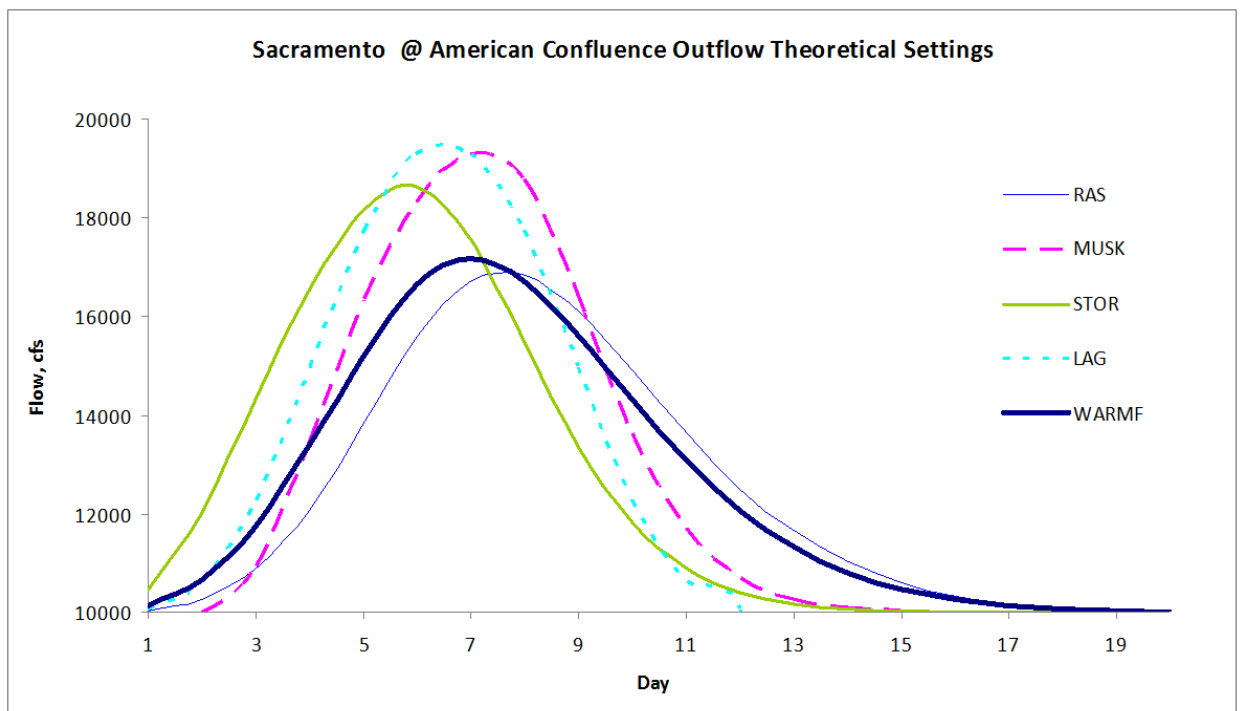


Figure 47. Outflow from C_SacAme at Hood with theoretically calibrated coefficients

Delta Flow Requirement Results

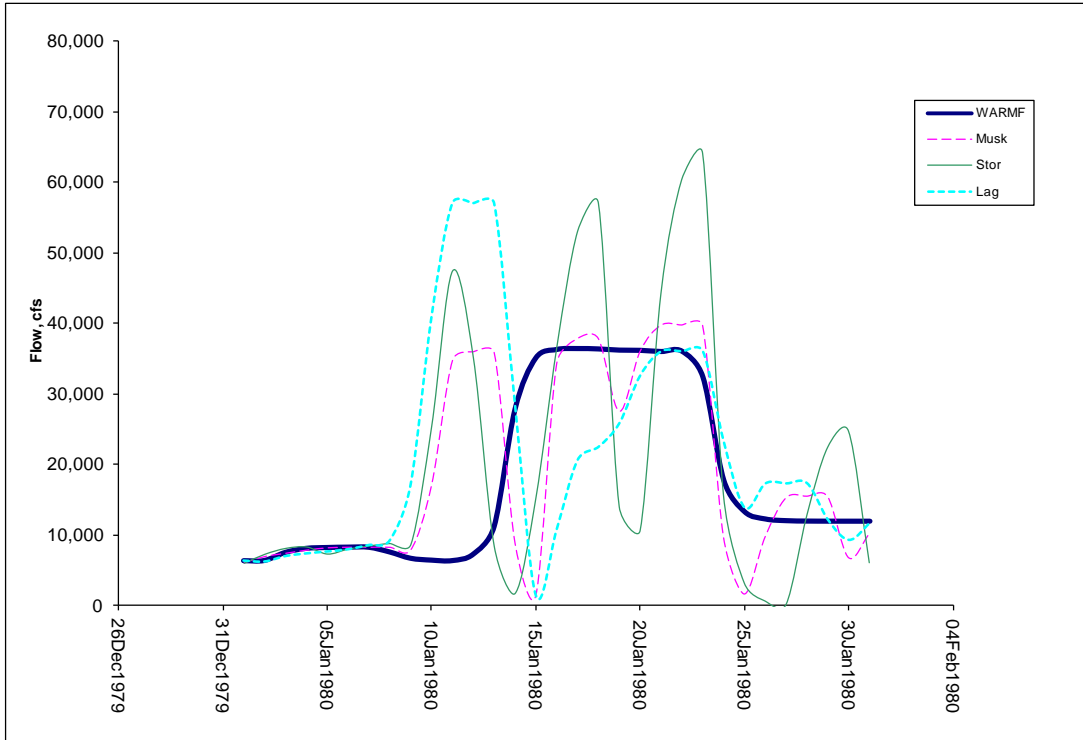


Figure 48. Outflow from C_Shsta at Keswick with Delta flow requirement using WARMF calibrated coefficients

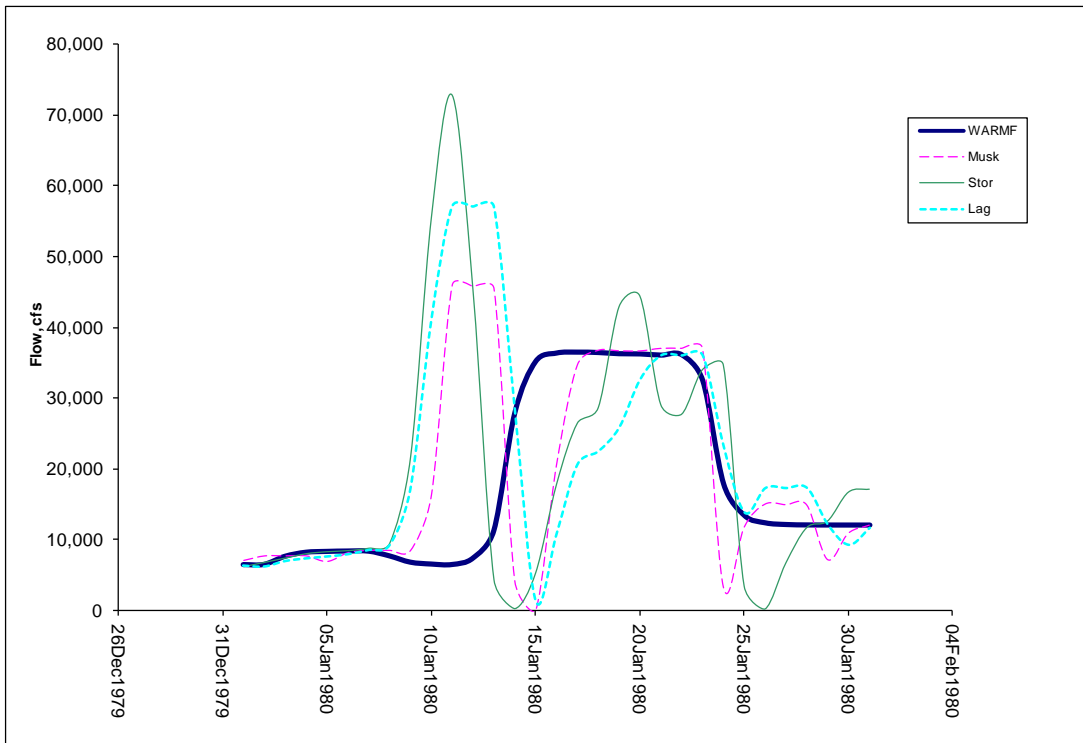


Figure 49. Outflow from C_Shsta at Keswick with Delta flow requirement using theoretically calibrated coefficients

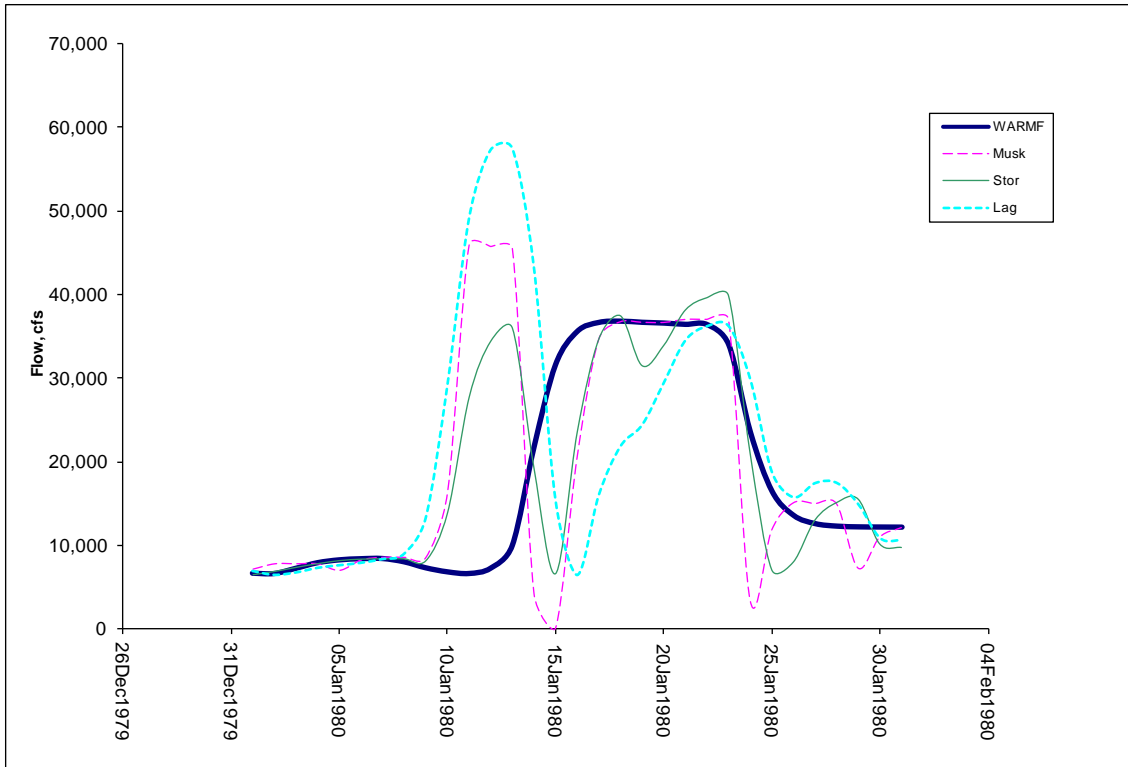


Figure 50. Outflow from C_Kswck at Red Bluff with Delta flow requirement using WARMF calibrated coefficients

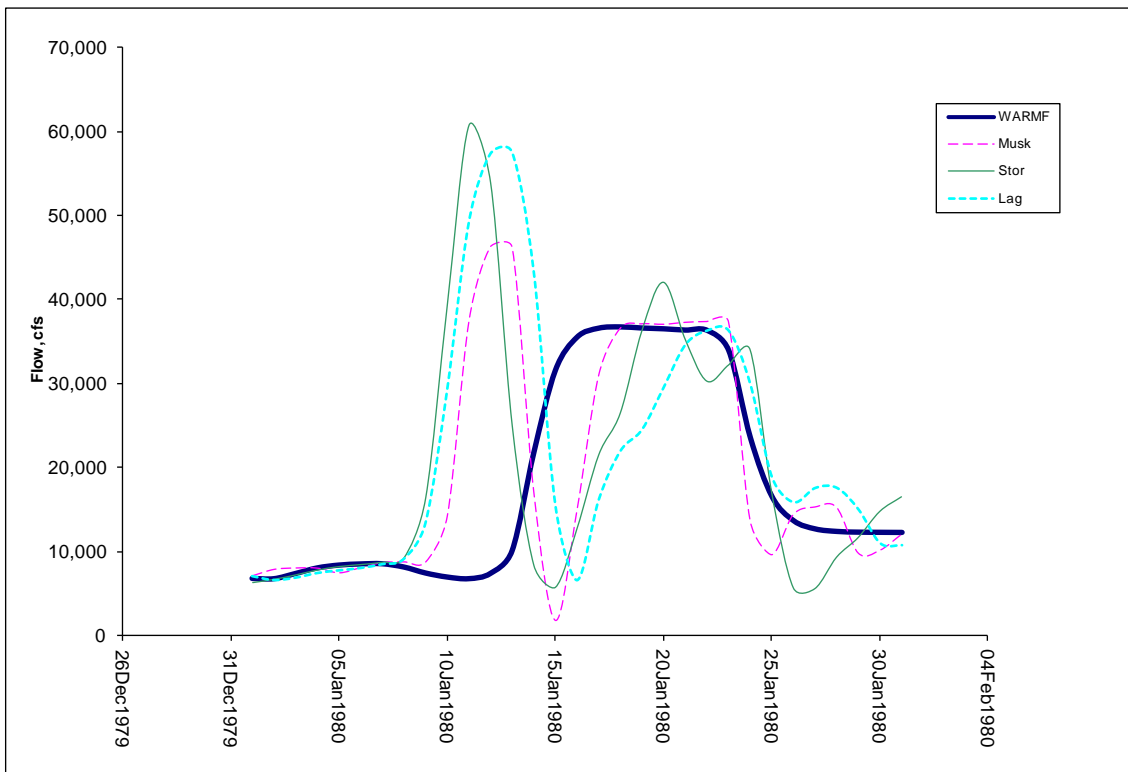


Figure 51. Outflow from C_Kswck at Red Bluff with Delta flow requirement using theoretically calibrated coefficients

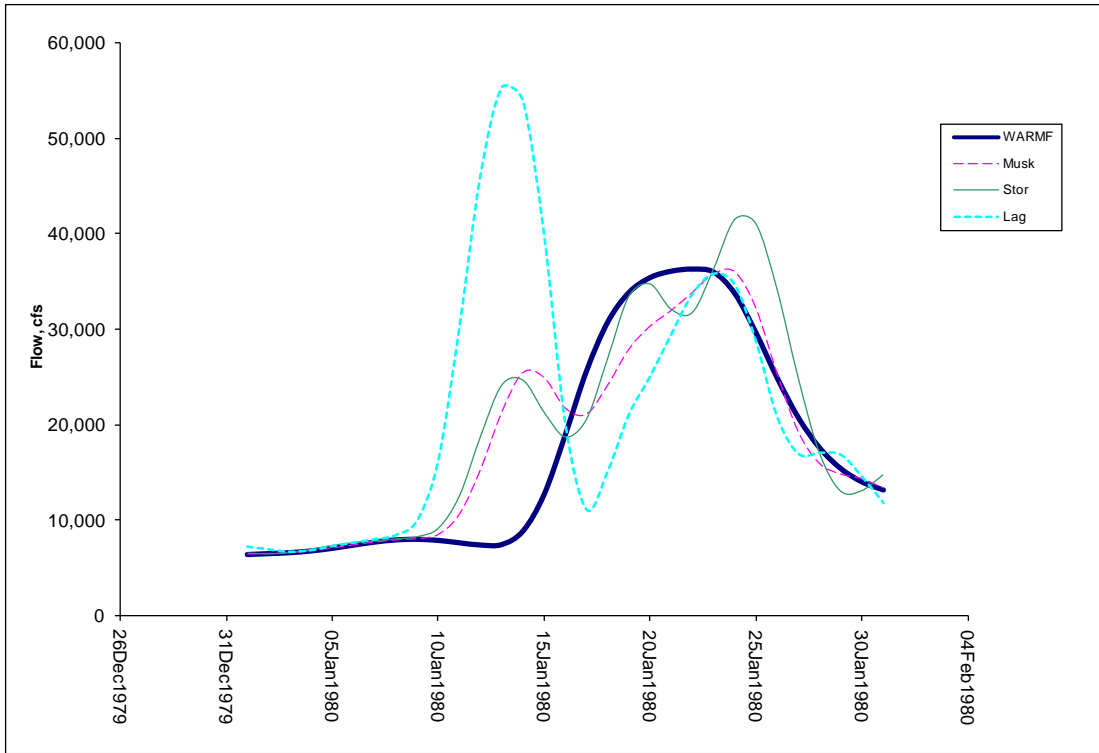


Figure 52. Outflow from C_RedBlf at Wilkins Slough with Delta flow requirement using WARMF calibrated coefficients

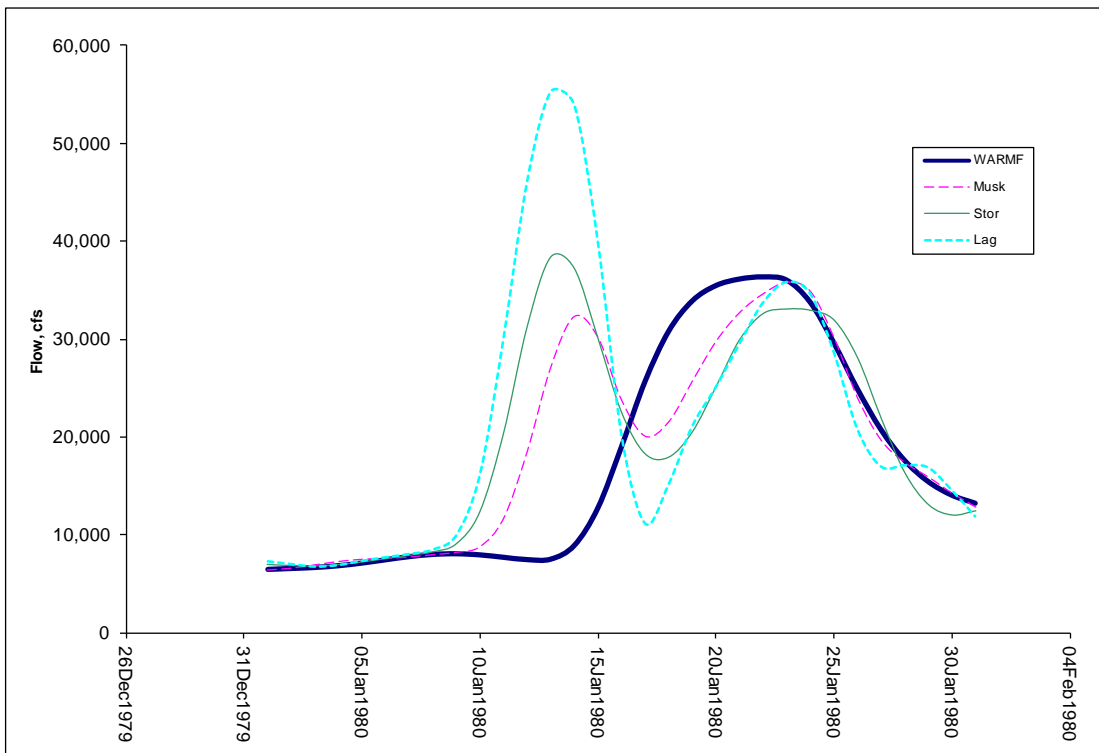


Figure 53. Outflow from C_RedBlf at Wilkins Slough with Delta flow requirement using WARMF calibrated coefficients

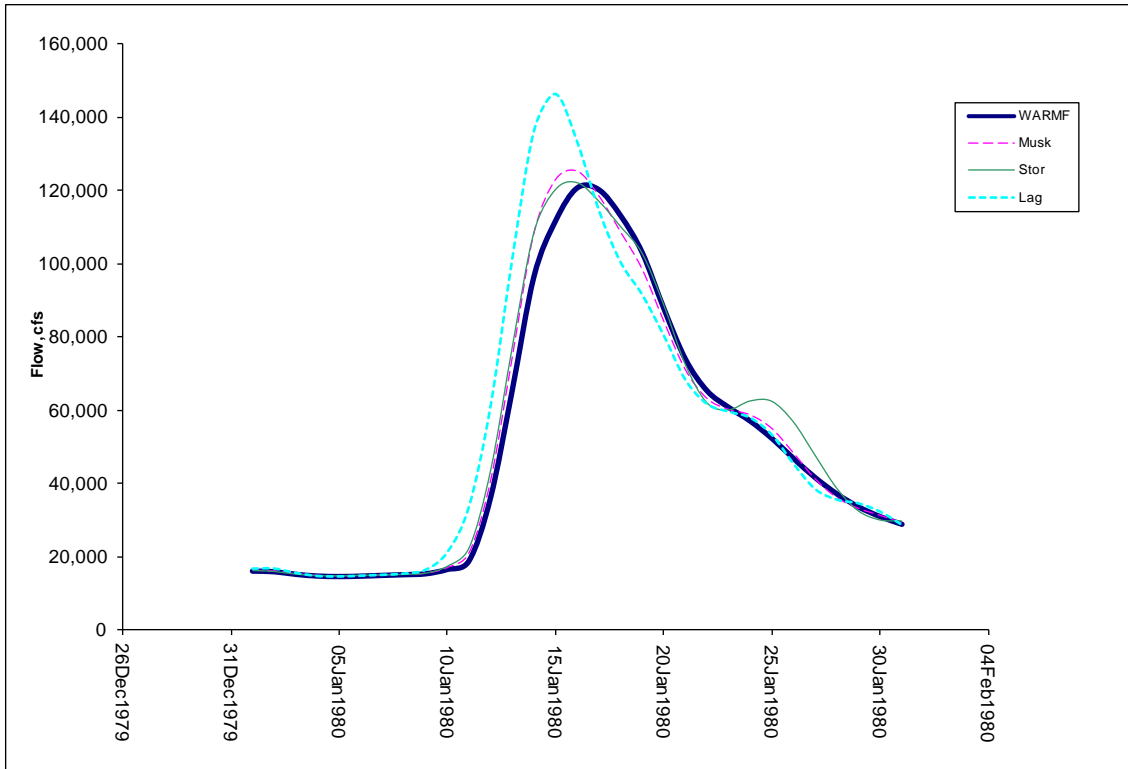


Figure 54. Outflow from C_Wilkins at Sacramento R. and Feather R. confluence with Delta flow requirement using WARMF calibrated coefficients

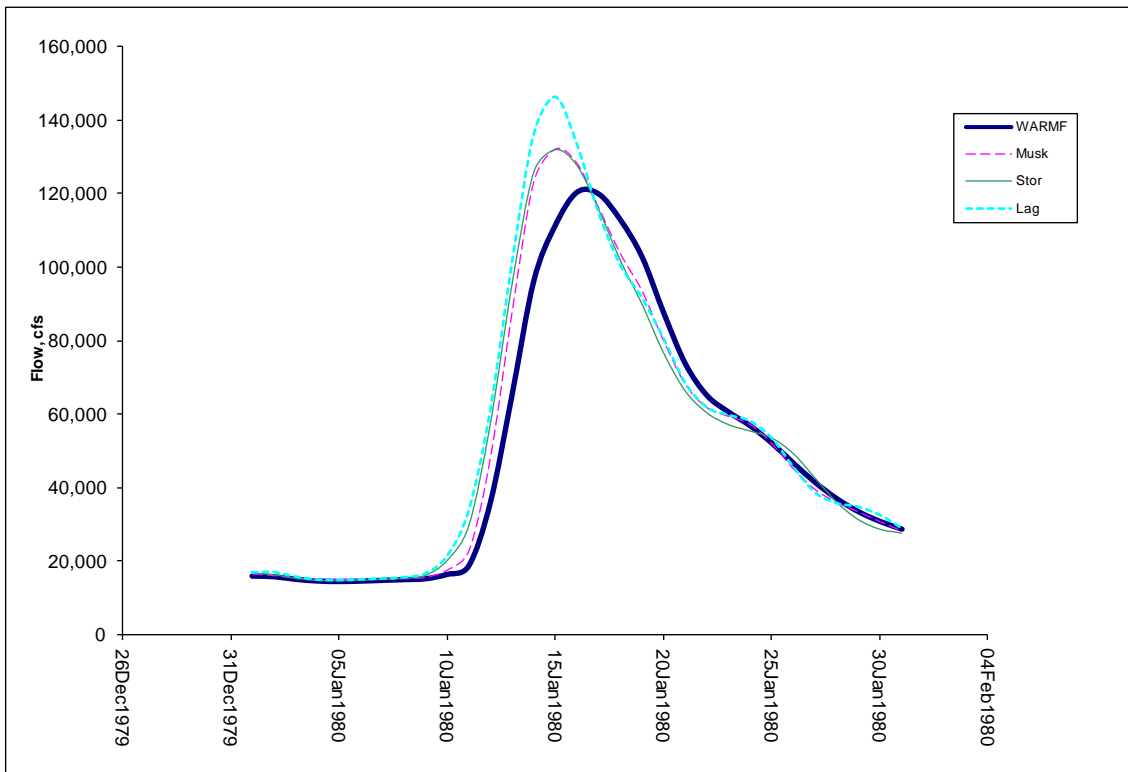


Figure 55. Outflow from C_Wilkins at Sacramento R. and Feather R. confluence with Delta flow requirement using theoretically calibrated coefficients

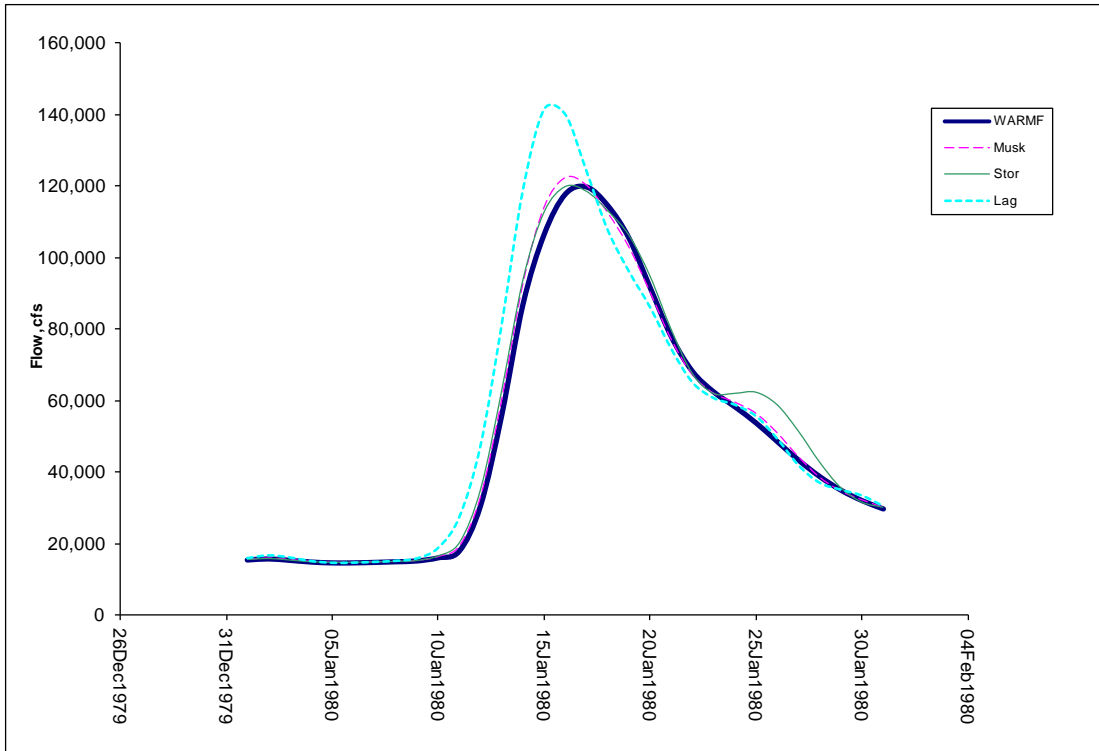


Figure 56. Outflow from C_SacFea at Sacramento R. and American R. confluence with Delta flow requirement using WARMF calibrated coefficients

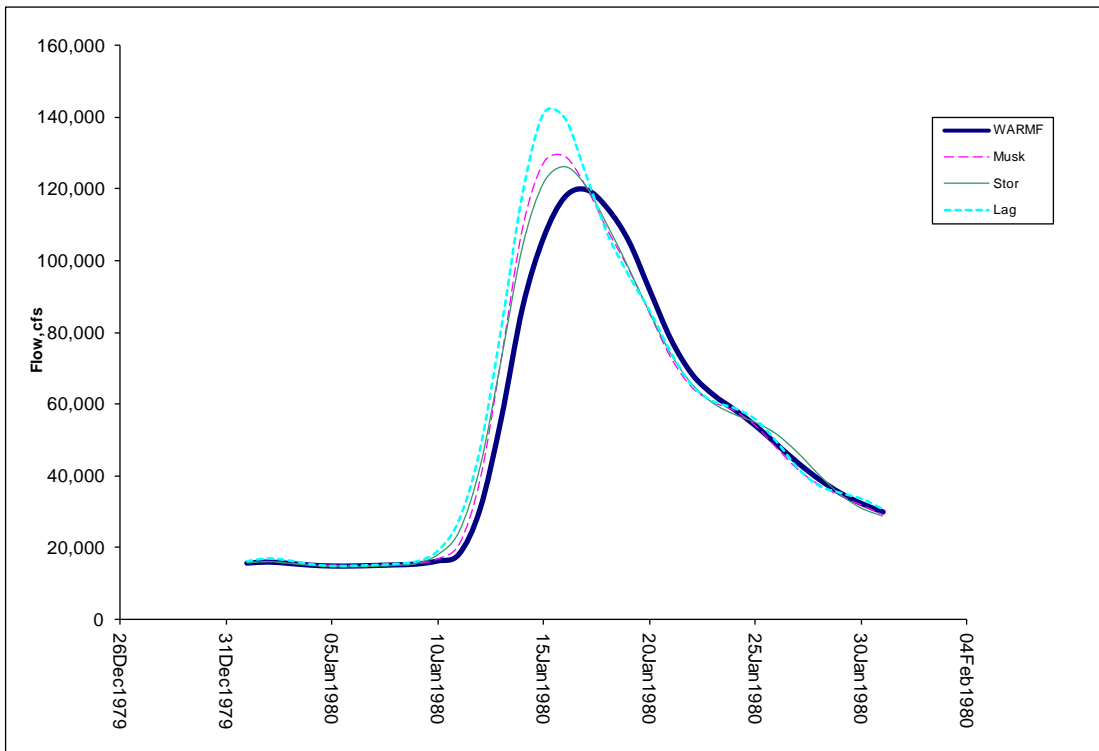


Figure 57. Outflow from C_SacFea at Sacramento R. and American R. confluence with Delta flow requirement using theoretically calibrated coefficients

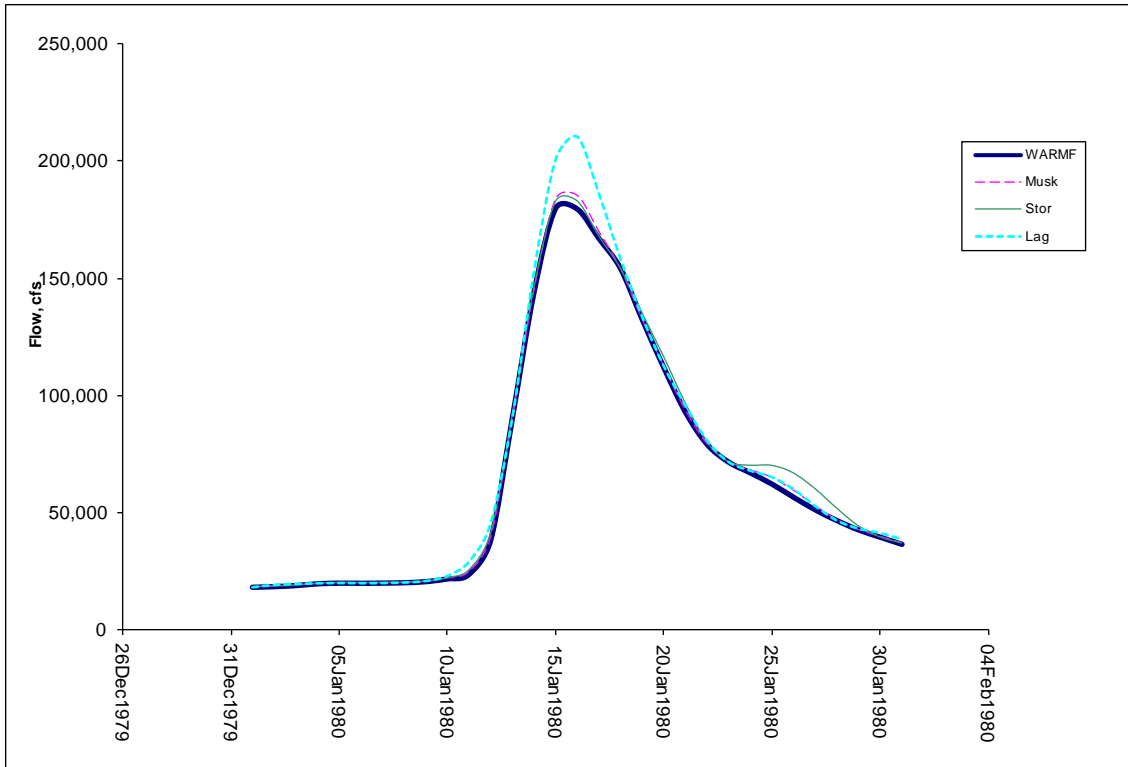


Figure 58. Outflow from C_SacAme at Hood with Delta flow requirement using WARMF calibrated coefficients

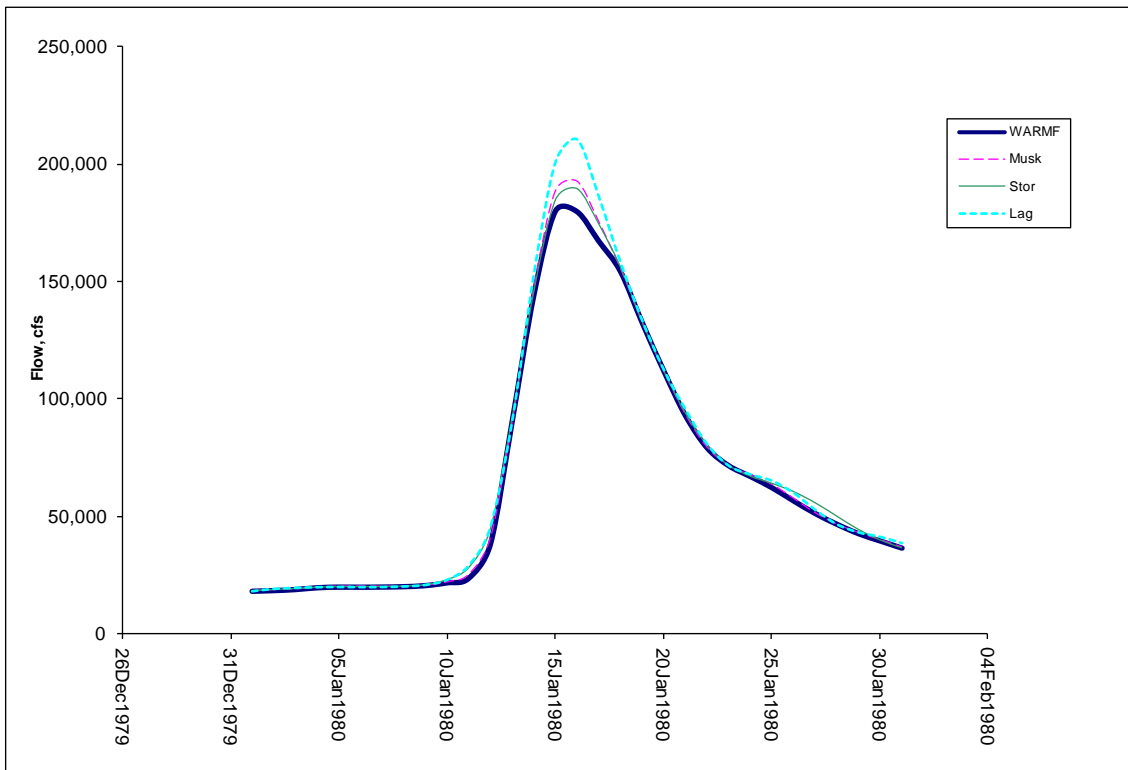


Figure 59. Outflow from C_SacAme at Hood with Delta flow requirement using theoretically calibrated coefficients

Upstream and Downstream Minimum Flow Results

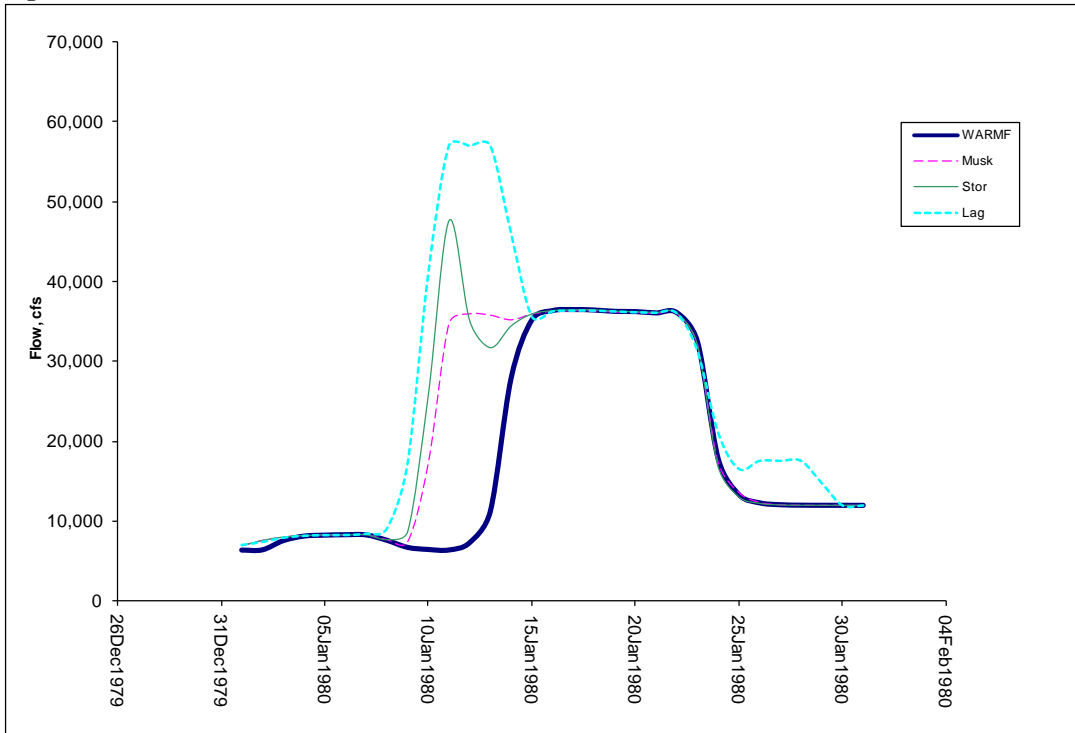


Figure 60. Outflow from C_Shsta at Keswick with Delta and upstream flow requirements using WARMF calibrated coefficients

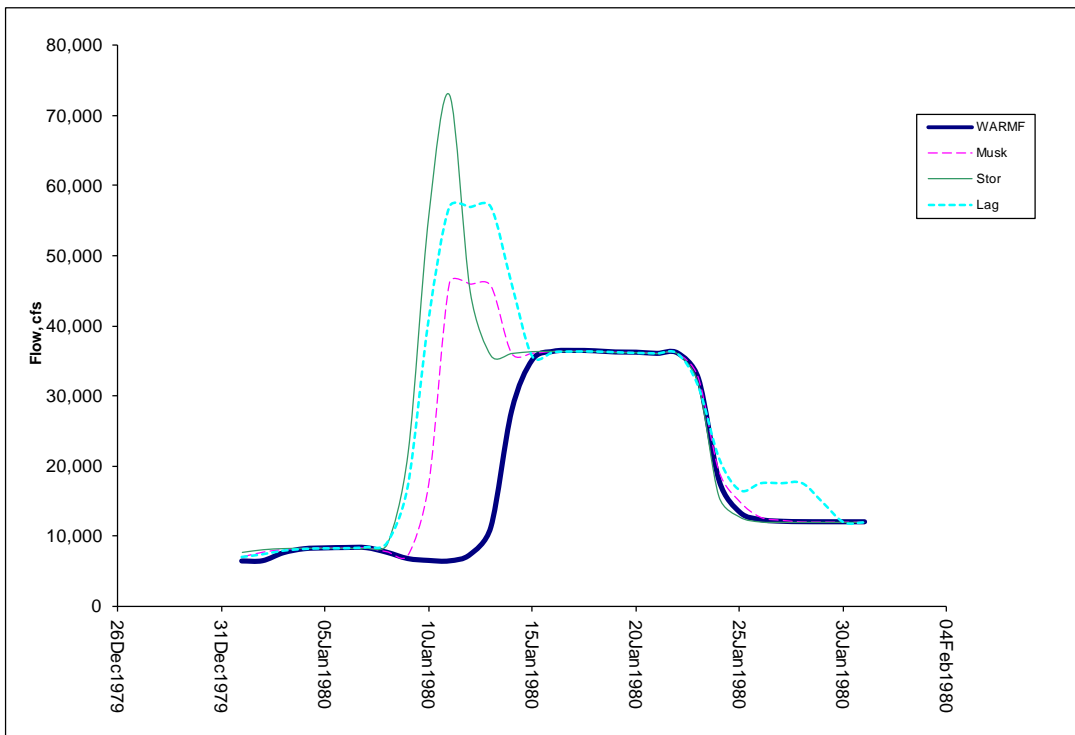


Figure 61. Outflow from C_Shsta at Keswick with Delta and upstream flow requirements using theoretically calibrated coefficients

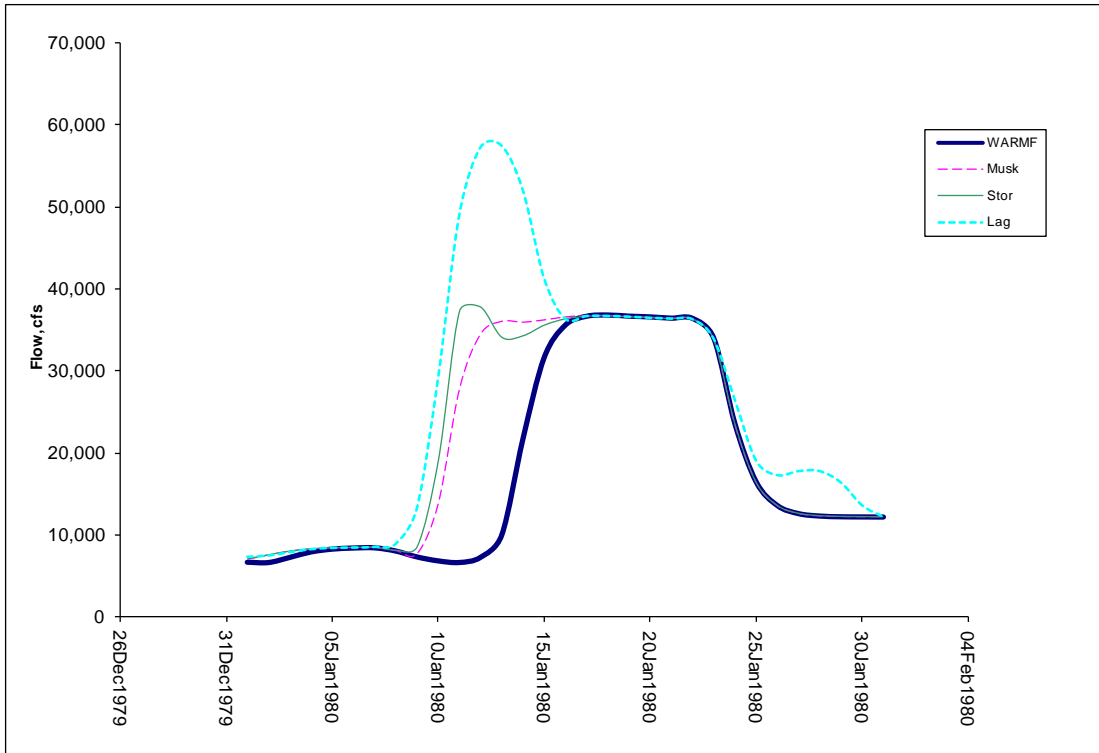


Figure 62. Outflow from C_Kswck at Red Bluff with Delta and upstream flow requirements using WARMF calibrated coefficients

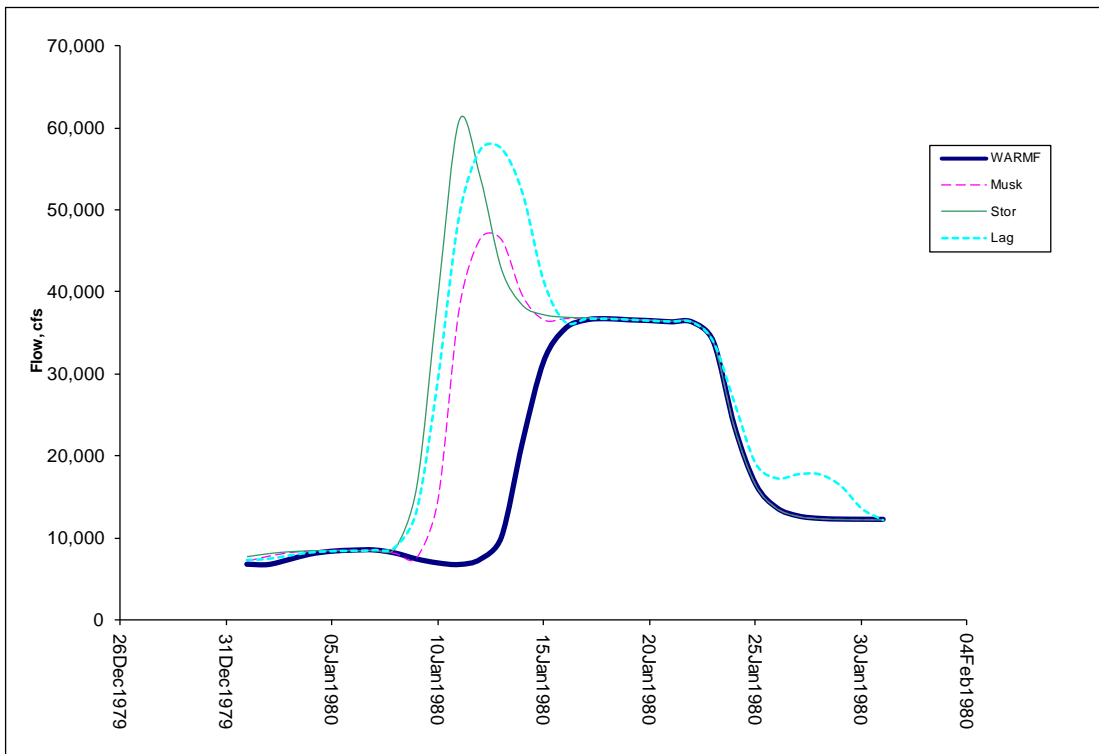


Figure 63. Outflow from C_Kswck at Red Bluff with Delta and upstream flow requirements using theoretically calibrated coefficients

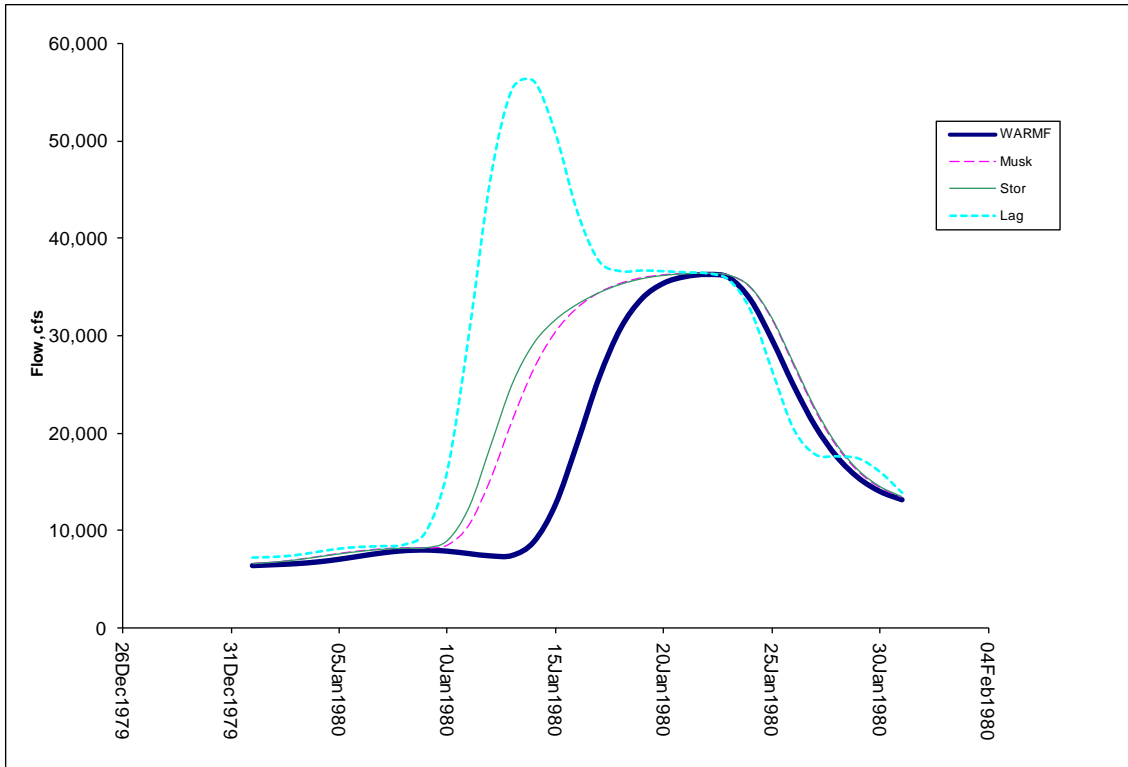


Figure 64. Outflow from C_RedBlf at Wilkins Slough with Delta and upstream flow requirements using WARMF calibrated coefficients

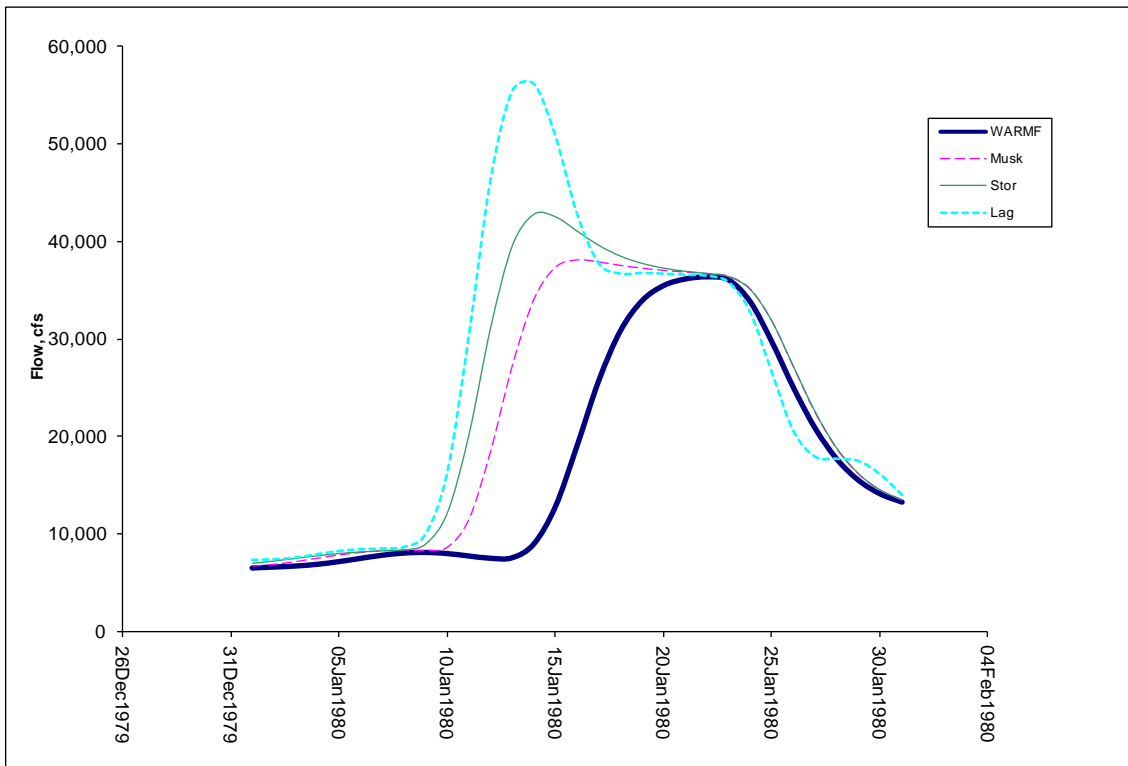


Figure 65. Outflow from C_RedBlf at Wilkins Slough with Delta and upstream flow requirements using theoretically calibrated coefficients

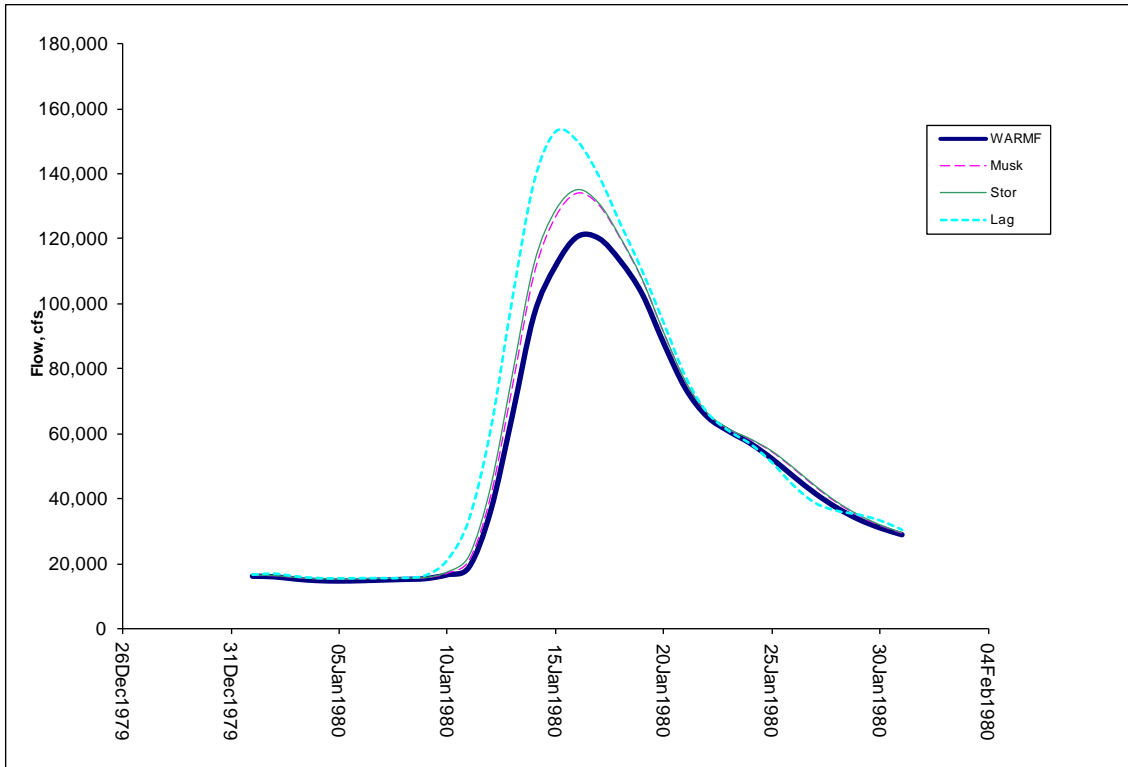


Figure 66. Outflow from C_Wilkins at Sacramento R. and Feather R. confluence with Delta and upstream flow requirements using WARMF calibrated coefficients

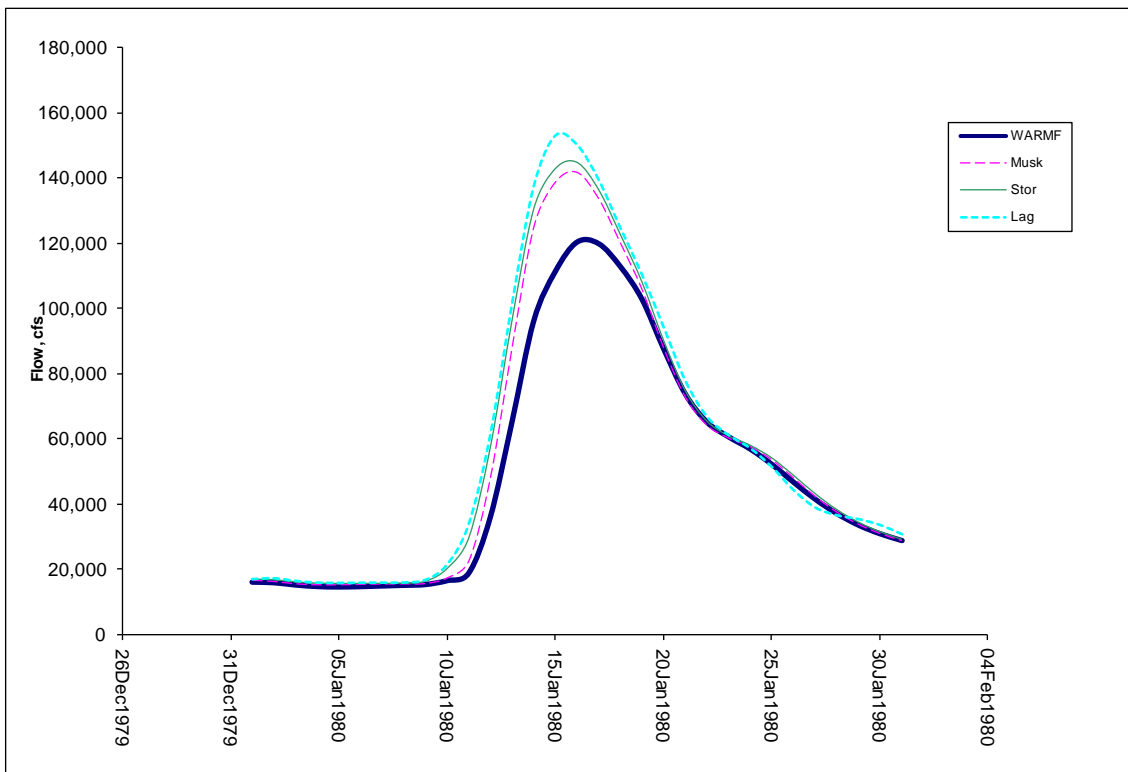


Figure 67. Outflow from C_Wilkins at Sacramento R. and Feather R. confluence with Delta and upstream flow requirements using WARMF calibrated coefficients

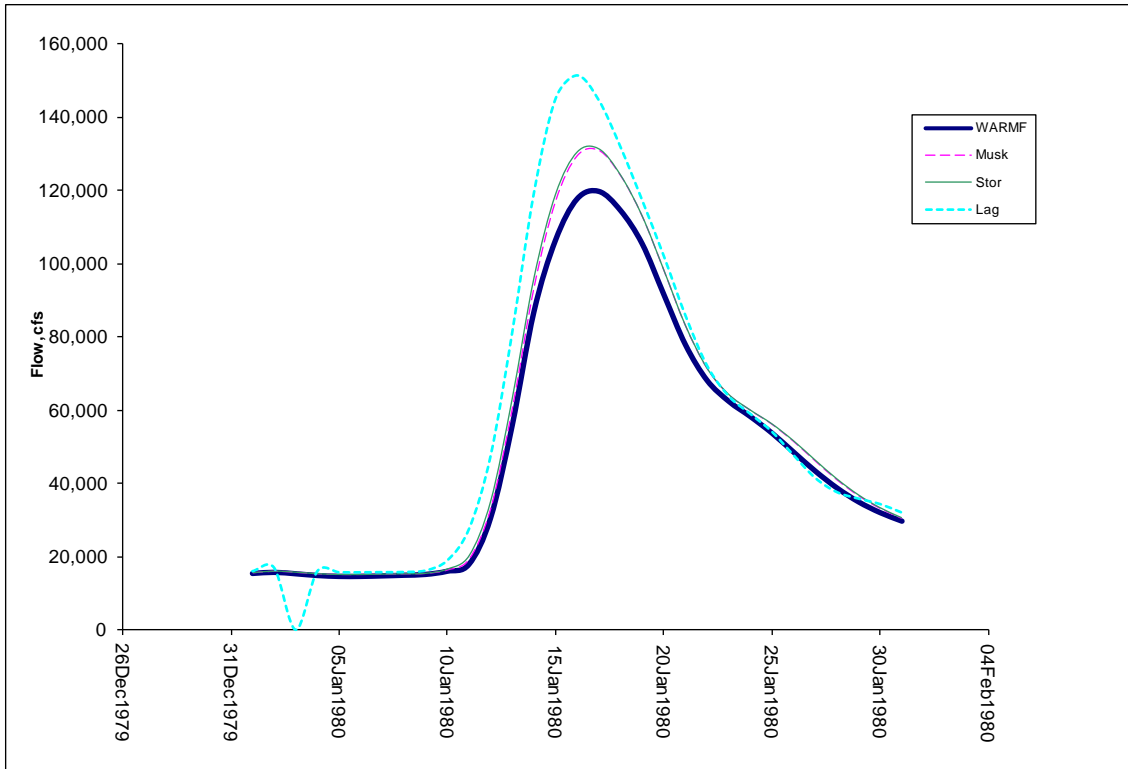


Figure 68. Outflow from C_SacFea at Sacramento R. and American R. confluence with Delta and upstream flow requirements using WARMF calibrated coefficients

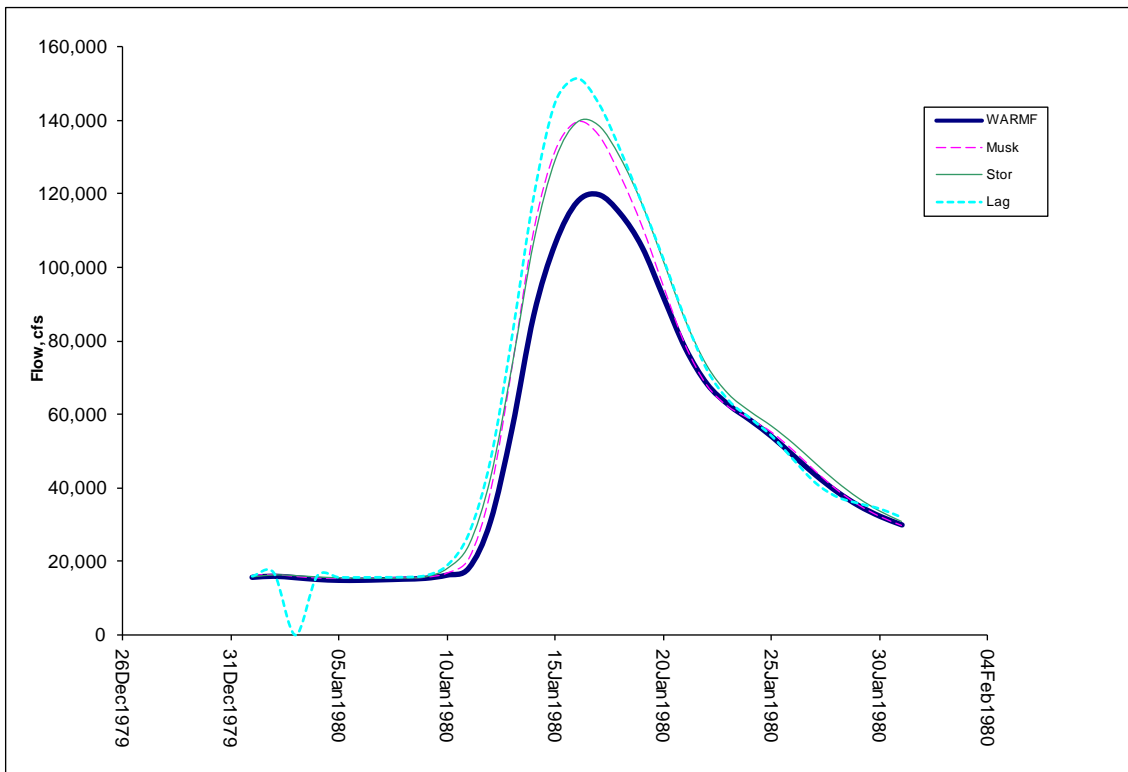


Figure 69. Outflow from C_SacFea at Sacramento R. and American R. confluence with Delta and upstream flow requirements using theoretically calibrated coefficients

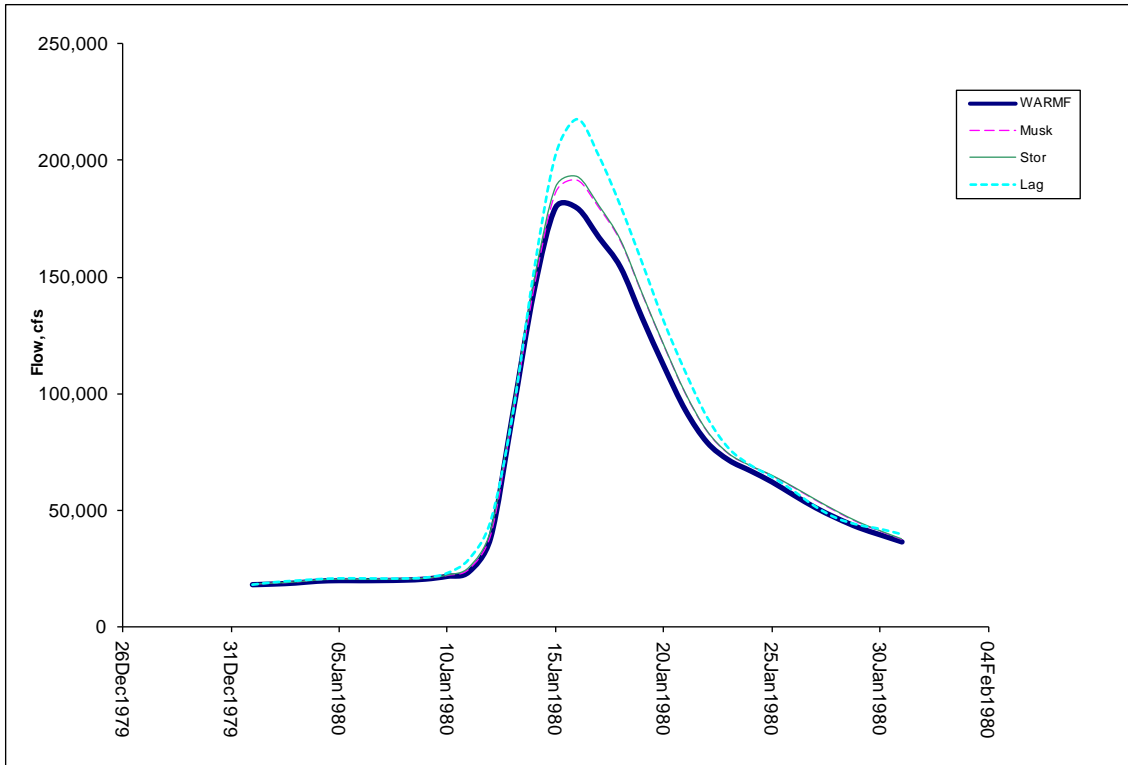


Figure 70. Outflow from C_SacAme at Hood with Delta and upstream flow requirements using WARMF calibrated coefficients

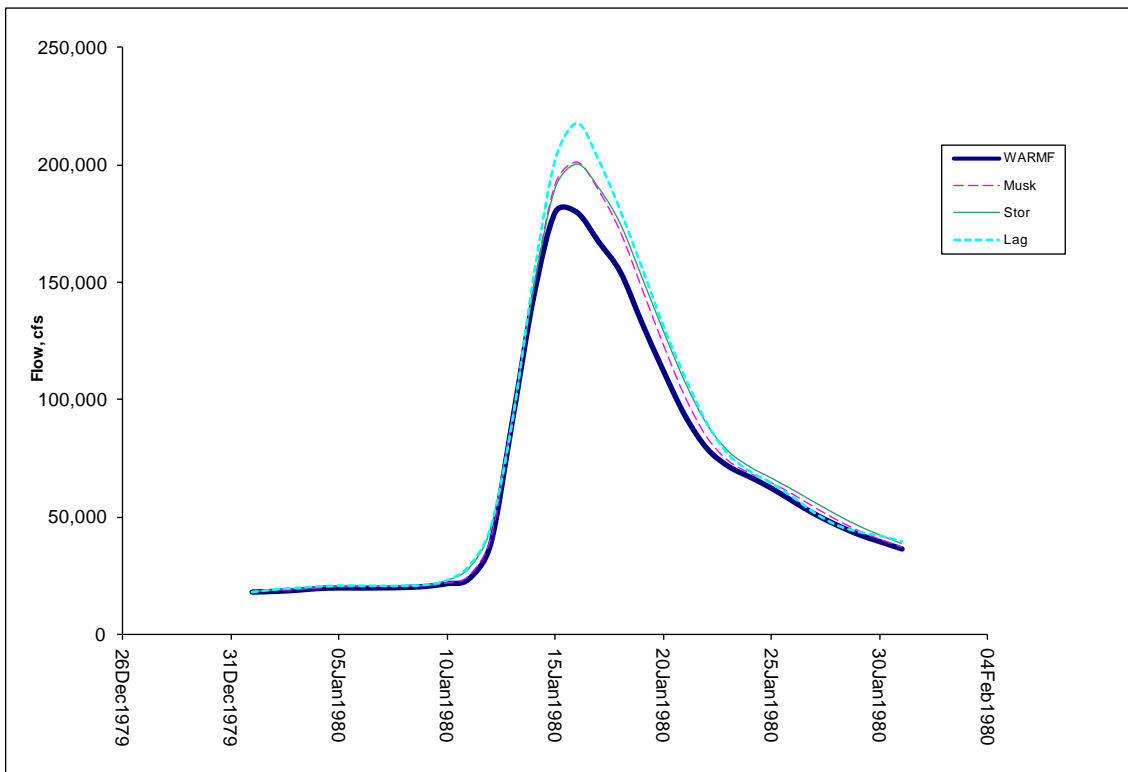


Figure 71. Outflow from C_SacAme at Hood with Delta and upstream flow requirements using theoretically calibrated coefficients